Microbial carbon processing in present-day lacustrine food webs

A multidimensional approach using stable isotopes, membrane lipid chemistry and modelling

Marieke Lammers

Utrecht Studies in Earth Sciences
No. 122

Promotoren:
Prof. dr. G.J. Reichart, Utrecht University and NIOZ, The Netherlands
Prof. dr. J.J. Middelburg, Utrecht University, The Netherlands

Members of the dissertation committee:
Prof. dr. T.I. Battin, University of Vienna, Switzerland
Prof. dr. L. Bouwman, Utrecht University, The Netherlands
Dr. A. de Kluijver, Utrecht University, The Netherlands
Prof. dr. G.A. Kowalchuk, Utrecht University, The Netherlands
Prof. dr. J.S. Sinninghe Damsté, Utrecht University and NIOZ, The Netherlands

Contact: jmlammers.vdbroeke@gmail.com

Lay-out and initial figure design (unless stated otherwise): Marieke Lammers
Final figure design: Ton Markus (Utrecht University, The Netherlands)
Design by Margot Stoete (Utrecht University, The Netherlands)
Cover: Photo: Naardermeer, The Neterlands.

ISBN 978-90-6266-446-7
Utrecht Studies in Earth Sciences (USES) No. 122
Printed by CPI – Koninklijke Wöhrmann, Zutphen

Microbial carbon processing in present-day lacustrine food webs

A multidimensional approach using stable isotopes, membrane lipid chemistry and modelling

Microbiële koolstofverwerking in hedendaagse zoetwater voedselwebben

Een multidimensionale aanpak met behulp van stabiele isotopen, membraanlipidenchemie en modellering (met een samenvatting in het Nederlands)

Proefschrift

ter verkrijging van de graad van doctor aan de Universiteit Utrecht op gezag van de rector magnificus, prof dr. G.J. van der Zwaan, ingevolge het besluit van het college voor promoties in het openbaar te verdedigen op vrijdag 24 februari 2017 des middags te 16.15 uur

door

Johanne Marieke Lammers

geboren op 17 april 1985 te Gouda

Promotoren:
Prof. dr. G.J. Reichart
Prof. dr. J.J. Middelburg

This research was partially funded by the Netherlands Organisation for Scientific Research (Earth and Life Sciences, grant 820.02.017).

Riding high amongst the waves
I can feel like I
have a soul that has been saved
I can see the light
Coming through the clouds in rays
- Pearl Jam –

Contents

Chapter 1

General introduction and synopsis

1.1 Climate change and the global carbon cycle in the Anthropocene

The chemical element carbon (C) is not only a key constituent of life on Earth but is also pivotal in Earth's energy balance and hence climate. Its gaseous forms carbon dioxide (CO_2) and methane (CH_4) are among the primary greenhouse gases in the atmosphere, trapping heat by absorbing long-wave (infrared) radiation emitted by Earth's surface. Recently, human activities have changed the natural global carbon cycle, by burning fossil fuels, clearing forests and cement production. As a result, atmospheric CO_2 concentrations increased at an unprecedented rate from ~280 parts per million (ppm) in the pre-industrial era to its current concentration of ~400 ppm [NOAA, Global monitoring Division]. This is a cause of concern, as there is strong evidence for a link between atmospheric CO_2 concentrations and rising global temperatures (IPCC 2013, Petit et al. 1999).

Although the observed increase in atmospheric CO_2 is substantial, it represents only ~50% of anthropogenic CO_2 emissions (Canadell et al. 2007, IPCC 2007, Le Quéré et al. 2009). The rest has been taken up by different reservoirs in the global carbon cycle. Earth's oceans have long been recognized as a sink since CO_2 dissolves in and subsequently reacts with (sea)water, resulting in carbonic acid (H_2CO_3), bicarbonate (HCO_3^-) and carbonate (CO_3^{2-}), the sum of which is called dissolved inorganic carbon (DIC). On land, carbon budget studies generally focus on the terrestrial biosphere as the primary carbon sink, storing ~30% of the emitted carbon (Canadell et al. 2007). Still, there are large uncertainties regarding the sustainability of these carbon sinks under changing environmental conditions, and gaps and discrepancies remain in carbon budgets (Battin et al. 2009, Heimann 2009, Le Quéré et al. 2009).

1.2 The role of lakes in the global carbon cycle

Only during the last couple of years have freshwater systems been recognized to process and potentially store substantial amounts of carbon (Battin et al. 2009, Cole et al. 2007, Raymond et al. 2013, Richey et al. 2002). Although lakes make up only ~1% of the Earth's surface, they have a large storage capacity compared to oceans as a consequence of their higher production rates and faster sedimentation rates (Cole et al. 2007). Freshwater systems receive 1.9 – 2.9 Pg C y^{-1} from their surroundings via runoff, groundwater and rivers (Battin et al. 2009, Cole et al. 2007), which for the largest part is processed or stored within the lakes themselves. Because of their relative importance lakes should be considered in estimates of the global carbon cycle (Fig. 1.1). However, complete lacustrine carbon budgets are scarce and need to be better constrained in order to provide a more consistent view on the function of freshwater systems in the global carbon cycle (Hanson et al. 2015). For example, despite their large storage capacity, lakes are mostly sources of CO_2 to the atmosphere (Battin et al. 2009, Cole et al. 2007, Tranvik et al. 2009) and although terrestrial organic carbon is generally assumed to be refractory and a poor food source (e.g. Brett et al. 2009), it may still be assimilated in parts of the food web (e.g. Cole et al. 2011, Pace et al. 2004). Many questions thus remain to be answered regarding not only the fluxes in- and out of lakes as a whole, but also concerning the fluxes within lakes and the organisms and processes involved in carbon cycling in lakes. This thesis aims at increasing the understanding of the internal processes (within food webs) that affect lacustrine carbon budgets in lakes with contrasting productivity.

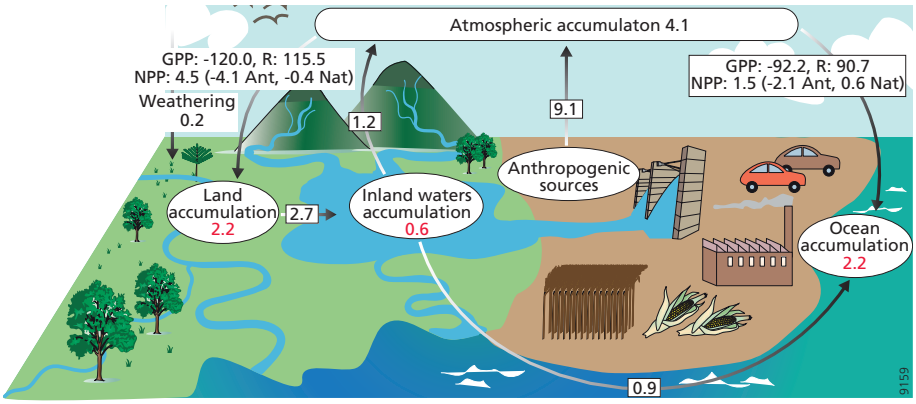

Fig. 1.1. Carbon fluxes in the global biogeochemical C cycle (in Pg C y^{-1}) through marine and terrestrial reservoirs. Red numbers represent rates of cycling within the reservoir. Positive fluxes denote sources of CO_2 to the atmosphere and negative fluxes are sinks of CO_2 from the atmosphere. Net primary production is divided between natural fluxes (Nat) and anthropogenic (Ant) components. Figure adapted from Battin et al. (2009).

1.3 Carbon cycling in lacustrine food webs

Whereas traditionally food-web studies were limited to analysing larger sized organisms and using indirect proxies for the microbial domain, nowadays microbial lipid chemistry allows for direct analysis of microbial producers and consumers (see Middelburg (2014) for an extensive review). This thesis focuses specifically on microbial carbon processing in four different freshwater systems with varying nutrient conditions: 1) Rotsee, a relatively shallow, eutrophic lake in Switzerland, 2) Lake Lucerne, a large, oligotrophic lake in Switzerland, 3) two basins of Lake Taihu (China), one of which is highly eutrophic and dominated by toxic algal blooms, and the other was subject to biomanipulation and restoration efforts and is now dominated by macrophytes, and 4) Lake Naarden (Naardermeer), a shallow peat lake in The Netherlands.

1.3.1 Primary production and carbon pools

At the base of the food web, phytoplankton (microphytes) and macrophytes take up DIC during photosynthesis to produce organic matter (Fig. 1.2). Freshwater DIC concentrations generally range between 100 and 1000 µmol C L^{-1} (Cole and Prairie 2009) and are rarely in equilibrium with the atmosphere because the rate of exchange with the atmosphere (timescale of months) is much slower than the rates of biological processes affecting DIC concentrations in the water column (Sarmiento and Gruber 2006). Concentrations of DIC species ($CO_{2(aq)}$, H_2CO_3, HCO_3^- and CO_3^{2-}) in lake water are a function of pH, with HCO_3^- being the dominant species in most natural waters and $CO_{2(aq)}$ contributing only minor amounts. To maintain production, most phytoplankton and macrophyte species have developed carbon concentrating mechanisms that aid in the conversion of HCO_3^- to $CO_{2(aq)}$ (Lucas and Berry 1985). Still, phytoplankton production is generally assumed to decrease when $CO_{2(aq)}$ concentrations are limiting (Riesebell et al. 1993).

The fresh organic matter photosynthesized by micro- and macrophytes can either be directly consumed by zooplankton or it can be converted to dissolved organic carbon (DOC) through microbial degradation (Fig. 1.2). Additionally, phytoplankton may directly exude excess organic matter when photosynthetic carbon fixation exceeds the production of biomass (Fogg 1983). Exudation of organic carbon (EOC) in freshwater systems increases with rates of primary production, albeit at a slower rate (Baines and Pace 1991). Furthermore, DOC in lakes can be produced by cell senescence, sloppy feeding by zooplankton, viral lysis and degradation of particulate organic carbon (POC). Through these pathways, all producers and consumers within a lake contribute to the pool of DOC, adding to allochthonous sources (allo-C, Fig. 1.2) derived from sediments and surrounding streams and soils. As a result, the composition (and hence degradability) and concentrations of DOC can be highly variable among freshwater systems (e.g. Lapierre and Del Giorgio 2014, Lapierre et al. 2015, Meili 1992, Waiser and Robarts 2000). In turn, differences in the DOC concentrations have been found to affect carbon fluxes in the microbial food web by e.g. limiting photosynthesis (as a result of decreased light availability) and stimulating bacterial metabolism (Del Giorgio and Peters 1994, Hessen 1992, Seekell et al. 2015, Sundh and Bell 1992).

All organisms within the food web contribute to the pool of particulate organic carbon, consisting of both living (biomass) and dead (detritus) fractions. POC is usually produced in the top water layers but degradation generally occurs deeper in the water column, hence concentrations are highest at the surface, decreasing with depth.

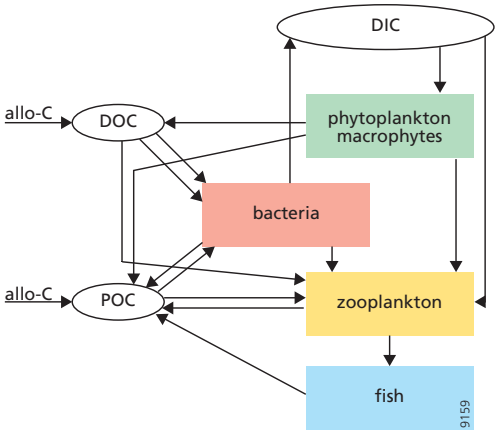

Fig. 1.2 Schematic of a classical lacustrine food web and its link to dissolved (DIC and DOC) and particulate (POC) carbon pools. Allochthonous contributions to DOC and POC pools are shown as allo-C.

1.3.2 Secondary production and respiration by bacteria

Bacteria play an important role in the food web as they remineralize organic compounds and contribute significantly to total secondary production (Fig. 1.2) (Cole et al. 1988 and references therein). Production by heterotrophic bacteria is strongly coupled to phytoplankton production, with bacterial production ranging between 20 to 30% of phytoplankton production (Cole et al. 1988). Most of the total bacterial carbon requirement derives from phytoplankton, with

calculated dependencies ranging from 70% (Lyche et al. 1996) to 91% (De Kluijver et al. 2010) to ~100% (Pace et al. 2007). Furthermore it was estimated that bacteria derive between 13 and 32% of their carbon requirement from EOC, depending on bacterial growth efficiencies (Baines and Pace 1991). Bacterial metabolism not only contributes significantly to total secondary production but also to respiration in lakes (Pace and Prairie 2005). In freshwater systems, respiration is often stimulated by allochthonous carbon sources, resulting in respiration rates that are higher than rates of primary production. Hence many aquatic systems are net heterotrophic and sources of CO_2 to the atmosphere (Del Giorgio and Peters 1994). Relative rates of production and respiration vary with water depth, thereby also affecting depth-profiles of e.g. oxygen and DIC concentrations. Primary production (oxygen production and DIC consumption) mainly occurs at the top of the water column, while remineralisation (consuming oxygen and producing DIC) also occurs in darker, deeper water layers. Depth-dependence of the composition and processing of carbon by microbial communities is investigated in chapters 2 and 3 of this thesis.

1.3.3 Zooplankton and fish

Zooplankton can either directly consume phytoplankton biomass or via the DOC-bacteria pathway (Fig. 1.2). These two sources are of approximately equal importance to zooplankton production, although both pathways seem to be relatively inefficient (Havens et al. 2000, Koshikawa et al. 1996). The size of the zooplankton population is controlled by planktivorous fish higher in the food web. Conversely, by providing shelter against predation, macrophytes reduce top-down control on zooplankton.

1.4 Effects of nutrients levels and eutrophication on microbial food webs

Especially in the microbial domain of the food web, production and consumption not only depend on the availability of carbon substrates but concentrations of nutrients, nitrogen (N) and phosphorous (P), also play an important role. Many studies have shown that the relative sizes of the compartments and the fluxes described above and in figure 1.2 change along a trophic gradient, as reviewed by Cotner and Biddanda (2002). In short, under low-nutrient conditions primary production is limited, but respiration is not as it can be stimulated by input of allochthonous organic carbon. Hence, in oligotrophic lakes, production rates are generally lower than respiration rates, making these lakes sources of CO_2 to the atmosphere (see above) (Del Giorgio and Peters 1994, Del Giorgio et al. 1997). Since most available nutrients and organic carbon in oligotrophic lakes are in the DOC-pool, bacteria have an advantage and play an important role (Cotner and Biddanda 2002 and references therein). When nutrient availability increases, phytoplankton production increases as well but the percentage of extracellular release decreases (Baines and Pace 1991). Because concentrations of particulate carbon substrates increase, particle feeders such as zooplankton, protozoans and fish become more important and hence the relative importance of bacteria decreases (Cotner and Biddanda 2002). Still, in absolute numbers, the role of the microbial food web becomes more important when nutrient availability increases because cyanobacteria become more important and the zooplankton community shifts to smaller crustaceans and rotifers (Fulton and Paerl 1988). Finally, in nutrient-rich (eutrophic) lakes with high rates of primary production, export of organic matter to the lake sediments may cause disequilibrium between $CO_{2(aq)}$ and the atmosphere, and lakes may become sinks of CO_2 instead of sources (Pacheco et al. 2013).

In addition to natural causes, eutrophication of lakes can also be caused by excessive nutrient loading resulting from anthropogenic activities, e.g. inflow of sewage water, agricultural runoff and atmospheric deposition. Anthropogenic eutrophication is one of the most severe environmental problems on a global scale, degrading ecosystems when phytoplankton production becomes dominated by algal blooms. This results in increased turbidity and reduced light penetration, killing macrophytes and the organisms that use macrophyte beds as habitats (zooplankton and fish). Finally, degradation of the large amounts of biomass produced during blooms reduces oxygen levels, also killing fish. Especially cyanobacteria are known to form blooms, as reviewed by Paerl et al. (2001), sometimes forming layers of scum on the water surface and producing substances that are toxic to humans and animals.

In order to counteract eutrophication, reduce phytoplankton (cyanobacterial) biomass and re-establish clear-water states, measures to reduce nutrient loading are crucial but often not enough. Hence they are often combined with biomanipulation measures aimed at increasing the grazing pressure on phytoplankton. Examples are re-planting of macrophytes, removal of planktivorous (zooplankton-eating) fish and stocking of piscivorous (fish-eating) fish. This way, phytoplankton production is not only limited from the bottom up (removal of nutrient sources), but also from the top down. The presence of macrophytes limits the size of the phytoplankton population by competing with phytoplankton for DIC and nutrients. Moreover, macrophyte abundance can increase zooplankton:phytoplankton ratios since they provide shelter for zooplankton, thereby increasing grazing pressure on phytoplankton. So far, restoration measures have had varying success and many questions remain regarding long-term effects. Generally, fish communities tend to recover to their pre-restoration states but macrophytes may permanently re-establish when grazing is not too severe and a source of seeds is available (Moore et al. 2010). There is also limited knowledge on the effects of biomanipulation measures in warm (sub)tropical freshwater systems where biological feedbacks and food-web interactions differ from those in temperate lakes (see Jeppesen et al. (2012) for a review). For example, shelter for zooplankton in macrophyte beds is lower in tropical lakes because fish tend to gather there (Iglesias et al. 2007, Meerhoff et al. 2006).

In this thesis, lakes of differing trophic states are studied, ranging from oligotrophic (chapter 3), to eutrophic (chapter 2) and hypereutrophic, dominated by cyanobacterial blooms (chapter 4). Additionally, in chapter 4 we compare carbon processing in a hypereutrophic, subtropical lake (Taihu, China) to a restored section of the same lake (Fig. 1.3).

Fig. 1.3 A similar project as in Lake Taihu was carried out in Huizhou West Lake (China). On the left side of the walkway lies the unrestored, eutrophic part of Huizhou West Lake.On the right side, restoration measures have turned a part of the basin into a clear-water system. Picture was taken by Angela Scharfbillig.

1.5 Effects of seasonality on carbon processing in lacustrine food webs

In addition to nutrient levels and input of allochthonous organic matter, phytoplankton production and thereby the entire (microbial) food web is also influenced by abiotic parameters such as light availability and temperature. All these parameters vary throughout the year, thereby affecting phytoplankton communities and production. For example, the severity of nutrient limitation in general, and also which nutrient limits production have been found to potentially switch between spring and fall (Kolzau et al. 2014, Morris and Lewis 1988). In Addition, by affecting metabolic rates, seasonal variation in temperature has long been recognized to influence primary production and respiration (e.g. Davison 1991), but it is also a controlling factor on carbonate chemistry (pH, pCO_2) (Zeebe and Wolf-Gladrow 2001) and hence inorganic carbon availability. The availability of light, as a prerequisite for photosynthesis, also affects primary production, hindering photosynthesis when photosynthetically active radiation (PAR) is either too low (low-light limitation, Smith 1938) or too high (photo-inhibition, Kok 1956). Production and respiration may respond differently and at different rates to seasonal changes such as described above, e.g. under increasing temperatures, respiration rates may increase at a faster rate than production (Hancke and Glud 2004). Hence the potential for burial of organic matter in a freshwater system depends strongly on seasonal changes in environmental parameters (Canuel and Martens 1993).

Due to their quick turnover, phytoplankton and bacteria rapidly respond to changes in environmental parameters resulting in seasonal algal blooms, in turn leading to seasonal stratification and possible oxygen depletion. Seasonal variation in microbial communities is also reflected in biomarker assemblages [Sushchik et al., 2010; Blaga et al., 2011; Huguet et al., 2011; Loomis et al., 2014] and phytoplankton isotopic compositions [Finlay, 2004; Van Breugel et al., 2006; Bontes et al., 2006; De Kluijver et al., 2015]. In this thesis, seasonal differences in phytoplankton and bacterial carbon sources and isotopes are studied in Dutch Lake Naarden (chapter 5).

1.6 Reconstructing microbial carbon processing using phospholipid-derived fatty acid biomarkers

Biomarkers are organic molecules, mostly lipids, which can be attributed to specific organisms and/or processes. In food-web studies, biomarkers such as phospholipid-derived fatty acids (PLFAs) are used to ascertain the occurrence and calculate the abundance of specific groups of organisms. Phospholipids are components of cell membranes consisting of a hydrophilic phosphate head group attached (via a glycerol molecule) to two hydrophobic fatty acid "tails" (Fig. 1.4). Saponification releases the fatty acid tails, which have variable chain lengths and highly diverse structures with e.g. straight chains and (iso- or anteiso) methyl branches, or cyclic moieties. The fatty acids tails can be saturated or unsaturated with varying amounts of double bonds at different positions of the carbon chain. This structural variability in PLFA molecules is expressed in their informal biogeochemical nomenclature as C*a*:*b*ω*c*, where *a* is the chain length, *b* is the number of double bonds and *c* is the position of the (first) double bound counted from the end (ω) of the fatty acid chain. PLFAs are especially useful in food-web studies as they they are hydrolyzed quickly after cell death (White et al. 1979) and thus mainly represent freshly produced biomass. The combination of PLFAs with stable isotope labelling experiments provide

a powerful tool to compare the food web community and trace carbon and nitrogen flows through the microbial food web.

PLFAs occur in a wide range of organisms and hence do not represent unique organisms. Nonetheless, they can be used to differentiate between groups of producers. Branched PLFAs (e.g. i/aC15:0) are predominantly produced by gram-positive bacteria (Kaneda 1991) but have also been detected in some gram-negative bacteria (Haack et al. 1994). Poly-unsaturated PLFAs such as C18:3ω3 (α-linolenic acid), C18:4ω3 (stearidonic acid) and C20:5ω3 (eicosapentaenoic acid) (Brett and Müller-Navarra 1997, Dijkman and Kromkamp 2006, Taipale et al. 2013) are produced by eukaryotic phytoplankton (green/red algae, diatoms, haptophytes etc.). Hence, by combining PLFA occurrence with isotope labelling it is possible to differentiate between primary producers (autotrophs), secondary producers (heterotrophic bacteria) and detritus (dead organic matter) and to quantify group-specific production.

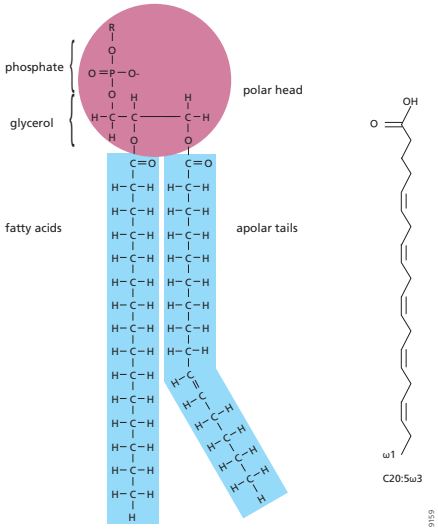

Fig. 1.4 Molecular diagram of a phospholid (left) and schematic structure of phospholipid-derived fatty acid C20:5ω3.

1.7 Scope and outline of this thesis

This thesis aims at increasing our understanding of carbon processing by microbial communities in lakes and the influence of trophic states (or nutrient levels), biomanipulation measures and seasonality. To this end, field studies were carried out to examine carbon processing and food-web functioning. Stable carbon ($\delta^{13}C$) and nitrogen ($\delta^{15}N$) isotopes at either natural abundance or after tracer addition were analysed for total carbon and nitrogen pools and carbon isotopes were analysed for specific membrane lipids (PLFAs).

Chapter 2 of this thesis describes the results of in situ ^{13}C-labelling experiments carried out at six different depth intervals in eutrophic Lake Rotsee, Switzerland. Twelve bottles were filled with water collected from six different depths. Six transparent bottles were labelled with ^{13}C-bicarbonate to trace total and group-specific primary production, and the transfer of this newly fixed carbon to secondary producers. Six dark bottles were labelled using ^{13}C-glucose as a deliberate tracer to quantify bacterial production in terms of assimilation and respiration. This

study shows depth-dependence of primary production and the microbial community, with 1) different PLFAs produced at different depths corresponding to different metabolic processes, 2) variability with depth of release of extracellular carbon by phytoplankton and 3) depth-dependence of consumption of recently fixed carbon by bacteria. The results suggest that Rotsee was net autotrophic during the experiments.

Chapter 3 discusses the results of two ^{13}C-tracer experiments in oligotrophic Lake Lucerne. First, a similar experiment as described in Chapter 2, using light and dark bottles, showed that productivity rates were substantially lower compared to nearby Lake Rotsee and that the greater depth of the photic zone could not compensate for differences in volumetric production rates. Bacteria in Lake Lucerne were well adapted to rapidly respond to periods of increased productivity as studied here (June) and fully consumed the newly produced organic matter. Chapter 3 also describes a mesocosm labelling experiment using ^{13}C-bicarbonate as a tracer, which was carried out earlier in the year during spring. This second experiment shows a much weaker coupling between phytoplankton and bacterial production indicating that potentially more organic matter can escape recycling at this time and can be transported to the lake floor.

In **Chapter 4**, the effects of restoration measures on carbon flows in a macrophyte-dominated (Wuli Lake) and phytoplankton-dominated (Meiliang Bay) section of a shallow Chinese lake were studied. Mesocosm labelling experiments using ^{13}C and ^{15}N as tracers were carried out in both lakes. Isotope analyses on microbial lipids, zooplankton, epiphytes and macrophytes were combined with a simple isotope model. As a result of restoration measures, carbon flows shifted from phytoplankton(cyanobacteria)-dominated in Meiliang Bay to macrophyte-dominated in Wuli Lake and primary production in the restored lake was 2-7 times higher compared to the unrestored lake. Severe CO_2 limitation in Wuli Lake apparently forced phytoplankton to derive significant amounts of carbon from DOC, while macrophytes only assimilated DIC-derived carbon. Nitrogen isotopes data were not well constrained but confirmed the carbon isotope results.

In **chapter 5**, seasonal variability in phytoplankton and bacterial stable carbon isotopes, and changes in bacterial carbon sources were studied in a shallow Dutch peat lake. During 17 months, samples were collected from two basins of Lake Naarden, with one basin in a restored state and the other somewhat eutrophic. Natural abundance stable carbon isotopes were analysed on carbon pools, macrophytes and microbial membrane lipids (PLFAs). Isotope fractionation between phytoplankton biomass and $CO_{2(aq)}$ was lowest during summer (11.6‰), when productivity is high. At both sites, correlations between phytoplankton and bacterial carbon isotopes were strong, with bacterial dependence on locally produced organic carbon highest during summer and lowest during winter. During winter months, bacterial dependence on DOC was higher at the restored site (39-77%) compared to the eutrophic site (17-46%).

In summary, the studies in this thesis demonstrate the strong variability in microbial carbon processing in different freshwater systems. Nutrient levels are of clear importance to microbial metabolic activities and hence in-lake carbon processing, and much variability was found in terms of absolute and relative amounts of production and consumption of organic matter. Remarkably however, in the restored, macrophyte-dominated part of Lake Taihu we found total ecosystem productivity to be much higher compared to the still eutrophic lake, despite lower nutrient levels. Carbon cycling pathways had shifted from phytoplankton-dominated to macrophyte-dominated, confirming the greater importance of the microbial food web in eutrophic systems. In addition to variation among lakes, also large variability with depth was found in the relative importance of production and consumption and the microbial communities

and metabolic processes dominating at each depth, showing that multiple sampling depths are of crucial importance, especially in vertically stratified lakes such as Rotsee. Coupling between phytoplankton and bacterial production seems related to trophic state with stronger coupling in oligotrophic Lake Lucerne compared to eutrophic Lake Rotsee. Additionally, phytoplankton-bacteria coupling was found to vary with water depth (chapters 2 and 3) and throughout the year (chapters 3 and 5). The potential for burial of organic matter in lake sediments is thus highly variable and mass flux calculations should be based on multiple sampling depths and campaigns.

Chapter 2

Carbon flows in eutrophic Lake Rotsee: a ^{13}C-labelling experiment

Can anybody out there see me?
– Losing My Way, Justin Timberlake -

Abstract

The microbial segment of food webs plays a crucial role in lacustrine food-web functioning and carbon transfer, thereby influencing carbon storage and CO_2 emission and uptake in freshwater environments. Variability in microbial carbon processing (autotrophic and heterotrophic production and respiration based on glucose) with depth was investigated in eutrophic, methane-rich Lake Rotsee, Switzerland. In June 2011, ^{13}C-labelling experiments were carried out at six depth intervals in the water column under ambient light as well as dark conditions, to evaluate the relative importance of (chemo)autotrophic, mixotrophic and heterotrophic production. Label incorporation rates of phospholipid-derived fatty acid (PLFA) biomarkers allowed us to differentiate between microbial producers and calculate group-specific production. We conclude that at 6 m, net primary production (NPP) rates were highest, dominated by algal photoautotrophic production. At 10 m – the base of the oxycline- a distinct low-light community was able to fix inorganic carbon, while in the hypolimnion, heterotrophic production prevailed. At 2 m depth, high label incorporation into POC could only be traced to nonspecific PLFA, which prevented definite identification, but suggests cyanobacteria as dominating organisms. There was also depth zonation in extracellular carbon release and heterotrophic bacterial growth on recently fixed carbon. Large differences were observed between concentrations and label incorporation of POC and biomarkers, with large pools of inactive biomass settling in the hypolimnion, suggesting late-/post-bloom conditions. Net primary production (115 mmol C m^{-2} d^{-1}) reached highest values in the epilimnion and was higher than glucose-based production (3.3 mmol C m^{-2} d^{-1}, highest rates in the hypolimnion) and respiration (5.9 mmol C m^{-2} d^{-1}, highest rates in the epilimnion). Hence, eutrophic Lake Rotsee was net autotrophic during our experiments, potentially storing large amounts of carbon.

2.1 Introduction

Within the global carbon cycle the cycling of organic matter in freshwater systems has only recently been recognized as a significant component, potentially with global impacts (Battin et al. 2008, Battin et al. 2009, Cole et al. 2007, Raymond et al. 2013, Richey et al. 2002). Carbon loading to freshwater systems ranges between 1.9 and 2.9 Pg C y^{-1} (Battin et al. 2009, Cole et al. 2007, Tranvik et al. 2009), most of which is processed and/or stored within the system itself. Due to higher biological production and faster sedimentation rates compared to the oceans, lakes have a large storage capacity and bury as much as 30-60% organic carbon per year compared to oceanic carbon storage, despite their limited surface area relative to the ocean (Cole et al. 2007). Still, lakes are generally net sources of CO_2 to the atmosphere, with CO_2 evasion rates estimated to range between 0.75 and 2.1 Pg C y^{-1} (Battin et al. 2009, Cole et al. 2007, Tranvik et al. 2009).

Within lakes, carbon cycling is determined by in situ primary and secondary production, depending on nutrient availability and light, and also by inputs of terrestrial organic carbon and methane (either locally produced or derived via groundwater from surrounding soils). The availability of these different carbon sources has a major impact on food-web functioning and structure by affecting the relative amounts of primary and secondary production (Cole et al. 2006, Pace et al. 2004). The microbial segment of food webs (phytoplankton and bacteria) therefore plays a crucial role in food-web functioning and transfer of organic matter through ecosystems to higher trophic levels (e.g. zooplankton, fish).

The microbial food web in particular is affected by present-day environmental changes in nutrient supply, oxygenation, temperature, light and atmospheric CO_2 levels (De Kluijver et al. 2013, Middelburg 2014, Travers et al. 2007) and must therefore be included in ecosystem studies. Most of these parameters vary with depth in freshwater ecosystems, allowing different microbial communities to occur simultaneously at different depths of the water column (Bossard et al. 2000, Galand et al. 2002, Humayoun et al. 2003, Koizumi et al. 2004, Øvreås et al. 1997). Hence, especially in stratified lakes, undersampling can easily lead to under- or overestimations of production and remineralization within different parts of the food web.

Different approaches have been used in the past, to investigate carbon processing in lakes, sometimes applying stable isotope ratios at natural abundances or after deliberate tracer additions (Brett et al. 2009, Cole et al. 2011, Pace et al. 2007). Under natural conditions, isotopic differences between substrates and consumers are typically small, and hence the isotopic signatures of producers often partially overlap. Adding ^{13}C-label to enrich certain substrates enables quantification of carbon assimilation and the transfer of recently fixed carbon through the food web. Over the last years, the emergence of compound-specific stable isotope analyses (CSIA) has enabled including part of the microbial food web in ecological studies (Boschker et al. 1998, Middelburg et al. 2000, Van den Meersche et al. 2004). Specifically, biomarker molecules (mostly lipids) linked to specific (groups of) organisms are well suited for CSIA and have expanded our knowledge on microbial food-web functioning over a wide range of settings. In this study, phospholipid-derived fatty acids (PLFAs) were used to differentiate between and zoom in on different primary producers (autotroph, mixotroph and chemoautotroph), secondary producers (heterotrophic bacteria) and detritus (dead organic matter) and to quantify group-specific production. PLFAs are produced by a wide variety of organisms, representing a wide range in trophic behavior. Although specific PLFAs do not uniquely represent one source organism, they can be very informative in labeling studies since DIC-derived enrichment directly or indirectly derives from autotrophic production, while DOC-derived enrichment of PLFAs results from heterotrophic production (Boschker et al. 1998, De Kluijver et al. 2013, Dijkman et al. 2009, Van den Meersche et al. 2004).

Here we contribute to further unravelling fluxes between lacustrine carbon pools and microbial groups using in situ ^{13}C-labelling under both dark and light conditions at six different depth intervals in a shallow methane-rich, eutrophic lake (Rotsee, Switzerland). The incubations under ambient light conditions were labelled with ^{13}C-bicarbonate to quantify total as well as group-specific primary production and to trace the transfer of newly fixed carbon to bacteria. Dark incubations were labelled with ^{13}C-glucose, which is used as a substrate by the majority of heterotrophic producers and is therefore well suited to quantify heterotrophic bacterial turnover in terms of assimilation and respiration. Combining light and dark incubations thus allows for a more complete reconstruction of microbial carbon transfer. PLFA concentrations were compared to production rates and the relative importance of phytoplankton production and bacterial production and respiration was evaluated at different water depths, each with their own set of environmental conditions such as light penetration, nutrient availability and microbial community. This allowed for elucidating the most relevant processes at the different water depths, quantifying carbons flows through the microbial food web.

2.2 Material and Methods

2.2.1 Study site

The experiment was carried out in Lake Rotsee, a prealpine Swiss lake. Rotsee (Fig. 2.1) is small (2.4 km long and 0.4 km wide), eutrophic and has a mean depth of 9 m and a maximum depth of 16 m. It has a drainage area of 4.6 km^2 and is fed by the Reuss-Rotsee canal, which draws from Reuss River. The lake is shielded from wind, allowing for the formation of a stable stratification from approximately May to November. Rotsee is monomictic and when stratified the oxycline is located between about 8 and 11 m, with an anoxic hypolimnion (Schubert et al. 2010). The lake is quite dark, with only 0.28% of light radiation reaching the oxycline, and 0.01% reaching 11 m depth (Oswald et al. 2015).

Rotsee has an intense methane cycle (Schubert et al., 2010); in the top few cm of sediment the methanogen acetoclastic *Methanosaeta* spp. is the main provider (>90%) of methane to the water column (Zepp Falz et al. 1999). It was found that during summer stratification, methane oxidation rates were highest within the oxycline with aerobic gammaproteobacterial methanotrophs (type I) being the main methane oxidizers, although alpha-methane oxidizing bacteria were also detected one year (Oswald et al. 2015). Aerobic oxidation of methane was found to be fuelled by light-dependent oxygenic photosynthesis (Oswald et al. 2015). Regardless, the epilimnion is still oversaturated in methane and thus serves as a source of methane to the atmosphere (Schubert et al. 2010).

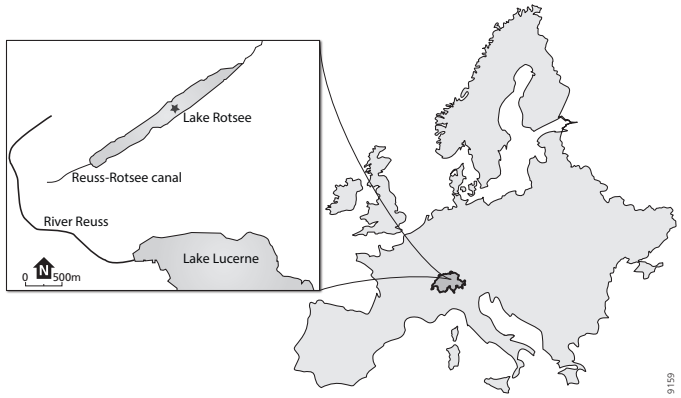

Fig 2.1 Map showing the location of Lake Rotsee in Switzerland and its in- and outflowing rivers. Rotsee is connected to the river Reuss via the Reuss-Rotsee canal. The location of the experiment is indicated by a star.

2.2.2 Incubation experiments and sample collection

In situ ^{13}C-labelling experiments were carried out from June 10 to June 14, 2011. During the experiment, twelve pre-cleaned 25 liter-bottles (transparent bottles: polycarbonate; dark bottles: Low Density Polyethylene) were filled with water, which was retrieved from 6 different depths using Niskin bottles. At the site of the experiment, prior to collecting water, a CTD probe (Seabird SBE19) was deployed to measure in situ oxygen, temperature, conductivity and pH. The water was transferred from Niskin to incubation bottle on the ship using a tube, as quickly as possible, but some exchange with the atmosphere cannot be ruled out. Additionally, due to the

shape of the caps, a small headspace remained in the incubation bottles. Clear bottles intended for light incubations were labelled with ^{13}C-Na-bicarbonate (8.4 mg >98 atom% ^{13}C) and bottles for dark incubations were covered in waterproof aluminium-tape and labelled with ^{13}C-glucose (2.3 mg >99 atom% ^{13}C), increasing DIC and DOC concentrations by about 0.16% and 1.0% respectively. Bottles were redeployed attached to a cable running from an anchor at the lake floor to a buoy, in such a way that each bottle was positioned at the original depth the incubated water was recovered from. The entire setup remained in situ for the four-day experiment. Before (T0) and after the experiment (T4), samples were collected from each bottle for oxygen, dissolved inorganic carbon (DIC), dissolved organic carbon (DOC), and particulate organic matter (POM) analyses.

Samples for dissolved oxygen analyses were fixed on site and measured by Winkler titration in the laboratory to ascertain the calibration of the CTD probe. Samples for DIC concentration and ^{13}C content were collected air-free in 20 mL headspace vials and sealed using airtight caps followed by mercury chloride poisoning. Samples were stored dark and upside down. Samples for DOC concentration and ^{13}C content were filtered through 0.45 µm GM/F filters and stored frozen (-20 ˚C) until further analysis. All remaining water was filtered through pre-weighed and pre-combusted GF/F filters (0.7 µm) for POM and the filter stored frozen (-20 ˚C) until extraction and further analysis.

2.2.3 Laboratory analyses

DIC concentrations were measured using a Total Organic Carbon (TOC) analyzer (Shimadzu TOC-5050 A), using an in-house seawater standard. A seawater standard is stable and can therefore also be used to check measurements of lacustrine DIC samples. For δ^{13}C analyses of natural abundance and labelled DIC, a helium headspace was created and samples were acidified with a H_3PO_4 solution. Stable isotopes of the DIC were analyzed using a gas bench coupled on line to an IRMS (Thermo Delta V advantage) and were calibrated to the Vienna PeeDee Belemnite (V-PDB) scale using international (Li_2CO_3) and in-house (Na_2CO_3) standards. For analyses of DOC concentration and δ^{13}C of the DOC, samples were treated and measured following (Boschker et al. 2008) using high-performance liquid chromatography-isotope ratio mass spectrometry (HPLC-IRMS, Thermo Surveyor system). From the filters, the particulate organic carbon (POC) concentrations were measured using an elemental analyzer (EA) (Fisons Instruments NA1500) and the isotopic composition was analyzed on an EA-IRMS (Thermo Deltaplus). Carbon stable isotope ratios are expressed in the delta notation (δ^{13}C) with respect to the V-PDB standard. Precision is <0.35‰ based on international (Graphite quartzite standard NAXOS) and in-house (Nicotinamide) standards. No systematic changes were observed in the concentrations of DIC, DOC and DIC between T0 and T4. Therefore, concentrations are reported as averages of T0 and T4, of both transparent and dark incubations.

POM samples were freeze dried and lipids were extracted using a modified Bligh and Dyer method (Dickson et al. 2009). Total lipid extracts (TLE) were fractionated into simple lipids (SL), glycolipids (GL) and phospholipids (PL) on activated silicic acid columns using chloroform/acetic acid (100:1 v/v), acetone and methanol respectively as eluents (Dickson et al. 2009). Phospholipid fractions, containing phospholipid-derived fatty acids (PLFAs), were converted to fatty acid methyl esters (PL-FAME) by mild alkaline transmethylation (White et al. 1979). C12:0 and C19:0 FAME were added as internal standards. Concentrations and compound-specific δ^{13}C of PL-FAME were determined using gas chromatography-combustion-isotope ratio mass spectrometry (GC-C-IRMS) using a column and oven program

as described in (Middelburg et al. 2000). Similar as for total carbon pools, no systematic changes were observed in PLFA concentrations between T0 and T4, hence concentrations are reported as averages of T0 and T4, of both light and dark incubations. Identification was based on comparing retention times using equivalent chain lengths. Carbon isotopic values were corrected for the one added carbon during methylation using the carbon isotopic value of the derivatizing agent, which was determined offline.

2.2.4 Data analysis

Production rates (in mol L^{-1} d^{-1}) for carbon pools and PLFAs were calculated following de Kluijver et al. (2013) and Middelburg (2014) as

$$Production\ rate = \frac{\Delta^{13}F_{produced}}{\Delta^{13}F_{DIC}} \times \frac{C_{produced}}{t} \quad (1)$$

Where $C_{produced}$ is the concentration of the C species or PLFA that is produced in mol L^{-1}; t is the duration of the experiment and

$$\Delta^{13}F = {}^{13}F_{sample} - {}^{13}F_{background} \quad (2)$$

With $^{13}F_{background}$ representing natural abundance ratios as measured at T0, before the label was added and where ^{13}F is the fraction ^{13}C, which is calculated as

$$\frac{{}^{13}C}{{}^{12}C + {}^{13}C} = \frac{R}{R+1} \quad (3)$$

Isotope ratios *R* were derived from $\delta^{13}C$ values using

$$R = [(\delta^{13}C/1000) + 1] \times R_{VPDB} \quad (4)$$

With R_{VPDB} = 0.0111796 (Coplen 2011). Only $\Delta\delta^{13}C$ values >1.5‰ were considered for calculations, with

$$\Delta\delta^{13}C = \delta^{13}C_{sample} - \delta^{13}C_{background} \quad (5)$$

Only bicarbonate-labelled incubations were corrected for $\Delta^{13}F_{DIC}$. For glucose-labelled incubations, the assumption was made that DOC was 100% labelled (see discussion).

PLFAs are produced by a wide variety of microbes. Branched PLFAs iC14:0, iC15:0 and aC15:0 all mainly derive from gram-positive bacteria (Kaneda 1991), although also occurring in some gram-negative bacteria (Zelles 1999). Here they are interpreted to represent bacteria in general. In Lake Rotsee, common phytoplankton PLFAs are C18:3ω3 (α-linolenic acid, or ALA), C18:4ω3 (stearidonic acid, or SDA) and C20:5ω3 (eicosapentaenoic acid, or EPA). These PLFAs are common in different phytoplankton phyla, e.g. Chlorophyta, Chrysophyta, Cryptophyta, Heterokontophyta and Haptophyta (Dijkman and Kromkamp 2006, Taipale et al. 2013). PLFA C16:1ω7c is a common lipid in many organisms, including heterotrophic bacteria (Kaneda 1991), sulfur-oxidizing bacteria (Van Gaever et al. 2009, Zhang et al. 2005), nitrifying bacteria (De Bie et al. 2002, Guezennec and Fialamedioni 1996, Lipski et al. 2001) and a range of phytoplankton species (Dijkman and Kromkamp 2006). C16:1ω7c has also been found in methane-oxidizing bacteria (Bodelier et al. 2009, Guckert et al. 1991).

Net primary production (NPP) was calculated using production rates of POC and DOC under light conditions. The percentage of extracellular release (PER) was calculated as the production of DOC divided by the total production (POC+DOC) under light conditions.

Total label incorporation into POC in dark incubations was used to calculate glucose-based, heterotrophic production. Glucose-based respiration was calculated using total label transfer to the DIC pool in dark incubations. Steady-state was assumed for the calculation of these rates. Glucose-based bacterial growth efficiency (BGE) was calculated by dividing the concentration of labelled POC by the concentrations of labelled POC + DIC in dark incubations labelled with ^{13}C-glucose. The isotopic composition of the respired carbon was determined as the y-intercept of a linear trend line in a Keeling plot of 1/[DIC] vs. natural abundance (T0) $\delta^{13}C_{DIC}$ for each depth.

2.3 Results

2.3.1 Oxygen and (in)organic carbon pools

Dissolved oxygen concentrations in Lake Rotsee are shown in figure 2.2a and clearly show the location of the oxycline between 7 and 10 m water depth, which corresponds well to earlier observations (Schubert et al. 2010). Oxygen concentrations in the epilimnion were ~400 µmol L^{-1}, while oxygen concentrations in the hypolimnion were below 10 µmol L^{-1}, with values close to zero at 15 m depth, near the lake floor.

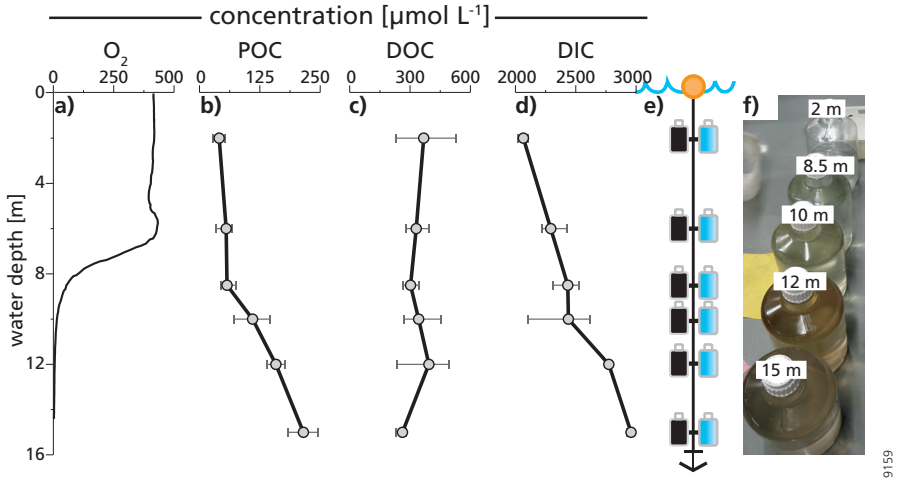

Fig. 2.2 Concentrations in µmol L^{-1} of a) oxygen, b) POC, c) DOC and d) DIC. Concentrations of POC, DOC and DIC are averages of T0 and both light and dark incubations; e) the experimental set-up showing two bottles at each sampling depth: one dark bottle in which glucose was labelled and one transparent bottle in which bicarbonate was labelled (bottle size is not to scale); f) Light incubation bottles derived from 2, 8.5, 10, 12 and 15 m water depth, showing an increase in suspended matter concentration with depth. The bottle from 6 meter water depth was being processed at the time this picture was taken.

Average POC concentrations (Fig. 2.2b) were relatively stable throughout the epilimnion, with values ranging from 41 to 57 µmol L^{-1}. From 8.5 m down to the maximum depth of 15 m, POC

concentrations rose to 215 µmol L^{-1}. Average DOC concentrations (Fig. 2.2c) decreased with depth in the epilimnion from 370 to 300 µmol L^{-1}, then increased to 390 µmol L^{-1} between 8.5 and 12 m and were lowest at 15 m (260 µmol L^{-1}). It should be noted that as a result of the 0.45 µm pore size of the filters used for DOC sampling (section 2.2.2), bicarbonate-based fixation by small, free-living microbes might also contribute to the DOC results. However, given the high DOC concentrations and production rates (see below), it seems unlikely that these small microbes had a large effect on calculated fluxes. Average DIC concentrations (Fig. 2.2d) increased with depth from 2.1 mmol L^{-1} at 2 m to 3.0 mmol L^{-1} at 15 m.

All PLFA concentrations showed the same overall trend, with low concentrations in the epilimnion, a strong increase in the chemocline and highest values reached in the hypolimnion at either 12 or 15 m water depth. This pattern closely mimics the changes observed in POC concentrations. PLFAs iC14:0, iC15:0 and aC15:0 (Fig. 2.3a-c) all showed peak concentrations at 15 m, with iC14:0 reaching 0.015 µmol C L^{-1}, and both iC15:0 and aC15:0 reaching highest values of 0.07 µmol C L^{-1}. PLFA C16:ω7c (Fig. 2.3d) showed the same trend as the iso- and anteiso PLFAs: peaking at 15 m with a maximum concentration of 1.04 µmol C L^{-1}. PLFAs C18:3ω3, C18:4ω3 and C20:5ω3 (Fig. 2.3e-g) showed the same trend, peaking at 0.05, 0.02 and 0.02 µmol C L^{-1} respectively at 12 m and reaching values of 0.04, 0.01 and 0.01 µmol C L^{-1} at 15 m.

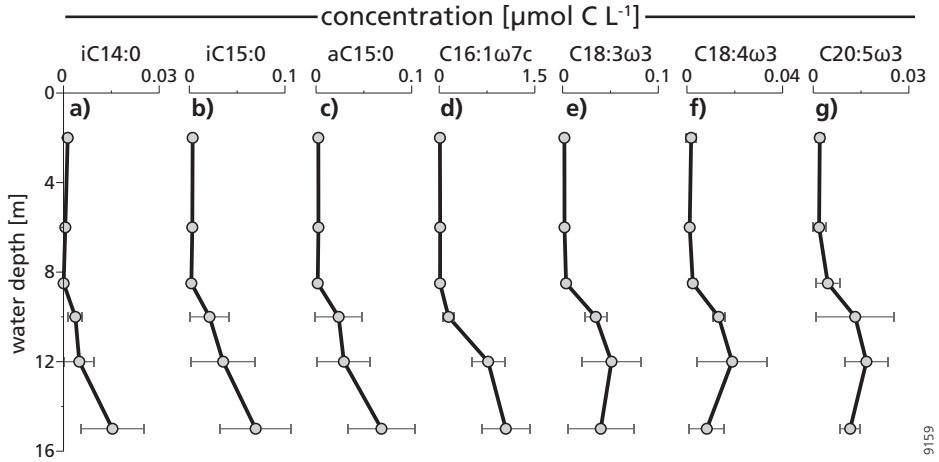

Fig. 2.3 PLFA biomarker concentrations in µmol C L^{-1} of a) iC14:0, b) iC15:0, c) aC15:0, d) C16:1ω7c, e) C18:3ω3, f) C18:4ω3, and g) C20:5ω3. Concentrations are averages of T0, light and dark incubations.

2.3.2 Tracer assimilation under light conditions

Because the same amount of ^{13}C-bicarbonate label was added at each depth whereas the DIC concentration varied, $\delta^{13}C$ enrichment of the DIC varied from 115 to 160‰ at the different depths, depending on initial DIC concentration (Fig. 2.2d) (Table S2.1). At T4, the $\delta^{13}C$ of DOC appreciably increased from 6 to 10 m by 13 to 24‰ (data not shown). Similarly, the $\delta^{13}C$ of POC increased appreciably between 2 and 10 m by 6 to 84‰ (data not shown). Production rates per day for DOC and POC showed that label incorporation into POC was strongest at 2

m (6.9 µmol C L^{-1} d^{-1}) and decreased with depth to zero at 12 m (Fig. 2.4a). Label transfer to DOC was zero at 2 m, increasing to 12.6 µmol C L^{-1} d^{-1} at 6 m, remaining high at 8.5 and 10 m (7.2 and 11.0 µmol C L^{-1} d^{-1} respectively) and decreasing again to zero at 12 and 15 m depth. During the experiments, a ^{13}C mass balance for inorganic and organic carbon pools was achieved within 15%, which is acceptable for our purposes.

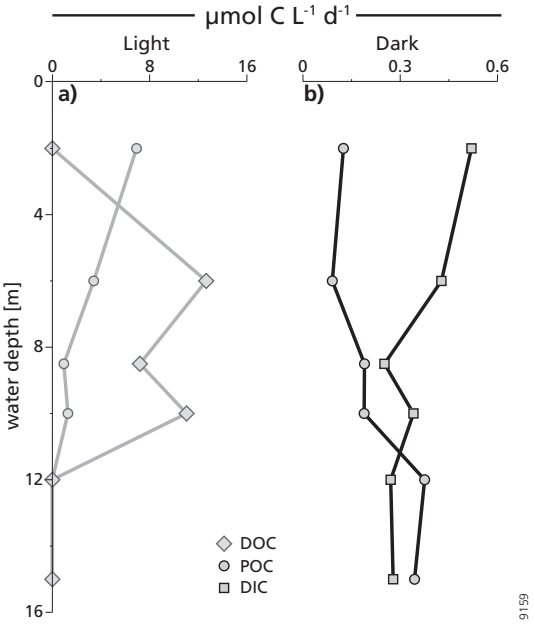

Fig. 2.4 Production rates with depth of POC, DOC and DIC in µmol C L^{-1} d^{-1} under a) light and b) dark conditions.

For PLFAs iC14:0, iC15:0 and aC15:0 (Fig. 2.5a-c, grey squares for light incubations), label incorporation was only observed in the upper 8.5 m. PLFA iC14:0 (Fig. 2.5a) had a maximum production rate, corresponding to 32 pmol C L^{-1} d^{-1} at 2 m, which decreased to zero at 8.5 m. Label incorporation into iC15:0 (Fig. 2.5b) corresponded to 35 pmol C L^{-1} d^{-1} at 2 m, increasing to 68 pmol C L^{-1} d^{-1} at 8.5 m. For PLFA aC15:0 (Fig. 2.5c) this was 32 pmol C L^{-1} d^{-1} at 2 m, decreasing to zero at 6 m and reaching a maximum value of 47 pmol C L^{-1} d^{-1} at 8.5 m. Production of PLFA C16:1ω7c (Fig. 2.5d) was highest of all PLFAs, with values of 208 pmol C L^{-1} d^{-1} at 2 m, increasing to 1326 pmol C L^{-1} d^{-1} at 6 m, then decreasing to 626 pmol C L^{-1} d^{-1} at 8.5 m with highest values observed at 10 m, corresponding to 4229 pmol C L^{-1} d^{-1}. PLFAs C18:3ω3 and C18:4ω3 (Fig. 2.5e, f) showed only minor label incorporation at 2 m (23 and 24 pmol C L^{-1} d^{-1}), but peaked at 6 m (388 and 197 pmol C L^{-1} d^{-1}) before decreasing again to 116 and 55 pmol C L^{-1} d^{-1} respectively at 8.5 m. C18:4ω3 had another peak in label incorporation at 10 m, corresponding to 206 pmol C L^{-1} d^{-1}. The trend in absolute label incorporation with depth for PLFA C20:5ω3 (Fig. 2.5g) was identical to that observed for C16:1ω7c: a small peak of 97 pmol C L^{-1} d^{-1} at 6 m and a maximum of 413 pmol C L^{-1} d^{-1} at 10 m depth. In the light incubations, labelling of all biomarkers was negligible at 12 and 15 m depth.

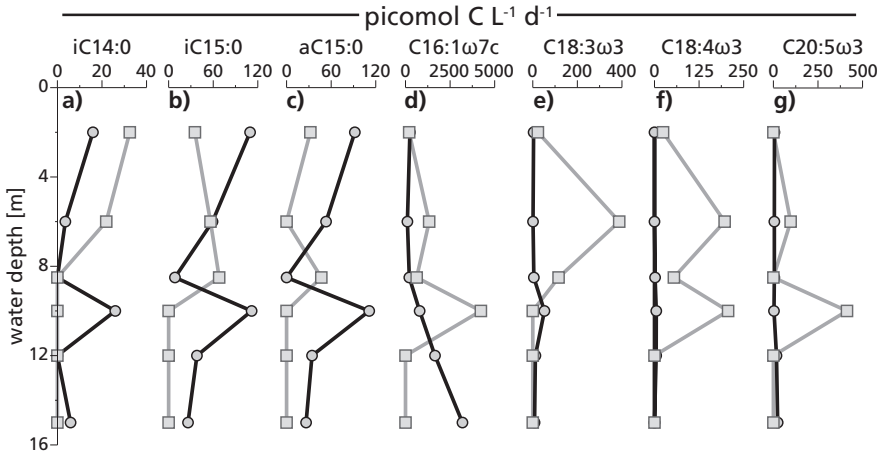

Fig. 2.5 Production rates of PLFA biomarkers in picomol C L^{-1} d^{-1} of a) iC14:0, b) iC15:0, c) aC15:0, d) C16:1ω7c, e) C18:3ω3, f) C18:4ω3 and g) C20:5ω3. Grey squares represent incubations under light conditions. Black circles represent dark incubations.

2.3.3 Tracer assimilation under dark conditions

Since the initial concentrations of DOC varied with depth and equal amounts of ^{13}C-glucose were added to the dark incubation bottles, the δ^{13}C increase of DOC varied from 512 to 1119‰ for the different bottles (Table S2.1). The absolute transfer of label from DOC to DIC (Fig. 2.4b), indicating respiration of added glucose, was highest at 2 and 6 m, with values corresponding to 0.52 and 0.43 µmol C L^{-1} d^{-1} respectively. In and below the chemocline, absolute label transfer to DIC was relatively constant at 0.25 to 0.28 µmol C L^{-1} d^{-1}, with the exception of a small peak at 10 m corresponding to 0.34 µmol C L^{-1} d^{-1}. Label transfer to POC reflects heterotrophic production in the epilimnion and was 0.12 and 0.09 µmol C L^{-1} d^{-1} at 2 and 6 m respectively, with values increasing to 0.19 µmol C L^{-1} d^{-1} in and just below the oxycline. Label incorporation values for POC were highest in the hypolimnion reaching 0.38 µmol C L^{-1} d^{-1} at 12 m and 0.34 µmol C L^{-1} d^{-1} at 15 m. Also in these incubations, mass balance for inorganic and organic carbon pools was achieved within 15%, which is again acceptable for our purposes.

Similar patterns were observed for PLFAs iC14:0, iC15:0 and aC15:0 (Fig. 2.5a-c with black circles representing dark incubations). Incorporation decreased with depth in the epilimnion from 16, 110 and 92 pmol C L^{-1} d^{-1} respectively at 2 m depth to zero at 8.5 m. All three showed a peak in incorporation at 10 m (26 pmol C L^{-1} d^{-1} for iC14:0; 112 pmol C L^{-1} d^{-1} for iC15:0 and aC15:0), decreasing to lower values deeper in the hypolimnion. In the dark incubations label incorporation was highest for PLFA C16:1ω7c (Fig. 2.5d), showing relatively low values in the epilimnion and at 8.5 m, varying between 109 and 249 pmol C L^{-1} d^{-1}, then increasing with depth to a maximum value of 3200 pmol C L^{-1} d^{-1} at 15 m. For PLFAs C18:3ω3 and C18:4ω3 (Fig. 2.5e, f), production rates in the dark incubations were very low throughout the water column, with maximum values corresponding to 12 pmol C L^{-1} d^{-1}, with the exception of a peak in C18:3ω3 at 10 m depth of 52 pmol C L^{-1} d^{-1}. Label incorporation rates for PLFA C20:5ω3 (Fig. 2.5g) were low as well, between 5.1 and 6 pmol C L^{-1} d^{-1} between 2 and 8.5 m water depth,

increasing to a maximum of 24 pmol C L^{-1} d^{-1} at 15 m, which is similar to the trend observed in PLFA C16:1ω7c.

Table 2.1 Net primary production, glucose-based production and glucose-based respiration in µmol C L^{-1} d^{-1} and bacterial growth efficiency with depth.

Water depth (m)	net primary production (µmol C L^{-1} d^{-1})	Percentage extracellular release (PER)	Glucose-based production (µmol C L^{-1} d^{-1})	bacterial growth efficiency	Glucose-based respiration (µmol C L^{-1} d^{-1})
2	6.93	0.00	0.12	0.19	0.52
6	16.05	78.8	0.09	0.17	0.43
8.5	8.15	88.4	0.19	0.43	0.25
10	12.32	89.6	0.19	0.36	0.34
12	0.00	-	0.38	0.58	0.27
15	0.00	-	0.34	0.55	0.28
Depth-integrated rates (mmol C m^{-2} d^{-1})	115	-	3.3	-	5.9

2.3.4 Production and respiration

Net primary production (NPP, the sum of label transfer from DIC to POC and DOC, Table 2.1) was highest at 6 m with a rate of 16.0 µmol C L^{-1} d^{-1}, decreasing with depth to 8.1 µmol C L^{-1} d^{-1} at 8.5 m. At 10 m water depth, NPP was somewhat higher with a value of 12.3 µmol C L^{-1} d^{-1}, decreasing to zero at 12 and 15 m depth. From 6 to 10 m depth label transfer from DIC to DOC was substantial, resulting in high percentages of extracellular relase (Table 2.1) increasing from 78.8% at 6 m to 89.6% at 10 m water depth. In the epilimnion and chemocline, glucose-based, heterotrophic production (Table 2.1) was much lower than NPP, with rates between 0.12 and 0.19 µmol C L^{-1} d^{-1}. Heterotrophic production rates were somewhat higher in the hypolimnion (0.38 to 0.34 µmol C L^{-1} d^{-1} at 12 and 15 m respectively). Bacterial growth efficiency (Table 2.1), the production of bacterial biomass relative to the total amount of ^{13}C-glucose substrate assimilated (Del Giorgio and Cole 1998), also increased with depth from 0.19 at 2 m to 0.55 at 15 m water depth.

Respiration rates (Table 2.1) were highest in the epilimnion, corresponding to values of 0.52 and 0.43 µmol C L^{-1} d^{-1} at 2 and 6 m respectively, decreasing to rates between 0.25 and 0.28 µmol C L^{-1} d^{-1}, with the exception of 10 m depth, where respiration was slightly higher with a rate of 0.34 µmol C L^{-1} d^{-1}. From unlabelled samples, using a Keeling plot (Fig. 2.6), it was derived that the respired DIC had an average δ^{13}C value of -21.8‰.

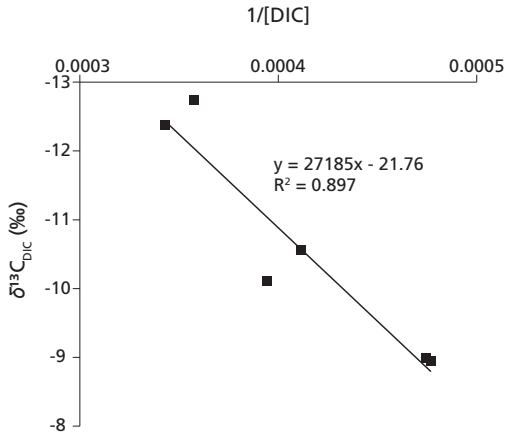

Fig. 2.6 Keeling plot showing 1/(DIC concentration) vs. the natural abundance value (T0) of $\delta^{13}C_{DIC}$. The y-intercept of the linear trendline indicates the $\delta^{13}C$ of respired carbon.

2.4 Discussion

Before discussing the results of the labelling experiments in detail, it is informative to first review the methodology used in this study. In our experiments glucose was added as a tracer to the dark incubations to quantify bacterial production rates and, given the complex and largely unknown composition of the natural DOC pool, it is not possible to extrapolate glucose-based rates to bulk DOC processing rates. Moreover, glucose is probably more readily usable as a substrate compared to the naturally available DOC, likely resulting in an overestimation of assimilation and respiration rates. Conversely, some microbes do not use glucose as a substrate, and their production and respiration could not be traced. Quantifying these effects would require dedicated experiments using a range of different substrates, which is beyond the scope of this research. Hence the rates of assimilation and respiration in the dark experiments discussed here are potential rates and represent glucose-based bacterial production and respiration.

Using PLFAs in isotope-labelling experiments allowed us to distinguish between metabolic pathways in the microbial communities. Still, there are limitations to what PLFAs can tell us about certain microbial groups. In this study, we were unable to identify cyanobacteria, which mostly produce non-unique PLFAs (Gugger et al. 2002). Although not produced by all cyanobacteria species (Gugger et al. 2002), the more specific PLFA C18:3ω6, which has previously been used as a marker for cyanobacteria, was either not present or detected in very low abundances in our samples. Heterocyst glycolipids (HGs) have also been studied as cyanobacterial markers (Bauersachs et al. 2009), but due to the work-up process prior to PLFA analyses it was unfortunately no longer possible to analyse HGs on our samples. Also, we were unable to trace methanotrophic bacteria using PLFAs. Specific PLFAs in methanotrophic bacteria are C16:1ω8c and C16:1ω5t for type I, while for type II C18:1ω8c (Bowman et al. 1991, Bowman et al. 1993, Nichols et al. 1985) and also C18:2ω7c,12c and C18:2ω6c,12c (Bodelier et al. 2009) are considered biomarker PLFAs. In the samples from Lake Rotsee, none

of the methanotrophic PLFAs were detected in quantities that allow for reliable isotope analysis. Only C18:2ω6c was detected, but both concentrations and enrichment values were low.

The incubation experiments were performed at multiple depths, but at a single location. Consequently, these incubations did not capture any potential horizontal spatial heterogeneity. Still, horizontal spatial differences are expected to be relatively small given the narrow shape of the lake. The incubation experiments lasted four days and the light treatment hence included natural day-night cycles. The four-day duration of the experiments was a compromise between detecting activity of slow-growing organisms on the one hand and preventing changes in environmental conditions, substrate depletion and isotope scrambling on the other hand (Middelburg, 2014). Concentrations of carbon pools and PLFAs did not significantly change over four days, suggesting steady-state conditions. However, only 2 to 32% of the added ^{13}C-glucose remained at T4, implying that glucose-based production and respiration rates may have been underestimated, in particular at depths 12 and 15 m where more than 97% was processed. Although we did not measure oxygen concentrations at T4, we have no indication of oxygen limitation in the oxygenated epilimnion. Only at the interface between oxygenated and anoxic water (8.5 m water depth), the small headspace that was present over the incubated sample, might have caused a switch in the microbial community. Since our experiment was carried out once, it is possible that on a longer timescale, the calculated rates and their relative importance in Lake Rotsee differ.

2.4.1 Carbon flows

Concentrations of POC were relatively low in the surface layers compared to deeper in the water column (Fig. 2.2b) possibly related to post and/or late-bloom conditions as debris of the bloom still remained at depth. This is not surprising since the experiment was performed in June when stratification is stable, the chemocline is well established and production rates are still high. Visual inspection of the incubated water and the filtered material showed a strong increase in the amount of suspended material with depth (Fig. 2.2f). Additionally, the observed increase in POC and PLFA concentrations in the hypolimnion is in line with settling of large amounts of organic matter during post and/or late-bloom conditions.

Label incorporation into POC and subsequent transfer to DOC under light conditions (Fig. 2.4a) together constitute net primary production (Table 2.1). Labelling of POC is in line with expected decreasing production with depth, as light conditions become less favorable for photosynthesis. After the four-day experiment, label incorporation into POC showed a somewhat smaller uptake than labelling of DOC (Fig. 2.4a). In short-term ^{13}C-bicarbonate tracer experiments, label transfer to DOC reflects exudation of organic carbon (EOC), which is the release of excess organic molecules by phytoplankton when carbon fixation is higher than incorporation into new cell material (Fogg 1983) and is generally highest under nutrient-poor conditions, when growth of phytoplankton is limited, but photosynthetic carbon fixation is not (Fogg 1983, Van den Meersche et al. 2004). For Lake Rotsee, EOC as a percentage of NPP (PER) is very high (Table 2.1), but it has been shown that the epilimnic nitrate content decreases to very low concentrations after spring and nitrite concentrations are low throughout the year (Schubert et al. 2010). Despite the overall eutrophic state of the lake, nutrient poor post-/late-bloom conditions at the time of the incubation experiments may have favored exudation of organic carbon by algae, causing the DOC pool to become labelled at several depths.

Production of labelled POC in the dark incubations (Fig. 2.4b) represents heterotrophic production (Table 2.1, see above) and was relatively stable in the epilimnion, but increased in the

hypolimnion as a result of more favorable conditions: less competition from other producers and increased nutrient availability. Compared to NPP, the potential heterotrophic production rates in the epilimnion and chemocline were substantially lower (Table 2.1). When integrated over the water column, the daily rate of net primary production was 115 mmol C m^{-2} d^{-1}, while the potential rate of heterotrophic production was only 3.3 mmol C m^{-2} d^{-1}.

Crucially important when studying net ecosystem metabolism is the relative rate of production compared to respiration as a function of water depth (Pace and Prairie 2005). Within heterotrophic lakes allochthonous carbon may stimulate part of the food web (Battin et al. 2008, Brett et al. 2009, Cole et al. 2006, Pace et al. 2004), resulting in higher rates for respiration than for primary production. This will lead to (1) oxygen diffusing into the lake since dissolved oxygen levels become lower than atmospheric levels and (2) the partial pressure of CO_2 increases to higher levels than in the atmosphere, causing it to diffuse out of the lake (Prairie et al. 2002). It has been found that many aquatic systems are net heterotrophic (Cole et al. 2000, Del Giorgio and Peters 1994, Del Giorgio et al. 1997), which may also be expected for Lake Rotsee, given its strong methane cycle (Schubert et al. 2010). The glucose-based respiration rate integrated over the water column was 5.9 mmol C m^{-2} d^{-1} in Lake Rotsee. The resulting difference between NPP and respiration is quite large (~109 mmol C m^{-2} d^{-1}) indicating that, despite the uncertainties in glucose-based respiration, Lake Rotsee was net autotrophic during our experiment. However, our assessment of the carbon flows is incomplete because high methane fluxes from the sediment and intense methane cycling in the water column should also be considered in the overall carbon balance. Moreover, as a consequence of the high rate of NPP, there was a large flux of organic matter to the sediment. Within the sediment, this organic matter will be processed, releasing methane to the overlying water column. Although unexpected, given that many lakes are net heterotrophic, the observed large difference between NPP and potential respiration in Lake Rotsee still falls within the range of net ecosystem productivity found among lakes and years by Cole et al. (2000), who observed daily rates up to +175 mmol C m^{-2} d^{-1}.

Respiration added DIC with a $\delta^{13}C$ of -21.8 ‰, while the DOC pool from which it was derived had a $\delta^{13}C$ of about -25‰ (Table S2.1), suggesting preferential degradation of heavy compounds such as sugars and also certain amino acids (Scott et al. 2006). Moreover, the relatively heavy signature of the substrate excludes a substantial contribution of soil derived organic matter, which consists mainly of trees, ferns, shrubs, reed and grassland (Naeher et al. 2014), which is generally isotopically depleted.

2.4.2 Phytoplankton production

Photoautotrophy – Enrichment of phytoplankton PLFAs (C18:3ω3, C18:4ω3 and C20:5ω3) in the bicarbonate-labelled (ambient light) incubations (Fig. 2.5e-g) derives from autotrophic production. The highest concentrations of autotrophic biomass were observed below the oxycline (Fig. 2.3e-g), similar to the other PLFA biomarkers (Fig. 2.3a-d) and in line with post-/late-bloom conditions as suggested above. Light conditions below the oxycline are not favorable for typical photoautotrophic production, implying that this biomass can fix little amounts of carbon. This is corroborated by the labelling experiment, showing that production rates of phytoplankton PLFAs (Fig. 2.5e-g) were in line with the epilimnion being the main site for photoautotrophic production, with maximum production values reached at a water depth of 6 m. Maximum production values at 6 m are in agreement with maximum Chlorophyll α concentrations found in Lake Rotsee around this depth in June by (Brand et al. 2016). At 6 m depth, photoautotrophs therefore seem to have been the dominant producers. The high production levels at 6 and

10 m mainly resulted in labelling of DOC (Fig. 2.4a). The low epilimnic algal biomarker concentrations imply that the biomass present was very active and, moreover, that recycling of biomass must have been important in the epilimnion. An intense internal nutrient cycle in Rotsee has been suggested by (Bloesch et al. 1977), who calculated that 35-75% of the nitrogen and 55-85% of the phosphorous required for primary production can be regenerated.

Based on the production rates of C18:3ω3, C18:4ω3 and C20:5ω3, photoautotrophy seems minor at 2 m water depth (Fig. 2.5). In contrast, figure 2.4a shows highest POC label incorporation at this depth. Evidently, another primary producer, not represented by the PLFA biomarkers studied here (see above), dominated production at this depth. Cyanobacteria are the most likely candidates, as they are ubiquitous photosynthesizers and have been found to account for 99% of total cell counts in a 2013 study (Brand et al. 2016). High cyanobacterial growth rates are in accordance with the observed lack of label transfer to the DOC pool at 2 m depth (Fig. 2.4a). Hence it is possible that cyanobacterial production is responsible for the observed high levels of label incorporation into POC and insignificant transfer to DOC at 2 m depth.

Light penetration in Lake Rotsee decreases to ±0.28% of surface light intensity at the oxycline and 0.01% at 11 m depth (Oswald et al. 2015). At water depths less than 10 m production of PLFAs C18:3ω3, C18:4ω3 and C20:5ω3 was detected (Fig. 2.5e,f,g). At 10 m water depth, only C18:4ω3 and C20:5ω3 were produced but no C18:3ω3. These results confirm an earlier report that oxygenic primary production (assumed to derive from oxygenic photoautotrophs) has been detected at and below the oxycline (Oswald et al. 2015). Moreover, our data suggest that the primary producer community differed in this low-light zone. Rhodophyta are a possible candidate as these algae are known to exhibit low-light adapted photosynthesis (Necchi Jr and Zucchi 2001) and produce C18:4ω3 and C20:5ω3 but not C18:3ω3 (Dijkman and Kromkamp 2006).

Chemoautotrophy – Anaerobic and potentially aerobic chemoautotrophy occur in the water column of Lake Rotsee, since sulphate, sulfide and ammonium have been detected (Schubert et al. 2010). In the past, rates of chemoautotrophic bacterial production (CBP) in other lakes were calculated using data from DIC labelled incubations in bottles covered with aluminium foil (Hama et al. 1983, Morana et al. 2016). Since in our setup DIC-labelled incubations were carried out under ambient light conditions only naturally dark depths (see above) are potentially suitable to calculate chemoautotrophic DIC uptake, though photoautotrophic production at 8.5 and 10 m has been detected at and below the oxycline in Lake Rotsee.

An estimate of chemoautotrophic production may still be made based on label incorporation into PLFAs. The redox gradients in the chemocline (8.5 to 10 m water depth) are the most likely location for chemoautotrophy. It can be observed in figure 2.5 that in addition to phytoplankton-derived PLFAs, also bacterial PLFAs iC14:0, iC15:0 and aC15:0 were labelled at 8.5 m depth and PLFA C16:1ω7c was labelled at 8.5 and 10 m depth. The observed incorporation of labelled carbon in the bacterial PLFAs at 8.5 m water depth (Fig. 2.5a-c) could result from heterotrophic assimilation of organic carbon exudated by phytoplankton or from chemoautotrophic production and we cannot be certain about the relative contributions of each. At 10 m water depth, no production of branched PLFAs was observed and hence at this depth labelling of C16:1ω7c is indicative of chemoautotrophy. Moreover, a comparison between the production rates of C16:1ω7c and other phytoplankton PLFAs, allows us to differentiate between low-light photosynthetic versus chemoautotrophic production of C16:1ω7c. In phytoplankton, C16:1ω7c contributes to a smaller or similar extent to total PLFAs as other PLFAs such as C18:4ω3 and

C20:5ω3 (Dijkman and Kromkamp 2006), which also showed label incorporation at 10 m. Highest fractions of C16:1ω7c are found in Heterokontophyta, which produce similar amounts of C16:1ω7c and C20:5ω3. However, both production rates and concentrations of C16:1ω7c were (at least) 10 times higher compared to C20:5ω3: concentrations were 0.15 vs. 0.013 μmol C L^{-1} (Fig. 2.3d,g) and production rates were 4230 vs 413 pmol C $L^{-1}d^{-1}$ respectively (Fig. 2.5d,g). This indicates that at 10 m water depth, at most 10% of the peak in labelling of C16:1ω7c can be explained by low-light adapted photosynthesis. The remainder most likely derived from chemoautotrophic production by sulfur-oxidizers and/or nitrifiers, which is in line with the observed lack of labelling at 12 and 15 m depth (Fig. 2.5), as these are both obligate aerobes.

Methanotrophy – Given that Lake Rotsee has a strong methane cycle and that methane-oxidizing bacteria have previously been detected in the water column (Oswald et al. 2015, Schubert et al. 2010), it should be kept in mind that C16:1ω7c has also been found in some methane-oxidizing bacteria (Bodelier et al. 2009, Guckert et al. 1991). In fact, highest methane oxidation rates, attributed to type I MOB, were found at and below the oxycline (Oswald et al. 2015), at the same depth of highest (chemo)autotrophic production rates of C16:1ω7c (Fig. 2.5d). The natural abundance $\delta^{13}C$ value of C16:1ω7c (and other nonspecific PLFAs) showed a shift towards more depleted values at 8.5 and 10 m (data not shown), which is the zone identified as having highest methane-oxidation rates by Oswald et al. (2015). Hence, a partially methanotrophic origin for these PLFAs cannot be ruled out, in which case the calculated production rates represent minimum values as the isotopic signal may have been mixed with ^{13}C-depleted methane-derived carbon.

Mixotrophy – The ability of phytoplankton to switch facultatively between DIC and DOC as substrates for the production of biomass is called mixotrophy (or osmotrophy). Many organisms are capable of mixotrophy, albeit to differing degrees. In our experiment, mixotrophy is observed when transfer of label to phytoplankton PLFAs occurs not only in bicarbonate-labelled light incubations but also in glucose-labelled dark incubations. From figure 2.5e-f it is clear that only PLFA C18:3ω3 with a glucose-based production rate of 52 pmol L^{-1} d^{-1} at 10 m could have a mixotrophic source at this water depth. Since its producers Cryptophyta and Dinophyta, are known to be mixotrophic (Jones et al. 1994, Roberts and Laybourn-Parry 1999, Sanders and Porter 1988) these are potential source organisms for this PLFA at 10 m water depth, as are diatoms. Diatoms are primarily photoautotrophic, although some also exhibit heterotrophic behavior dependent on conditions (e.g. limited light availability, high DOC concentrations) (Lewin 1953). Additionally, heterotrophic production of PLFA C20:5ω3 by diatoms provided with glucose as a source of carbon and energy has been demonstrated (Shishlyannikov et al. 2014, Tan and Johns 1996). It is noteworthy that in our experiment PLFA C20:5ω3, which derives from diatoms, Cryptophytes and Dinophyta, did not show glucose-based enrichment (Fig. 2.5g). This implies that C20:5ω3 is only produced autotrophically in Lake Rotsee, confirming our earlier suggestion that C20:5ω3 has a different source organism than C18:3ω3.

2.4.3 Heterotrophic bacterial production

Heterotrophic production, or production of PLFAs in glucose-labelled incubations, was eminent in bacteria-derived PLFAs iC14:0, iC15:0, aC15:0 (Fig. 2.5a-c) and also in C16:1ω7c (Fig. 2.5d). Below the chemocline, production of C16:1ω7c only occurred in dark, glucose-labelled incubations, attesting to heterotrophic production.

Glucose-based production rates of PLFAs iC14:0, iC15:0 and aC15:0 (Fig. 2.5a-c) matched the DOC concentration profile (Fig. 2.2c), with high rates at 2 m, which decreased with depth until 8.5 m. Similarly, following high DOC concentrations and high (glucose-based) bacterial growth efficiencies (Table 2.1) in the hypolimnion, high bacterial production rates were also expected for 12 and 15 m water depth. This was however not the case, suggesting that in the hypolimnion the bacteria that produce PLFAs iC14:0, iC15:0 and aC15:0 were outcompeted by the heterotrophic source organism of C16:1ω7c.

Labelling of bacterial PLFAs in light incubations indirectly derives from autotrophic production, via consumption of exuded organic carbon (assuming bacteria do not feed directly on labelled phytoplankton). So far, no indication has been found that the exuded substances are used as a substrate by phytoplankton itself or that it significantly contributes to their growth (Fogg 1983), leaving the exudates altogether available for utilization by heterotrophic producers. Organic carbon exudates mainly consist of glycolic acid (Fogg 1983), which can be respired and taken up by many bacterial species. Growth yield, however, seems to be low (Fogg 1983, Smith et al. 1977, Wright and Shah 1975) and it has been suggested that glycolic acid functions as a co-metabolite, providing energy for the assimilation of other substances (Wright and Shah 1975). In Lake Rotsee, however, label transfer to heterotrophic bacteria in the DIC-labelled incubations resulted in relatively high production rates (compared to glucose-based production rates). At 2 m, even though phytoplankton production based on PLFA-labelling seems low, there was substantial uptake of labelled carbon by bacteria. Since no label was recovered in the DOC pool at this depth, it appears that heterotrophic bacteria were feeding on organic carbon produced by the inferred cyanobacteria, suggesting that their growth is tightly coupled at 2 m depth. Alternatively, the much larger pool of refractory DOC may obscure rapid turnover of labile DOC used by bacteria as a substrate. Below 10 m water depth, heterotrophic producers did not show an appreciable uptake of bicarbonate label, which was expected for 12 and 15 m, since no label was incorporated into phytoplankton biomass or DOC. At 10 m however, the DOC pool became substantially labelled (Fig. 2.4a), but the heterotrophic bacteria did not (Fig. 2.5a-c). Although it may have been used as a co-metabolite, other substances were used for growth, since incorporation of labelled glucose in the dark incubations showed (maximum) DOC uptake at 10 m water depth.

2.4.4 Conclusions and implications

By combining the tracer experiments with compound-specific stable isotope analyses of PLFAs we were able to identify and quantify the metabolic processes that affect the concentration and composition of DOC, DIC and POC pools at each depth. Figure 2.7 shows the main production types with depth, with photoautotrophic production dominating at 2 and 6 m, chemoautotrophic production dominating at 10 m depth and glucose-based heterotrophic production being most important at 12 and 15 m. At 8.5 m water depth, production rates of PLFAs showed that multiple processes occurred simultaneously. Furthermore we showed that the depth-dependence of primary production is also reflected in the microbial communities, with different PLFAs produced at different depths (Fig. 2.5). Using PLFA isotopes, we were able to show that high concentrations, or large biomass, does not necessarily indicate high production rates (Fig. 2.3 and 2.5), which would otherwise have required several sampling campaigns.

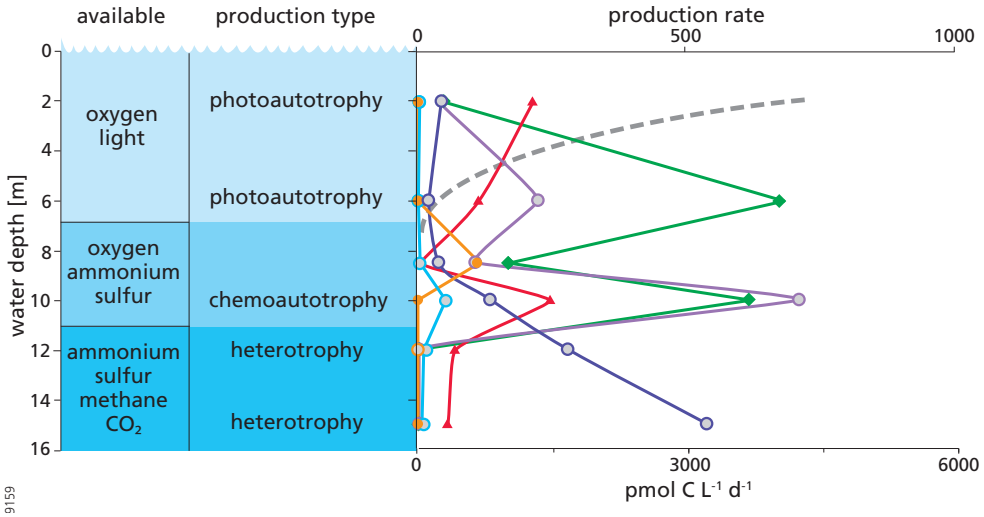

Fig. 2.7 Conceptual plot of dominant production types recognized at different depths (middle). On the left, available sources for production are shown; on the right, production rates in pmol C L^{-1} d^{-1} of producers versus depth are shown. The dashed grey line represents best guess cyanobacterial production (not quantified directly, but based on missing sink), the green line represents photoautotrophy, the blue line mixotrophy, the orange line chemoautotrophy and the red line heterotrophy. Autotrophic production of C16:1ω7c is represented by the light purple line while heterotrophic production of C16:1ω7c is shown in dark purple. Both shades of purple are plotted on the secondary axis at the bottom.

These findings have implications for monitoring carbon flows in lakes and linking activity and identity of organisms. Total particulate primary production (POC production) showed clear depth-dependence linked to light penetration, but the communities involved differed. Cyanobacteria dominated the upper layer, eukaryotic phytoplankton the subsurface water and a distinct low-light community was able to fix inorganic carbon at 10 m depth. There was also depth zonation in extracellular carbon release and heterotrophic bacterial growth on recently fixed carbon. Accordingly, lake monitoring programs based on one single depth provide an incomplete picture of the diversity and dynamics of photoautotrophs in this type of lakes. In lakes such as Rotsee, where light penetration and the oxycline occur at similar depths, we have found as one would expect that a diversity of communities is involved in carbon cycling (low-light phototrophs, chemo-autotrophs, mixotrophs, methanotrophs and heterotrophs).

Supplementary table S2.1 Average concentrations of DIC and DOC and also the isotopic compositions of DIC (under ambient light) and DOC (dark) at T0 and after labelling (T1).

Water depth (m)	DIC concentration (mmol C L^{-1})	DOC concentration (mmol C L^{-1})	$\delta^{13}C_{DIC}$ T0	$\delta^{13}C_{DIC}$ T1	$\delta^{13}C_{DOC}$ T0	$\delta^{13}C_{DOC}$ T1
2	2.1	0.37	-9.0	151	-25.7	1093
6	2.3	0.33	-10.6	128	-25.2	892
8.5	2.4	0.30	-10.1	123	-24.6	943
10	2.4	0.34	-9.0	152	-24.9	532
12	2.8	0.39	-12.7	108	-24.3	488
15	3.0	0.26	-12.4	103	-26.7	1078

Chapter 3

Microbial carbon processing in oligotrophic Lake Lucerne (Switzerland): results of in situ ^{13}C-labelling studies

Vechten bij het opstaan, twijfelen en doorgaan
- Niet Weglopen, Typhoon -

Abstract

Although clearly of major importance, the role of lakes in the processing and storage of organic carbon is still not very well characterized. Whether a lake functions as a net source or sink for carbon depends on relative rates of primary production, inputs of terrestrial organic matter and respiration. The microbial community will affect the efficiency of carbon cycling and thereby potential carbon storage. In this respect oligotrophic lakes have been studied less intensively than eutrophic lakes. Although the volumetric organic matter fluxes are smaller in these lakes, they might play an appreciable role in freshwater carbon cycling due to their deep photic zones. A detailed investigation of primary and secondary production is needed to clarify this role. Here we present such results for the oligotrophic Lake Lucerne, Switzerland. Based on in situ carbon isotopic labelling experiments using dark, glucose-labelled and transparent, DIC-labelled bottles positioned at different depths in the water column, we conclude that productivity was substantially lower than in a nearby eutrophic lake, showing that the deeper photic zone did not compensate for differences in volumetric production rates. The efficiency of the heterotrophic producers was such that photosynthesized organic matter was fully consumed, even during times of maximum productivity as studied here. This implies that the heterotrophic producers are well adapted to rapidly respond to a temporary increase in primary productivity, which is in line with calculated bacterial growth efficiencies in the surface water layer. Highest glucose-based productivity was observed in the deepest parts of the water column. Chemoautotrophy was recognized at 60 m water depth and is of relatively minor importance for overall fluxes. Mixotrophy was recognized possibly as a strategy to keep up production when light conditions become less favorable for autotrophic growth. A mesocosm experiment earlier in the year indicated lower primary production, which agrees well with the timing of this experiment preceding the annual spring bloom. During the low-productivity season the coupling between phytoplankton and bacterial production is much weaker and potentially more organic matter could escape recycling at that time.

3.1 Introduction

Of all processes influencing the release and uptake of carbon globally, the terrestrial carbon cycle is probably one of the least constrained compartments (Battin et al. 2009, Heimann 2009). Lakes play a major role in the terrestrial carbon cycle as sites of primary production and processing of organic matter, and are not just conduits of terrestrial carbon to oceans (Cole et al. 2007, Raymond et al. 2013, Tranvik et al. 2009, Weyhenmeyer et al. 2015). In general, the degree to which in situ produced or allochthonous organic matter contributes to secondary production in lakes is still under debate (Brett et al. 2009, Brett et al. 2012, Cole et al. 2011, Pace et al. 2004). Additionally, lakes differ in terms of size, trophic state and carbon loading, resulting in different relative rates of production and respiration which makes extrapolation to the global scale difficult. Eutrophic lakes are of clear importance but also relatively oligotrophic lakes potentially play an important role as such lakes can be of appreciable size. Studies targeting food webs and organic matter processing in oligotrophic lakes are hence needed to quantify their role in the terrestrial carbon cycle.

Many of the world's largest lakes are oligotrophic and they can be found from southern Siberia (Lake Baikal) to North America (Lake Superior, Lake Michigan, Lake Huron) and Africa (Lake Malawi, Lake Tanganyika) (www.globalgreatlakes.org). Together these lakes make

up roughly 50% of world's freshwater supply, making them crucially important for the supply of drinking water. They are also important in terms of biodiversity, ecology, economics and public service. These lakes do not only affect climate on a regional scale through heat and water exchange with the atmosphere, but they are also important players in the global carbon cycle (Cole et al. 2007). For unproductive systems it has been suggested that respiration often exceeds primary production, resulting in CO_2 diffusion into the atmosphere (Del Giorgio et al. 1997).

Although smaller than some of the afore-mentioned lakes, Lake Lucerne, Switzerland, is a textbook example of a large, oligotrophic lake. Lake Lucerne is a hard-water lake with a volume of 11.8 km^3. It has returned to an oligotrophic state (since 1989) after a brief period of eutrophication (1970-1977), with current total (dissolved) phosphorous concentrations ranging between 5 and 10 mg m^{-3} and nitrate-nitrogen concentrations of 600 to 700 mg m^{-3} (Bürgi and Stadelmann 2002). Plankton communities and food-web structure and functioning have been studied in Lake Lucerne, mainly in the context of the changes in trophic conditions (Bloesch et al. 1977, Bürgi et al. 1999, Bürgi and Stadelmann 2002). Currently the lake is considered well restored with recovered species diversity and evenness, although the species composition is still different from the pre-eutrophication period (Bürgi and Stadelmann 2002).

Here we present a study on the relative importance of primary production versus glucose-based heterotrophic production and respiration in Lake Lucerne. In 2011, a four-day bottle-labelling experiment was carried out which was designed to quantify and compare primary and heterotrophic production at different depth intervals of the water column. Incubations under light conditions were labelled using ^{13}C-bicarbonate to quantify total as well as group-specific primary production and trace the transfer of freshly produced organic matter to bacteria. Dark incubations at the same depths were labelled with ^{13}C-glucose in order to trace bacterial heterotrophic production and respiration. Combining light and dark labelling experiments thus allows us to calculate respiration and assess microbial carbon cycling.

Phospholipid-derived fatty acids (PLFAs) were used to zoom in on group-specific activities that contribute to net primary production (NPP) and microbial heterotrophic production, and to trace the transfer of labelled substrates to different producers. PLFAs are cell membrane constituents (lipids) that are produced by a wide variety of organisms and hence represent a range of feeding types. PLFAs represent viable biomass, since they are hydrolyzed within minutes to hours after cell lysis, releasing the polar head groups (White et al. 1979). Although PLFAs are rarely unique for specific source organisms, they have been successfully applied in trophic studies e.g. to differentiate between producers such as (chemo)autotroph and mixotroph phytoplankton and heterotrophic bacteria (De Kluijver et al. 2010, Van Gaever et al. 2009, Van Oevelen et al. 2006). Especially in labeling studies with ^{13}C-bicarbonate or ^{13}C-glucose, a distinction can be made between (chemo)autotrophic and heterotrophic produced PLFAs. PLFA ^{13}C-enrichment in bicarbonate-labelled incubations (in)directly results from photoautotrophic or chemoautotrophic production, while enrichment in glucose-labelled incubations results from heterotrophic production. Label incorporation in combination with phospholipid-derived fatty acids is used here to, (1) distinguish between different groups of primary producers (photoautotroph, mixotroph and chemoautotroph), secondary producers (heterotrophic bacteria) and detritus and, (2) quantify group-specific production.

Coupling between primary and secondary production is important because of the effects on carbon recycling or storage. Strong coupling between phytoplankton and heterotrophic bacteria, results in efficient remineralization of photosynthesized organic matter and in recycling of CO_2. When substantial time lags exist between bacterial responses to increases in phytoplankton

production, dead organic matter may escape bacterial degradation in surface water, resulting in export to deeper water. Therefore, in addition to the relatively short (4-day) bottle experiments, a 16-day mesocosm experiment was carried out in early spring 2012, using ^{13}C-bicarbonate as a tracer. This experiment serves as a pilot study aiming to quantify label transfer to bacteria, providing insight into dependence of bacteria on locally produced versus allochthonous organic matter.

3.2 Material and Methods

3.2.1 Study site

Experiments were carried out in Lake Lucerne, a large, oligotrophic prealpine lake in Switzerland (Fig. 3.1). Lake Lucerne is located 434 m above sea level, has a surface area of 113 km^2, a mean depth of 104 m and a maximum depth of 214 m. The lake water has a residence time of 3.4 years and the lake itself is oligomictic with complete overturn occurring on average every six years. The total catchment area of the lake is 2124 km^2, with four major rivers flowing into Lake Lucerne: Reuss, Muota, Engelberger Aa and Sarner Aa, together contributing ~80% of the lakes' water supply. Dominating phytoplankton during summer are pennate diatoms, chrysophyte algae and cryptophyte algae, while *Rhodomonas* (Cryptophyta) and centric diatoms dominate during winter (Bossard et al. 2001).

The bottle experiments in Lake Lucerne were located near the edge of the Chrüztrichter Basin. This location is relatively far away from major in- or outflowing rivers and has limited direct input of allochthonous organic matter (Blaga et al. 2011). To facilitate the comparison of flux rates the experimental location was also selected close to a previous sediment trapping study (Blaga et al. 2011). The mesocosm experiment was located at the opposite side of the basin in a much shallower part, to be relatively shielded from wave and wind interaction with the setup.

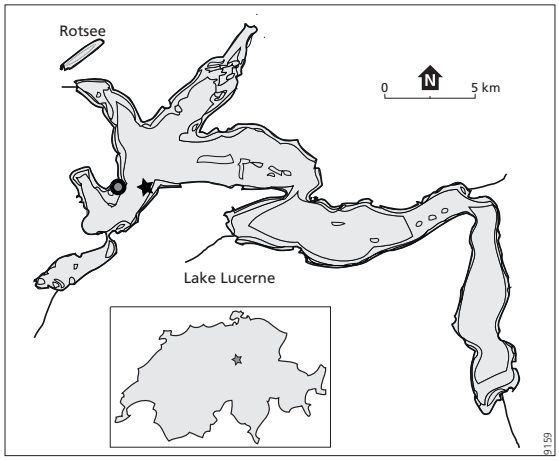

Fig 3.1 Map showing the location of Lake Lucerne and its major in- and outflowing rivers. The location of the 2011 bottle experiments is indicated by a star; the 2012 mesocosm experiment is indicated by a circle.

3.2.2 Incubation experiments and sample collection

In 2011, an in situ ^{13}C-labelling experiment was carried out from June 16 to June 20. Using Niskin bottles, twelve 25-liter bottles were filled with lake water from 6 different depths (5, 10, 20, 40, 60 and 75 m). Using a tube the water was quickly transferred from Niskin to incubation bottles. For each depth, a transparent (polycarbonate) bottle was labelled with ^{13}C-bicarbonate (6.6 mg $NaHCO_3$ per bottle, >98 atom% ^{13}C) and a (Low Density Polyethylene) bottle covered in waterproof, reflecting aluminum tape was labelled with ^{13}C-glucose (1.6 mg, >99 atom% ^{13}C). Label addition increased DIC and DOC concentrations by 0.16% and ~1% respectively. Transparent and dark bottles were attached side by side to a cable connecting an anchor at the lake floor to a buoy at the water-air interface, so that the bottles were placed at the original depth the water was recovered from. This setup was left in situ for four days. At the start of the experiment, in situ oxygen, temperature, conductivity and pH were measured using a CTD probe (Seabird SBE19). At the start (T_0) and end (T_4) of the experiment, samples were collected for dissolved organic carbon (DOC), dissolved inorganic carbon (DIC), and suspended particulate matter (SPM, for bulk organic carbon and lipid biomarkers) analyses.

The mesocosm incubation was performed in 2012 using a custom made set-up. A ten-meter-deep mesocosm (1 m diameter, 7800 liter, Fig. 3.2) was deployed in Lake Lucerne from March 22 to April 6 (16 days). The mesocosm consisted of a metal frame with floats and a black synthetic bag suspended from the frame. The frame was anchored to the lake floor. The rim of the mesocosm was positioned 1 meter above the lake level to avoid exchange of surface water with the lake during the experiment. The experiment was performed earlier in the year compared to the 2011 incubations, both in an attempt to capture onset of the spring bloom and also for logistical reasons. Samples were taken at 2.5 m water depth within the mesocosm. In situ oxygen concentrations, temperatures and pH were measured using a CTD probe (Seabird SBE19) at T_0, T_4, T_7, T_{11} and T_{14}, when samples were also collected for alkalinity. Samples for DIC and particulate organic carbon (POC) were collected daily for the first eight days and after that at T_{11} and T_{15}. Samples for lipid biomarker analyses were collected daily for the first seven days and at T_{15}.

Fig. 3.2 Setup of the 2012 mesocosm labelling experiment.

For analyses of concentrations and stable carbon isotope composition of DOC, samples were filtered over GM/F filters (0.45 µm) and stored frozen (-20 °C) in clean vials until further analysis. Samples for DIC were collected without air in 20 ml headspace vials and sealed using airtight caps, preventing further microbial activity by mercury chloride poisoning. Samples were stored in the dark and upside down. For SPM, the remaining water from the bottles was filtered over 0.7 µm GF/F filters (pre-weighed and pre-combusted). Filters were stored frozen (-20 °C) until extraction.

3.2.3 Laboratory analyses

Alkalinity was determined on 50 ml of water by potentiometric titration with 0.01M HCl, monitoring pH and using a Gran plot. For the bottle-experiment alkalinity was analyzed for each depth and values represent averages of T_0 and T_4 from light and dark incubations. Samples for the analyses of concentrations and $\delta^{13}C$ of DOC were first acidified, then flushed with helium (removing DIC) and finally oxidized (using peroxidisulfates). DOC samples were then analyzed following Boschker et al. (2008) using high-performance liquid chromatography-isotope ratio mass spectrometry (HPLC-IRMS, Thermo Surveyor system coupled to a Delta V Advantage using an LC-Isolink interface). DIC concentrations of water samples were measured on a Shimadzu TOC-5050A Carbon analyzer, using an in-house seawater standard. For carbon stable isotope analyses of DIC a helium headspace was made over the DIC samples, which were subsequently acidified using a H_3PO_4 solution. The $\delta^{13}C$ of the resulting CO_2-gas were then measured using a gas bench coupled online to an IRMS (Thermo Delta V advantage). Using in-house (Na_2CO_3) and international (Li_2CO_3) standards, $\delta^{13}C_{DIC}$ was calibrated to the Vienna Peedee Belemnite (V-PDB) scale. Filters for SPM were freeze dried and concentrations and stable carbon isotopic composition of particulate organic carbon (POC) were measured on small pieces (6-13 circles of 5 mm diameter) cut from these filters. POC concentrations were measured using an elemental analyzer (EA) (Fisons Instruments NA1500), with the $\delta^{13}C$ being analyzed with the online coupled IRMS (Thermo Deltaplus). Precision was better than 0.35‰ based on in-house standards (Graphite quartzite and Nicotinamide). The relatively small amounts of material did not permit true replication, but consistent trends confirm that the internal precision is representative. Concentrations of the organic and inorganic carbon pools showed no systematic changes during incubations and are hence reported as the averages of T_0 and T_4 of both bicarbonate-labelled and glucose-labelled incubations.

Lipids were extracted from the remainders of the freeze-dried SPM filters according to a modified Bligh and Dyer extraction method, which was followed by separation into simple lipid (SL), glycolipid (GL) and phospholipid (PL) fractions based on polarity (Dickson et al. 2009). Phospholipid-derived fatty acids in the PL fractions were converted to fatty acid methyl esters (PL-FAMEs) by mild alkaline transmethylation (White et al. 1979) and internal standards were added (C12:0 and C19:0 FAMEs). For the 2011 (bottle incubation) samples, concentrations and carbon isotopic composition of the individual FAMEs were determined using gas chromatography combustion isotope ratio mass spectrometry (GC-C-IRMS), following Middelburg et al. (2000). Concentrations and $\delta^{13}C$ of PL-FAMEs from the mesocosm experiment were determined using a different set-up. Concentrations were analyzed using a gas chromatograph (HP 6890) with Helium as carrier gas set at constant pressure and fitted with a flame ionization detector (FID) and a VF-23ms column (0.25 mm i.d.). Similar as for carbon pools, concentrations of PLFAs did not show systematic changes and are shown as the averages of T_0 and T_4 of both bicarbonate-labelled and glucose-labelled incubations. Mass spectrometry

was performed using a Thermo Trace GC Ultra, with Helium set at constant flow. Compounds were identified based on retention times and mass spectra and double-bond positions were determined after derivatization with dimethyl-disulfide (DMDS). DMDS was activated with iodine in diethyl ether at 40°C overnight (Buser et al. 1983). Compound-specific $\delta^{13}C$ values of the mesocosm PL-FAMEs were determined using GC-C-IRMS with a ThermoFinnigan Delta Plus XP using the same type of column as for GC. Oven programming of GC-FID, GC-MS and GC-C-IRMS followed Middelburg et al. (2000). For all PLFAs, values are reported in ‰ vs. V-PDB and were corrected for the added carbon atom during methylation. Carbon isotopic values of the derivatizing agents were determined offline.

3.2.4 Data analyses

From the incorporation of ^{13}C into carbon pools (DIC, DOC, POC) and PLFAs, production rates (in mol L^{-1} d^{-1}) were calculated following De Kluijver et al. (2013):

$$Production\ rate = \frac{\Delta^{13}F_{produced}}{\Delta^{13}F_{DIC}} \times \frac{C_{produced}}{t} \quad (1)$$

With $C_{produced}$ representing the concentration of the C pool or PLFA (in mol L^{-1}); t was equal to the duration of the experiment, and the difference in the carbon isotopic fractions between sample and background is

$$\Delta^{13}F = {}^{13}F_{sample} - {}^{13}F_{background} \quad (2)$$

following Middelburg (2014), where $^{13}F_{background}$ is the natural abundance ratio as measured before label addition (T_0), and $^{13}F_{sample}$ the ratio after the experiment (T_4) and with ^{13}F representing the fraction ^{13}C, calculated as:

$$\frac{{}^{13}C}{{}^{12}C + {}^{13}C} = \frac{R}{R+1} \quad (3)$$

R, the isotope ratios were derived from $\delta^{13}C$ values as

$$R = [(\delta^{13}C/1000) + 1] \times R_{VPDB} \quad (4)$$

using R_{VPDB} = 0.0111796 (Coplen 2011). Specific enrichment ($\Delta\delta^{13}C$, Middelburg (2014)) values >1.5‰ were used in calculations, with

$$\Delta\delta^{13}C = \delta^{13}C_{sample} - \delta^{13}C_{background} \quad (5)$$

The correction for $\Delta^{13}F_{DIC}$ (formula 1) applies for bicarbonate-labelled incubations only. For glucose-labelled incubations we assume the DOC-pool to be completely labelled since glucose is likely more easily consumed than naturally available, more refractory DOC.

The 2011 bottle-incubations allow calculating rates of net primary production (NPP), glucose-based production (GP) by microbes and respiration. For these calculations, steady-state is assumed, which considering the duration of the experiment and the absence of systematic changes in concentrations of carbon pools seems reasonable. NPP rate is calculated from the sum of label that was transferred to POC and DOC in bicarbonate-labelled incubations (light conditions), while label transfer to POC in glucose-labelled incubations under dark conditions represents GP (or heterotrophic microbial production). Respiration was calculated from label transfer to DIC in the dark incubations. From the glucose-labelled incubations, bacterial growth efficiency (BGE) was calculated as

$$BGE = \frac{[POC]_{labelled}}{[POC+DIC]_{labelled}} \quad (6)$$

To calculate the isotopic composition of the respired carbon at natural abundance, a linear trend line was fitted to a Keeling-plot (1/[DIC] vs. $\delta^{13}C_{DIC}$ at T_0 for each depth) using background DIC isotope values.

3.3 Results

3.3.1 Bottle labelling experiments

3.3.1.1 Physical and chemical parameters

A temperature profile of Lake Lucerne is shown in figure 3.3a and shows the thermocline during the 2011 bottle experiments starting at ~3 m depth, with temperatures decreasing strongly from 18 to 13 °C between 3 and 5 m. Below 5 m temperatures decreased more gradually, reaching stable values around 5 °C from 30 m depth downwards. Concentrations of dissolved oxygen (Fig. 3.3b) were around 370 µmol L^{-1} in the top 3 m, increasing in the thermocline to reach a maximum of 460 µmol l^{-1} at 10 m water depth. Oxygen concentrations decreased again below 10 m, reaching relatively stable concentrations below 30 m between 350 and 380 µmol L^{-1}. The 100% saturation line of dissolved oxygen is shown as a grey line in figure 3.3b and indicates supersaturation in surface waters and undersaturation below 30 m water depth. Alkalinity (Fig. 3.3c) values decreased from 1.98 mM to 1.94 mM between 5 and 10 m depth, below which alkalinity gradually increased, reaching a maximum of 2.07 mM at 75 m depth.

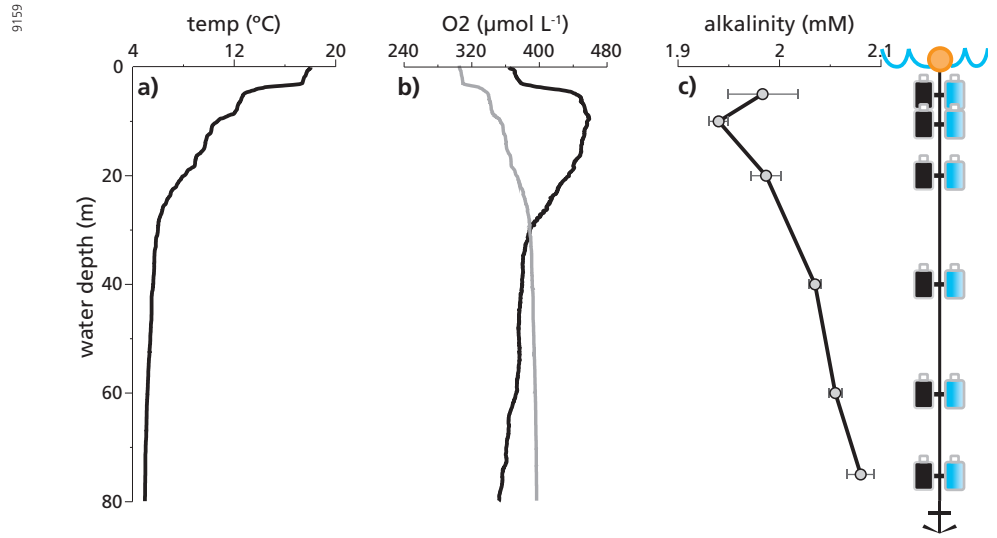

Fig. 3.3 Physical parameters in 2011: a) Temperature in °C, b) dissolved oxygen concentration in µmol L^{-1} as measured (black line) and the saturation concentration (grey line), and c) alkalinity in mM. Alkalinity concentrations are average values of T_0 and light and dark incubations.

3.3.1.2 Carbon pools

Average DIC concentrations (Fig. 3.4a) were 1850 and 1840 µmol C L^{-1} at 5 and 10 m respectively, increasing sharply to 1910 µmol C L^{-1} at 20 m and then gradually increasing to 2010 µmol C L^{-1} at 75 m depth. Average DOC concentrations (Fig. 3.4b) decreased from 320 µmol C L^{-1} to 210 µmol C L^{-1} between 5 and 10 m depth, below which they remained stable throughout the water column. At 5 and 10 m, average POC concentrations (Fig. 3.4c) were relatively stable, with values of 25 and 24 µmol C L^{-1} respectively, decreasing sharply to 16 µmol C L^{-1} at 20m. At greater depths POC concentrations remain relatively stable around 12 µmol C L^{-1}.

Since the same amount of ^{13}C-bicarbonate was added at each depth, but initial DIC concentrations varied, the δ^{13}C of DIC after tracer addition increased by 114 to 127‰, with a larger increase corresponding to lower initial DIC concentrations. Transfer of label from DIC to DOC (Fig. 3.4d) was negligible during the incubations under light conditions. Label incorporation into POC (Fig. 3.4d) was highest at 5 m with values of 1.0 µmol C L^{-1} d^{-1}, decreasing to zero µmol C L^{-1} d^{-1} at 40 m depth. A ^{13}C mass balance for organic and inorganic carbon pools was achieved within 18%, which is acceptable for our purposes.

Similar to bicarbonate labelling, the same amount of ^{13}C-glucose was added to each depth for dark incubations, while initial DOC concentrations varied. The resulting enrichment of DOC therefore varied between 250 and 680‰, with the exception of 20 m depth, for which $\Delta\delta^{13}$C values were 1250‰, likely resulting from the accidental double addition of label at the start of the experiment. Transfer of ^{13}C to DIC in dark incubations (Fig. 3.4e) was 0.14 and 0.16 µmol C L^{-1} d^{-1} at 5 and 10 m, decreasing to relatively low values around 0.03 µmol C L^{-1} d^{-1} at greater depth, with the exception of 40 and 75 m, where production rates reached higher values of 0.07 and 0.11 µmol C L^{-1} d^{-1} respectively. Label transfer to POC (Fig. 3.4e) showed a similar trend except that values were somewhat lower at the surface (0.09 and 0.08 µmol C L^{-1} d^{-1} at 5 and 10 m depth respectively) and somewhat higher below 20 m. Excluding 20 m depth, a ^{13}C mass balance for organic and inorganic carbon pools was achieved within 15%.

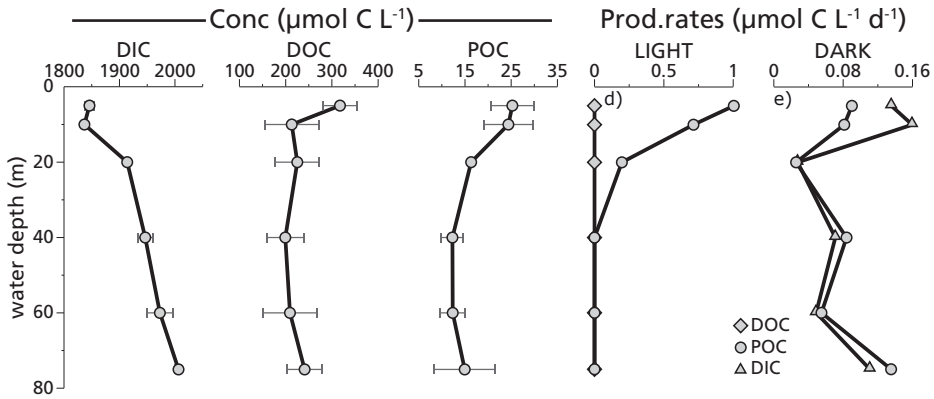

Fig. 3.4 Average concentrations (T_0 and light and dark incubations) of a) DIC, b) DOC and c) POC in µmol C L^{-1}. Production rates (absolute label incorporation per day) under d) bicarbonate-labelled light conditions and e) glucose-labelled dark conditions in µmol C L^{-1} d^{-1}.

3.3.1.3 Production and respiration

Since no appreciable transfer of ^{13}C to DOC was observed under light conditions (Fig. 3.4e), NPP derives solely from label incorporation into POC (section 3.3.1.2). Heterotrophic production rates (Table 3.1, calculated as label transfer to POC in glucose-labelled incubations) were positive at all depths, albeit much lower than NPP rates. Glucose-based heterotrophic production rates at 5, 10 and 40 m were similar, ranging between 0.08 and 0.09 μmol C L^{-1} d^{-1}, while relatively low rates of 0.03 and 0.05 μmol C L^{-1} d^{-1} were observed at 20 m and 60 m depth. Maximum rates of 0.14 μmol C L^{-1} d^{-1} were reached at 75 m water depth.

Respiration rates (Table 3.1, calculated as transfer of label to DIC in dark incubations) followed the same trend with depth as glucose-based production rates, with the exception that respiration rates were higher at 5 and 10 m, and lower below 20 m depth. By plotting natural abundance (T_0) samples in a Keeling-plot (not shown), it was derived that the $\delta^{13}C$ of respired DIC was -31.4‰. Bacterial growth efficiency (BGE, Table 3.1) decreased from 0.40 to 0.34 between 5 and 10 m, below which it increased with depth to a maximum value of 0.55 at the deepest incubation depth of 75 m.

Table 3.1 Net primary production (NPP), glucose-based heterotrophic production (GP) and respiration (R) in μmol L^{-1} d^{-1} and bacterial growth efficiency (BGE) with depth. Depth integrated primary production, glucose-based production and respiration rates in mmol C m^{-2} d^{-1}.

Water depth (m)	net primary production (μmol C L^{-1} d^{-1})	Glucose-based production (μmol C L^{-1} d^{-1})	Glucose-based respiration (μmol C L^{-1} d^{-1})	bacterial growth efficiency
5	1.00	0.09	0.14	0.40
10	0.71	0.08	0.16	0.34
20	0.20	0.03	0.03	0.48
40	0.00	0.08	0.07	0.54
60	0.00	0.05	0.05	0.53
75	0.00	0.14	0.11	0.55
Depth-integrated rates (mmol C m^{-2} d^{-1})	15.8	7.8	7.7	-

3.3.1.4 PLFA concentrations and label uptake

The main labelled PLFAs in the bicarbonate-labelled incubations during the 2011 bottle experiment were C16:2ω7, C16:3ω3, C16:3ω4, C16:4ω1, C18:3ω6, C18:3ω3 (α-linolenic acid, or ALA), C18:4ω3 (stearidonic acid, or SDA), C20:5ω3 (eicosapentaenoic acid, or EPA) and C20:4ω6 (arachidonic acid, or ARA). These PLFAs are produced by a variety of phytoplankton groups (e.g. Bacillariophyceae, Haptophytes, Chlorophytes, Chrysophytes, Cryptophytes, and also cyanobacteria) (Dijkman and Kromkamp 2006, Gugger et al. 2002, Taipale et al. 2013), but based on incorporation of labelled bicarbonate compared to glucose, these PLFAs were split into two groups: autotroph and mixotroph. PLFAs C16:3ω3, C18:3ω6, C18:3ω3, C18:4ω3 and C20:4ω6 showed minor (2 to 3 orders of magnitude less) incorporation of glucose compared to bicarbonate. Accordingly, they are combined to represent (photo)autotrophic producers. Glucose-derived label incorporation was higher for PLFAs C16:2ω7, C16:3ω4, C16:4ω1 and C20:5ω3,

hence their weighted sum is used to represent mixotrophic phytoplankton. In glucose-labelled dark incubation, heterotrophic production is represented by branched PLFAs iC14:0, i/aC15:0 and iC16:0, which derive primarily from gram-positive bacteria (Kaneda 1991), although they have also been found in gram-negative bacteria (Zelles 1999). Labelling of branched PLFAs in bicarbonate-labelled incubations derives indirectly from autotrophic production via consumption or from production by chemoautotrophic bacteria. PLFA C16:1ω7c is a common PLFA in many organisms (including (chemo)autotroph and heterotroph producers) and should therefore normally not be used as a biomarker for a specific group. However, in labelling studies such as the bottle experiments, label transfer into PLFA C16:1ω7c is informative and can be interpreted when taking the labelled substrate, labelling conditions and environmental context into account. Enrichment of C16:1ω7c in dark glucose-labelled incubations derives from heterotrophic production, while in bicarbonate-labelled light incubations it derives from autotrophic production. In bicarbonate-labelled incubations at greater depth, where light penetration is not sufficient to sustain considerable photoautotrophic production, chemoautotrophic production is responsible for enrichment of C16:1ω7c. Nevertheless, for clarity C16:1ω7c is shown separately in figures and has not been included in the summed values for autotroph and heterotroph production (Fig. 3.5). Concentrations and production rates of PLFA C18:1ω7c, which can derive from both phytoplankton (Dijkman and Kromkamp 2006, Taipale et al. 2013) and bacteria (White et al. 1996), were similar to concentrations and production rates of heterotroph-derived branched PLFAs and will not be discussed separately.

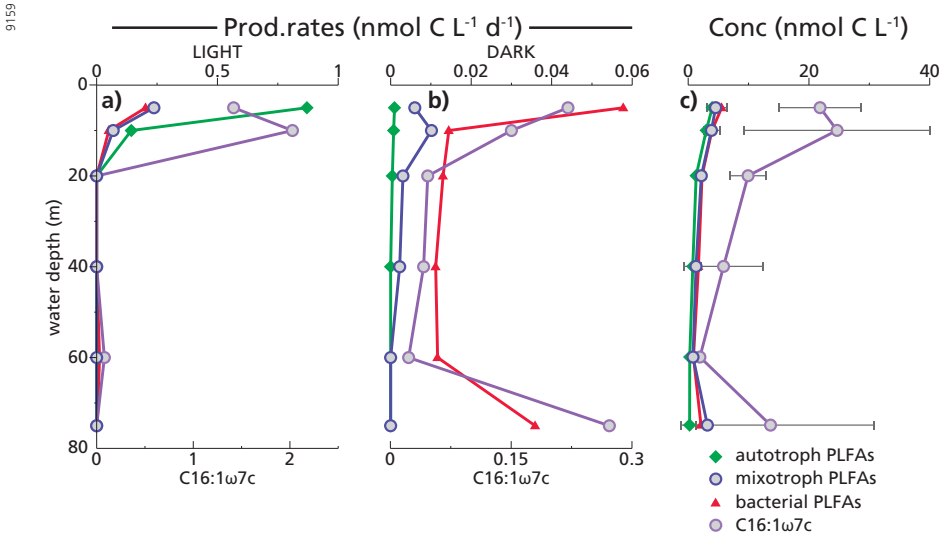

Fig. 3.5 Production rates in a) light and, b) dark incubations are plotted in nmol C L^{-1} d^{-1}. c) PLFA concentrations (± SD) as averages of T_0, T_4 light and T_4 dark in nmol C L^{-1}. Autotrophs shown in green are represented by PLFA C16:3ω3, C18:3ω6, C18:3ω3, C18:4ω3 and C20:4ω6. Mixotrophs (blue) are PLFA C16:2ω7, C16:3ω4, C16:4ω1 and C20:5ω3. Bacteria (red) are represented by PLFA iC14:0, iC15:0, aC15:0 and iC16:0. PLFA C16:1ω7c, which can derive from different producers (see section 3.3.1.4) is plotted in purple.

Production rates in nmol C L^{-1} d^{-1} for incubations under light conditions are shown in figure 3.5a. Autotrophic production rates decreased from 0.9 nmol C L^{-1} d^{-1} at 5 m to zero nmol C L^{-1} d^{-1} at 20 m and below. Production rates for mixotroph PLFAs showed the same trend but were somewhat lower (0.24 nmol C L^{-1} d^{-1} and 0.07 nmol C^{-1} L^{-1} d^{-1} at 5 and 10 m respectively). Bacterial production rates were highest at 5 m depth with a values of 0.2 nmol C L^{-1} d^{-1}, decreasing to zero nmol C L^{-1} d^{-1} at 20 m and below, except for 60 m depth where production reached the still quite low rate of 0.01 nmol C L^{-1} d^{-1}. The ratio of the weighted averages of bacterial versus phytoplankton specific enrichment ($\Delta\delta^{13}C_{bact}/\Delta\delta^{13}C_{phyto}$) was 0.28, indicating that 28% of the bacterial carbon was derived from newly fixed phytoplankton biomass. PLFA C16:1ω7c showed highest production rates in Lake Lucerne with values increasing from 1.4 nmol C L^{-1} d^{-1} at 5 m to 2.0 nmol C L^{-1} d^{-1} at 10 m, subsequently decreasing to zero nmol C L^{-1} d^{-1} at 20 m and below, with the exception of 60 m depth, where a relatively low production rate of 0.08 nmol C L^{-1} d^{-1} was observed.

Production rates for glucose-labelled incubations under dark conditions (Fig. 3.5b) show values close to zero for autotrophic production, reaching 0.001 nmol C L^{-1} d^{-1} at 5 m, decreasing to zero nmol C L^{-1} d^{-1} at 40 m and below. Production of mixotroph PLFA increased from 0.006 to 0.01 nmol C L^{-1} d^{-1} between 5 and 10 m water depth, decreasing to zero nmol C L^{-1} d^{-1} at 60 m and below. A maximum production rate for bacterial PLFAs of 0.06 nmol C L^{-1} d^{-1} was observed at 5 m depth, decreasing to 0.01 nmol C L^{-1} d^{-1} at 40 m depth and then increasing again to 0.04 nmol C L^{-1} d^{-1} at 75 m water depth. PLFA C16:1ω7c showed the highest glucose-based production rates in Lake Lucerne with values reaching 0.22 nmol C L^{-1} d^{-1} at 5 m, decreasing to values between 0.02 and 0.05 nmol C L^{-1} d^{-1} between 20 and 60 m depth. A maximum value of 0.27 nmol C L^{-1} d^{-1} was observed at 75 m, about 5 meters above the sediment-water interface.

Autotrophic phytoplankton showed a maximum concentration of 4.0 ± 1.0 nmol L^{-1} at 5 m, decreasing to 1.3 ± 0.1 nmol L^{-1} at 20 m, below which values were close to zero, ranging between 0.8 ± 0.2 and 0.3 ± 0.0 nmol L^{-1} (Fig. 3.5c). Mixotroph concentrations were highest at the top of the water column with a value of 4.5 ± 0.7 nmol L^{-1} at 5 m, decreasing to 0.8 ± 0.4 nmol L^{-1} at 60 m. Between 60 and 75 m, concentrations increased to 3.2 ± 0.0 nmol L^{-1}. Bacterial concentrations showed a decrease from 5.6 ± 0.9 to 0.9 ± 0.1 nmol L^{-1} between 5 and 60 m depth, below which concentrations increased to 2.1 ± 0.9 nmol L^{-1} at 75 m depth. Concentrations of PLFA C16:1ω7c increased from 21.8 ± 6.9 to 24.7 ± 15.5 nmol L^{-1} between 5 and 10 m depth, decreasing to 1.9 ± 0.4 nmol L^{-1} at 60 m. A higher concentration of 13.6 ± 17.2 nmol L^{-1} was observed at the maximum incubation depth of 75 m.

3.3.2 Mesocosm labelling experiment

3.3.2.1 Physical and chemical parameters

During the 2012 mesocosm experiment, water temperatures (Fig. 3.6a) steadily increased from 6.7 °C at T_0 to 9.8 °C at T_{14}. Dissolved oxygen concentrations are shown in figure 3.6b and were high and relatively stable, ranging between 440 and 476 µmol L^{-1}, although values at T_7 were even higher at 512 µmol L^{-1}. Alkalinity (Fig. 3.6c) somewhat increased during the experiment from 2.08 mM at T_0 to 2.14 mM at T_7, subsequently decreasing again to 2.08 mM at T_{14}.

The carbon isotopic composition of DIC before label addition (T_0) was -7.1‰ (Fig. 3.6d). The ^{13}C-bicarbonate addition resulted in constant-labelling with the $\delta^{13}C$ of DIC increasing to 441‰ at T_1, and stabilizing around 370‰ from T_2 until the end of the experiment.

Light penetration was somewhat reduced inside the mesocosm because of the material used, with Secchi depths ranging between 2.5 and 5 m, in contrast to the 9-11 m depth outside the mesocosm. Productivity in the mesocosm may have been hindered by this, but water within the mesocosm was well-mixed and phytoplankton was thus intermittently exposed to sufficient light.

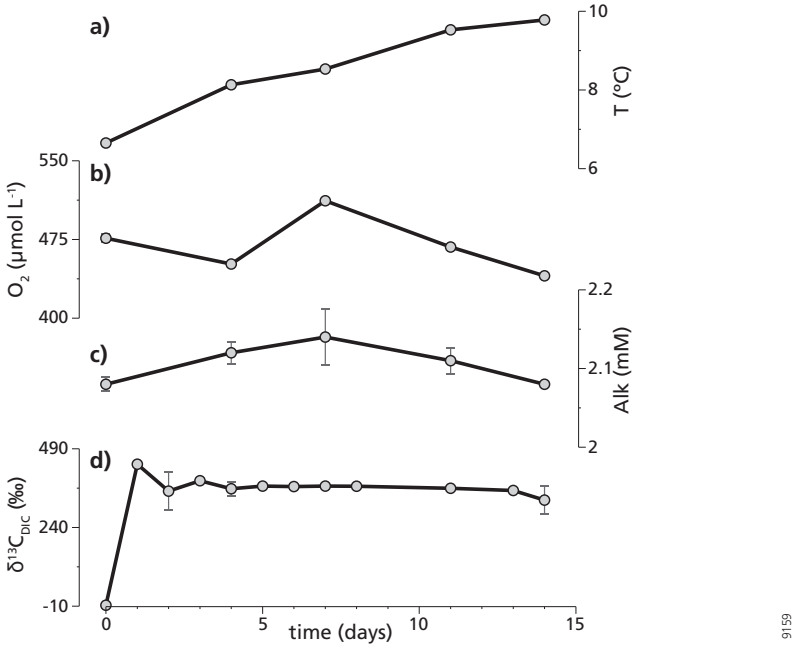

Fig. 3.6 Physical parameters during the 2012 mesocosm experiment. From top to bottom: a) water temperature in ˚C; b) dissolved oxygen concentrations in µmol L^{-1}; c) alkalinity in mM; d) Carbon isotopic composition of DIC in ‰ vs. VPDB.

3.3.2.2 PLFA concentrations and label uptake

After the mesocosm labelling experiment only a limited number of PLFAs showed isotopic enrichment values >1.5‰: branched PLFAs iC15:0 and aC15:0 and also phytoplankton-derived PLFAs C18:3ω3, C18:4ω3, C20:4ω6 and C20:5ω3. Stable carbon isotope values of the phytoplankton PLFAs showed that label incorporation took place at different rates: rapid (within one day) and late (from day 6) (Fig. 3.7). PLFA C18:3ω3 showed rapid label incorporation and is therefore used to represent early-growing phytoplankton. In the bottle labelling experiments above, PLFA C18:3ω3 was produced by autotrophs. The sum of PLFA C18:4ω3, C20:4ω6 and C20:5ω3 is used to calculate enrichment and production rates of late-growing phytoplankton. These PLFAs were produced both autotrophically (C18:4ω3 and C20:4ω6) and mixotrophically (C20:5ω3) during the bottle experiments. Weighted averages of branched PLFA iC15:0 and aC15:0 are used to represent heterotrophic bacteria (hereafter heterotrophs) (see above).

Relative label incorporation expressed as $\Delta\delta^{13}C$ (specific enrichment) for PLFAs is shown in figure 3.7 and shows that enrichment was not only fastest but, during our experiment, also highest for PLFA C18:3ω3, with a 4.1‰ enrichment at T_1, increasing to a $\Delta\delta^{13}C$ of 21.5‰ at T_7. Unfortunately, peak separation for C18:3ω3 in the T_{15} sample was poor, and low

concentrations did not allow for duplicate analyses, preventing calculation of a proper $\Delta\delta^{13}C$ value. Relative enrichment of late-growing PLFAs shows $\Delta\delta^{13}C$ values at or close to zero until T_5. After T_5, PLFA enrichment increased strongly with the exception of a 2‰ decrease at T_7. Final enrichment values at T_{15} varied between 16 and 25‰. Concentrations of C18:3ω6 (γ-linolenic acid or GLA), which can be used to represent cyanobacteria (De Kluijver et al. 2012, Gugger et al. 2002) were very low or not present. This indicates that they are either minor producers in Lake Lucerne during this period, or that the cyanobacterial community consists of species that do not produce this specific PLFA. Bacterial PLFAs (Fig. 3.7, purple shades) were not considerably labelled until after seven days, subsequently reaching a maximum $\Delta\delta^{13}C$ of 4.6‰ at T_{15}. The ratio of the weighted averages of the bacterial versus phytoplankton specific enrichments ($\Delta\delta^{13}C_{bact}/\Delta\delta^{13}C_{phyto}$) was 0.22, indicating that 22% of the bacterial carbon was derived from newly fixed phytoplankton biomass at that time.

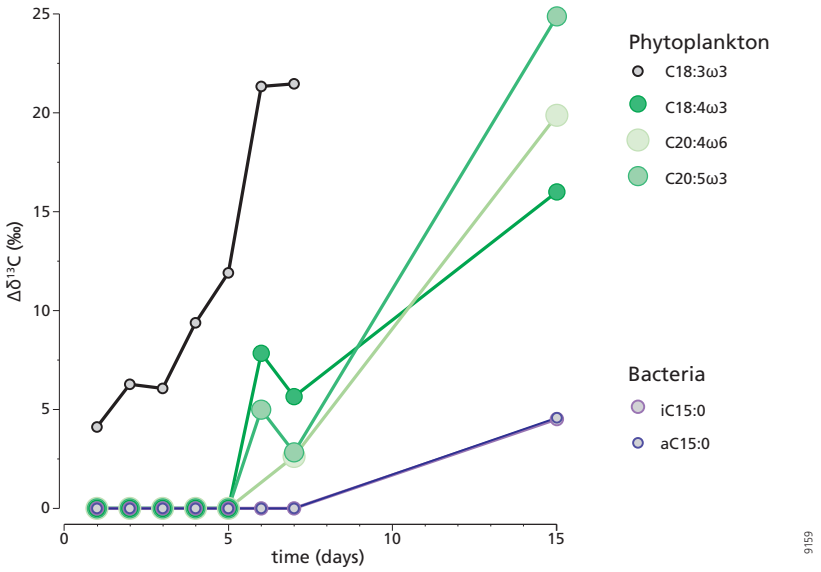

Fig. 3.7 Relative label incorporation into biomarker PLFA expressed as Δδ13C in ‰ vs. VPDB. Phytoplankton-derived PLFA are shown in black and green shades. Bacterial PLFA are plotted in shades of purple.

Production rates in nmol C L^{-1} d^{-1} for PLFAs grouped as early-/late-growing phytoplankton and heterotrophic bacteria are given in table 3.2. For early-growing phytoplankton, production rates based on ^{13}C-labelling were observed from day 1 ranging between 0.007 and 0.014 nmol C L^{-1} d^{-1} with a mean of 0.011 nmol C L^{-1} d^{-1}. For late-growing phytoplankton production rates were zero until T_5, then ranging between 0.005 and 0.009 nmol C L^{-1} d^{-1}, with a mean of 0.007 nmol C L^{-1} d^{-1}. Heterotroph production rates were zero until T_{15}, reaching 0.002 nmol C L^{-1} d^{-1}.

Table 3.2 Minimum, maximum and average production rates as measured during the mesocosm experiment in nmol C L^{-1} d^{-1} for phytoplankton and heterotrophic bacteria. The slow label transfer to heterotrophs did not allow for the calculation of minimum or maximum production rates.

	Early-growing phytoplankton	Late-growing phytoplankton	Heterotroph
Min (nmol C L^{-1} d^{-1})	0.007	0.005	-
Max (nmol C L^{-1} d^{-1})	0.014	0.009	-
Mean (nmol C L^{-1} d^{-1})	0.011	0.007	0.002

3.4 Discussion

3.4.1 Depth-profile of carbon flows

In this study, net primary production (NPP) is based on label incorporation into POC in light incubations, which partly might be transferred also to the DOC pool. In Lake Lucerne, however, no substantial transfer to the DOC pool was observed and hence NPP is solely based on production of POC (Fig. 3.4d, Table 3.1). NPP showed a clear decrease with depth, with a maximum rate of 1.0 µmol C L^{-1} d^{-1} at 5 m and a low production rate of 0.2 µmol C L^{-1} d^{-1} at 20 m water depth. Below 20 m, no substantial labelling of POC (>5‰) was observed, indicating that NPP (photosynthesis) at those depths is insignificant. This is consistent with summer Secchi depths of about 5.8±1.4 m in Lake Lucerne (Bossard et al. 2001).

To quantify bacterial production and respiration, labelled glucose was added as a substrate. Compared to the naturally available DOC, glucose is likely degraded more easily and hence the glucose-based production and respiration rates used here are likely overestimates of the actual rates, representing potential rates. Conversely, production and respiration by some microbes that do not use glucose could not be traced. During the bottle experiments, GP values were low (around 0.08 µmol C L^{-1} d^{-1}, Fig. 3.4e, Table 3.1) and relatively stable throughout the water column with only somewhat higher rates observed near the surface and deeper in the water column. GP at 5 and 10 m water depth is likely related to photoautotrophic production given that heterotrophic activies are positively correlated with primary production (Cole et al. 1988). This was confirmed in our light incubation showing transfer of ^{13}C-DIC via phytoplankton to heterotrophic bacteria (Fig. 3.5a). At 75 m water depth, near the lake floor, higher GP may derive from settled or re-suspended material, since no local primary production was observed (Fig. 3.4d). A higher GP rate may also be observed at 40 m, although there was no evidence for increased supply of substrate to explain higher rates of GP and differences are small. Since the low POC concentrations did not allow for true replication it is difficult to quantify error propagation and we therefore refrain from explaining such minor features.

The relative rates of NPP and respiration provide crucial information about the potential for storage or release of carbon from the lake system. In many unproductive systems, respiration is higher than NPP, indicating that microbes must consume external (allochthonous) organic matter, resulting in higher lake pCO_2 and a subsequent net flux of CO_2 into the atmosphere (Del Giorgio and Peters 1994, Del Giorgio et al. 1997). Integrated over the water column, respiration rates are approximately 50% lower than rates for NPP, indicating Lake Lucerne was net

autotrophic during our experiment (Table 3.1). It should be noted however, that the experiment took place during the most productive season of the year.

Transfer of ^{13}C-glucose to DIC exceeds that to POC near the surface, showing that glucose-catabolism is more important than glucose-anabolism, possibly as a result of competition for nutrients with phytoplankton (Bratbak and Thingstad 1985). The strong coupling between DIC and POC labeling below 10 m water depth suggests growth of heterotrophic producers is not nutrient limited deeper in the water column. Relative rates of GP and respiration can be expressed in bacterial growth efficiencies (BGE, Table 3.1), which increase below 10 m water depth. Although reports are inconclusive whether glucose-addition stimulates growth under oligotrophic conditions (Del Giorgio and Cole 1998), this seems likely in our experiment since BGE's in oligotrophic systems are usually much lower than those observed here. More complex substrates that make up most of the natural DOC pool are likely more refractory and hence extrapolation from a single compound such as glucose may lead to overestimation of BGEs (Del Giorgio and Cole (1998) and references therein).

3.4.2 Phytoplankton production

Photoautotrophy – Autotroph-derived PLFAs in bicarbonate-labelled light incubations (Fig. 3.5a) show decreasing photosynthetic production rates with depth. The relatively shallow zone of high productivity is in line with summer Secchi depth observations of about 5.8±1.4 m for Lake Lucerne (Bossard et al. 2001). Maximum oxygen concentrations at 10 meter depth exceeded maximum solubility of oxygen at the in situ temperatures (Fig. 3.2b), indicating highest NPP occurs at this depth. Below this depth productivity is much lower, decreasing to a production rate of 0.2 μmol L^{-1} d^{-1} at 20 m water depth. Since individual PLFAs at the same depth do not show substantial label incorporation this may indicate photosynthesis without growth of biomass, e.g. producing storage carbohydrates (sugars) as a result of nutrient and/or light depletion (Granum et al. 2002, Grosse et al. 2015). Also in the dark experiments low production rates for autotroph-derived PLFAs were observed, albeit that these rates are two to three orders of magnitude lower than bicarbonate-based production at the corresponding depths (Fig. 3.5b).

Chemoautotrophy – Production of biomass by bacteria or archaea using energy obtained from inorganic electron donors rather than sunlight is called chemo(litho)autotrophy. In the DIC-labelled incubations the isotopic signatures of branched bacterial PLFAs and the more general PLFA C16:1ω7c showed some isotopic enrichment at 60 m water depth, indicating this was probably the main depth for chemoautotrophic production, which is in line with Blaga et al. (2011). Production rates are, however, low compared to those in the top 10 m of the water column and only these specific PLFAs were labelled. Consequently, chemoautotrophic production rates were too low to be reflected in the POC pool and contribute little to primary production in Lake Lucerne.

Mixotrophy – The ability of certain phytoplankton species to switch between inorganic and organic carbon sources for the production of biomass is called mixotrophy. From amongst others diatoms it is known that they are able to take up carbohydrates to metabolize (Lewin 1953). Mixotroph-derived PLFAs observed in this study (C16:2ω7, C16:3ω4, C16:4ω1 and C20:5ω3) can be produced by Bacillariophyceae (diatoms), although C20:5ω3 is also produced by Rhodophyta, Cryptophyta and Haptophyta (Dijkman and Kromkamp 2006). Mixotrophic production was substantial in the bottle experiments (Fig. 3.5a,b), with production rates

(summed production based on bicarbonate and glucose) at 5 and 10 m of 28% and 55% of autotrophic production rates respectively. At 5 m water depth, DIC was more important as a substrate for the production of these PLFAs, whereas at 10 m depth production rates in light and dark (DOC) incubations are the same order of magnitude. More similar production rates for autotrophs and mixotrophs at 10 m depth compared to 5 m indicate that mixotrophy is a metabolic advantage for mixotrophs to keep up production at this depth, where conditions become less favorable for autotrophic growth.

3.4.3 Bacterial production

Glucose incorporation into bacterial branched PLFAs and PLFA C16:1ω7c in the dark incubations derives from heterotrophic production (Fig. 3.5b). It should be noted that PLFA C16:1ω7c is produced by both bacteria and phytoplankton and hence in the dark bottle incubations at 5 and 10 m water depth may partly derive from mixotrophs. Diatoms, the inferred mixotrophic producers at these depths (see above) produce lower amounts of C16:1ω7c compared to PLFAs used here to represent mixotrophs (Dijkman and Kromkamp 2006), yet production rates of C16:1ω7c are much higher and show a different trend with depth. It thus seems unlikely that production by mixotrophs has substantially contributed to the labelling of C16:1ω7c in dark incubations. In general the pattern in C16:1ω7c corresponds well with the bacterial-derived branched PLFAs and calculated GP. Only at 10 m water depth, branched bacterial PLFAs and C16:1ω7c likely derive from different source organisms since the production rate of production of C16:1ω7c is still high, while branched PLFA production has decreased substantially.

Production of labelled branched bacterial PLFAs at 5 and 10 m water depth in the light incubations most likely derives from organic carbon exudation by phytoplankton: the release of excess organic molecules when carbon fixation is higher than incorporation into new cell material (Fogg 1983). Although exudation of organic carbon by phytoplankton was not sufficient to change the carbon isotopic composition of the DOC pool (Fig. 3.4d), it is likely that some labelled organic carbon was produced nonetheless and preferentially used as a substrate by bacteria, since consumption of the extracellular compounds by heterotrophs was found to be both substantial and rapid (Fogg 1983).

From 5 to 10 m water depth a decrease in alkalinity was observed (Fig. 3.3c), which can result from different processes. Biological precipitation of $CaCO_3$ by organisms such as coccolithophores (Haptophyta) leads to a decrease in alkalinity (Zeebe and Wolf-Gladrow 2001), primary production based on ammonium (Soetaert et al. 2007), and oxidation of reduced nitrogen (nitrification) and sulfur, generated during remineralization of algae, can also decrease alkalinity (Wolf-Gladrow et al. 2007). In Lake Lucerne remineralization is a possible explanation for the lower alkalinity values at 10 m depth, since it is in line with the observed maximum in glucose-based respiration rates at this depth. Moreover, at 10 m water depth, a maximum can be observed in bicarbonate-based production of C16:1ω7c, which is produced by many organisms including nitrifying bacteria (De Bie et al. 2002, Guezennec and Fialamedioni 1996, Lipski et al. 2001) and sulfur-oxidizing bacteria (Van Gaever et al. 2009, Zhang et al. 2005). In Lake Lucerne, a maximum in calcite precipitation caused by picocyanobacteria was previously identified at 10 m water depth during summer. The PLFA concentration profiles show no indication for higher cyanobacterial abundance at 10 m although cyanobacterial production cannot be ruled out, since not all cyanobacteria produce unique PLFAs.

3.4.4 Comparison to eutrophic Lake Rotsee

Bottle labelling experiments similar to those described above in Lake Lucerne were carried out in Rotsee during the same month (Chapter 2). Rotsee is a eutrophic lake north of Lake Lucerne (Fig. 3.1), which is connected to Lake Lucerne via the Reuss-Rotsee canal. Because of their proximity, surface light conditions, air temperatures and precipitation in winter and spring leading up to the experiments were very similar. Therefore, differences in the carbon fluxes between Lake Lucerne and Rotsee result from their contrasting trophic states and corresponding microbial communities.

The depth-integrated NPP rate was ~24 times higher in eutrophic Rotsee (Table 2.1) compared to oligotrophic Lake Lucerne (Table 3.1). The much deeper photic zone in oligotrophic Lake Lucerne apparently does not compensate for the much higher volumetric NPP rates in Rotsee. However, rates of glucose-based production and respiration were only 3.5 and 4.5 times higher in Rotsee respectively, indicating a closer coupling with NPP in Lake Lucerne, which is as expected since availability of alternative substrates is limited in oligotrophic Lake Lucerne. Overall, in Lake Lucerne the sum of glucose-based production and respiration rates are approximately equal to the rate of NPP and the sedimentary C_{org} content was relatively low at 1.5-3% (Blaga et al. 2011). In Rotsee, the much higher NPP rate compared to the sum of glucose-based production and respiration rates potentially results in net carbon storage in the sediment, in line with a C_{org} content of 10-11% (data not shown).

3.4.5 Mesocosm labelling: carbon transfer to bacteria

3.4.5.1 Mesocosm conditions

During the mesocosm labelling experiment in spring, water temperatures rapidly increased by about 3 degrees in 14 days (Fig. 3.6a). From T_{11}, a thermocline starts to develop around 5 m water depth, with deeper water not warming to temperatures >7.5 °C (data not shown). Surface water temperatures however, are still about 7.5 degrees colder than during the bottle incubations in June (Fig. 3.3a), allowing for higher dissolved oxygen concentrations. At the observed temperatures between 6 and 10 °C, dissolved oxygen saturation concentrations range between ~400 and 353 µmol L^{-1} respectively. Higher observed concentrations between 440 and 510 µmol L^{-1} (Fig. 3.6b) indicate biological production of oxygen. Decreasing oxygen concentrations follow increasing water temperatures from T_7 onward, but a cause for the variability in oxygen concentrations before T_7 is not known.

3.4.5.2 PLFA production

Production rates during the mesocosm experiment were substantially lower for both phytoplankton and bacteria compared to the bottle experiments. The difference between production in the mesocosm and the bottles is in line with the timing of the experiments. The observed rapid increase in water temperatures during the mesocosm experiment usually precedes the onset of the spring bloom. Additionally, the difference in bacterial production rates may partly be related to the so-called bottle-effect, with enhanced substrate-availability for heterotrophs in the bottle incubations stimulating productivity. However, there were also substantial differences between the experiments in terms of light climate, temperatures and turbulence. Because of the mysterious and somewhat controversial nature of the bottle-effect (Hammes et al. (2010) and references therein), and the inherent difficulty to quantify this effect,

we will not discuss it further here and fully attribute the observed differences in production rate to seasonal variability. It should be noted that the lower values (< 5‰) of relative label incorporation during the mesocosm are close to the detection limit of the method, bringing uncertainty to the calculated production rate for heterotrophic bacteria.

Production of phytoplankton PLFAs occurred at two different rates (Fig. 3.7 and Table 3.2). The difference in isotopic enrichment and production rates of PLFA C18:3ω3 compared to C18:4ω3, C20:4ω6 and C20:5ω3 (Fig. 3.7) is suggestive of a change in the phytoplankton population as a result of changing conditions in the mesocosm.

Transfer of newly fixed (labelled) carbon to bacteria lags behind early-growing phytoplankton more than 6 days and behind late-growing phytoplankton more than 2 days. A wide range in lag time has been observed in previous studies. De Kluijver et al. (2010) observed a lag of 2-3 days in incubations under different CO_2 levels. A lag of ~1 day was found in a mesocosm labelling study in a Danish estuary (Van den Meersche et al. 2004). Much longer lag times of 14 days (Hoppe et al. 2008) and ~1 month (Ducklow et al. 2001) have also been observed, likely related to colder (winter) temperatures. The relatively slow bacterial response during the Lucerne mesocosm experiment renders it impossible to statistically correlate phytoplankton dynamics with bacterial dynamics or to determine whether bacteria had reached isotopic equilibrium during the 15-day experiment. Nevertheless, we calculate that only 22% of the bacterial carbon was derived from recently fixed phytoplankton at the end of the experiment, which is more or less consistent with the bottle experiments in which 28% of bacterial carbon was derived from labelled phytoplankton after the experiment (4 days). In a whole-lake DIC ^{13}C-labelling experiment (56 days), an almost complete dependency (88-100%) of heterotrophic bacteria on autochthonous carbon was found (Pace et al. 2007). Mesocosm labelling experiments found bacterial dependency on recently fixed phytoplankton material as high as 70% (Lyche et al. 1996) and 87% (De Kluijver et al. 2010). Although it is questionable whether isotopic equilibrium was achieved in our experiment, the observed dependence seems to be relatively low, which, in combination with the observed time-lag shows uncoupling between phytoplankton and heterotrophic bacteria on the timescale of weeks.

Uncoupling between phytoplankton and bacteria can have several explanations, one being that it may take a while to produce labelled substrate available to heterotrophs. The transfer of carbon from phytoplankton to heterotrophs occurs mainly via the pool of labile dissolved organic matter (DOM), which becomes enriched through exudation of organic carbon. Since phytoplankton production rates were low it likely took some time to enrich the pool of labile DOM sufficiently to manifest itself in newly produced bacterial matter. A second explanation is a potential state of dormancy in bacteria when there is a lack of suitable energy-yielding substrates (Morita 1982). This may also explain faster labelling of bacterial biomass during the bottle experiment in early summer. Seasonal evolution in the occurrence and the length of lag periods has been demonstrated in seawater culture experiments (Ducklow et al. 1999). When there is strong coupling between phytoplankton and heterotrophic bacteria, degradation results in an almost instant remineralization of photosynthesized organic matter and in recycling of CO_2. When there is a long time lag, dead phytoplankton biomass may sink and not be available for bacterial degradation in surface water, resulting in carbon export to deeper water.

3.5 Conclusions

The depth-integrated rate of NPP during the early summer bottle experiments in Lake Lucerne was 15.8 mmol C m^{-2} d^{-1}. During a similar experiment in nearby eutrophic Rotsee depth-integrated rates of NPP were ~24 times higher, showing that the deeper photic zone in Lake Lucerne didn't compensate for the higher volumetric NPP rates in Rotsee. In Lake Lucerne, autotrophic production was primarily located in the upper 20 m of the water column, but labelling of PLFAs provided evidence for some chemoautotrophic production at 60 m water depth. During the bottle experiments, label was transferred from phytoplankton to bacteria at 5 and 10 m depth and at the end of the experiment 28% of bacterial carbon was derived from freshly produced phytoplankton organic matter.

Depth-integrated glucose-based production and respiration rates were each ~50% of NPP rates (7.8 and 7.7 mmol C m^{-2} d^{-1} respectively). This close coupling between bacterial production and respiration with NPP was much stronger than in the Rotsee bottle experiments, where the depth-integrated NPP rate was >12 times higher than the sum of glucose-based production and respiration. This indicates that heterotrophic producers are well adapted to rapidly respond to an increase in primary productivity, which is in line with calculated bacterial growth efficiencies in the surface water layer.

During the spring mesocosm experiment, phytoplankton and bacterial production rates were 1-2 orders of magnitude lower than during the bottle experiments, agreeing with the timing of the experiment preceding the spring bloom. Bacterial production lagged ±6 days compared to early-growing phytoplankton. A low fraction of ~22% of bacterial carbon was derived from phytoplankton production at the end of the experiment. Compared to the bottle experiment, coupling between phytoplankton and bacteria is weaker and potentially more organic matter could escape recycling. This uncoupling is likely related to slow transfer of phytoplankton organic carbon to the pool of labile DOM.

Chapter 4

Carbon flows in macrophyte- and phytoplankton-dominated sections of a hypereutrophic, subtropical shallow lake (Taihu, China)

But still, like dust, I'll rise. Into a daybreak that's wondrously clear, I rise
– Maya Angelou –

Abstract

Eutrophication is one of the most serious and extensive environmental problems worldwide, which in lakes often results in cyanobacterial blooms, degrading ecosystems by reducing oxygen concentrations and lowering biodiversity. Lake Taihu (China) is a subtropical, shallow, hypereutrophic lake characterized by severe *Microcystis* blooms. In a section northeast of the lake (Wuli Lake) a series of biomanipulation measures were taken (planting of macrophytes, removal of fish and stocking of piscivorous fish) in an attempt to improve biodiversity and water quality. Here we present the results of mesocosm labelling experiments in two sections of the lake: unrestored Meiliang Bay and the restored Lake Wuli, using ^{13}C and ^{15}N as deliberate tracers to follow carbon and nitrogen flows through the food web. Samples were taken for zooplankton, epiphytes and macrophytes, while compound-specific isotope analyses on biomarker lipids allowed us to also include microbial producers (phytoplankton) and consumers (bacteria). A simple isotope model was used to determine turnover rates and to assess C and N sources for these components. Results show that carbon flows shifted from phytoplankton-dominated in Meiliang Bay to macrophyte-dominated in Wuli Lake, with primary production in Wuli Lake being up to 3 times higher than in Meiliang Bay. Interestingly, Wuli Lake was severely CO_2-limited ($CO_{2(aq)}$ was 0.6 µmol C L^{-1} and HCO_3^- was 681 µmol C L^{-1}), forcing phytoplankton to derive significant amounts of their carbon consumption from dissolved organic carbon in addition to dissolved inorganic carbon, in contrast with macrophytes which incorporated only labelled DIC-derived carbon. Bacterial production rates were similar in both lakes, but zooplankton production was higher in Meiliang Bay, likely using cyanobacteria-derived material as a food source. Zooplankton:phytoplankton biomass ratios of 0.2 and 0.16 in Meiliang Bay and Wuli Lake respectively indicate that restoration measures were not successful in increasing grazing pressure on phytoplankton. Nitrogen isotope data were not well constrained, but confirmed the rapid cycling inferred from carbon isotopes in both the restored and unrestored parts of this highly eutrophic lake.

4.1 Introduction

Eutrophication of freshwater lakes is one of the most pervasive and also one of the most severe environmental problems on a global scale since lakes provide many ecological services including fisheries and freshwater supply for drinking water and irrigation. Eutrophication results in loss of oxygen, biodiversity, fish and aquatic plant beds, thereby degrading ecosystems (Carpenter et al. 1998). Additionally, eutrophication often leads to extensive and persistent cyanobacterial blooms (Schindler 2006), which reduce light permeability and increase turbidity, and thereby suffocate macrophytes and degrade fish habitats. During post-bloom conditions, oxygen concentrations can decrease, also killing aquatic life. Some cyanobacteria (e.g. *Microcystis*) produce toxic substances (microcystins), potentially causing liver damage and neurological and skin diseases in humans. Global warming is expected to intensify cyanobacterial blooms (Paerl and Huisman 2008), making the problem of lake eutrophication even more urgent.

According to the theory of alternative stable states, lakes with similar nutrient inputs can be in either a eutrophic, turbid state characterized by high phytoplankton biomass, or a clear state dominated by macrophytes (Scheffer et al. 1993). Based on this theory, restoration of shallow eutrophic systems by reducing nutrient loading alone is rarely successful since water clarity and (re)colonization by plants also depend on internal phosphorous recycling (Søndergaard et al.

2003) and biological feedbacks from macrophytes, zooplankton and fish (Jeppesen et al. 1997, Jeppesen et al. 1999, Scheffer et al. 1993, Schindler 2006). Therefore, in addition to nutrient reduction, biomanipulation measures are commonly used in lake restoration, consisting of the addition of macrophytes and addition/removal of certain fish species in order to facilitate change from the turbid towards the clear state. Reduction of phytoplankton biomass can be achieved in several ways. First, macrophyte addition increases nutrient competition with phytoplankton. Second, macrophytes also provide shelter for zooplankton against predation by fish, leading to increased grazing pressure on phytoplankton (higher zooplankton:phytoplankton ratio). The removal of plankti-benthivorous fish or the addition of piscivorous fish may reduce grazing pressure on zooplankton, also favouring higher zooplankton concentrations. In addition to these effects, removal of predators and the introduction of macrophytes can also influence other variables such as pH, concentrations of CO_2 and O_2, and impact carbon flows in the microbial food-web (Bontes et al. 2006, Schindler et al. 1997). Hence, manipulation of fish and submerged macrophytes may have substantial impact on ecosystem structure and functioning, especially in shallow, eutrophic lakes as these lakes exhibit stronger top-down control (Jeppesen et al. 1997).

Though less frequently studied, biomanipulation in warm lakes seems to be more complex than in temperate lakes due to differences in fish community and lower sheltering effect of macrophytes due to accumulation of fish among the plants (see Jeppesen et al. (2012) for an extensive review). For example, in tropical freshwater systems omnivorous fish are more abundant (Moss 2010, Teixeira-de Mello et al. 2009), fish density and biomass are higher (Gyllström et al. 2005) and reproduction takes place throughout the year instead of seasonally (Fernando 1994), all of which have a negative effect on macrophyte recolonization. Moreover, the effects of biomanipulation on overall carbon flows are not well studied since most studies focus on fish and macrophytes rather than the microbial part of the food web (Jeppesen et al. 2012). Yet, the microbial food web generally becomes more important during eutrophication due to increasing cyanobacterial dominance and subsequent shifts in zooplankton community structure towards smaller crustaceans and rotifers (Fulton and Paerl 1988).

Here we examine differences in food-web dynamics and carbon flows between two parts of subtropical, shallow Lake Taihu (China): an unrestored hypereutrophic bay and a biomanipulated section. In 2010, a section of Lake Taihu (Wuli Lake) was subjected to a dual-treatment biomanipulation project, with removal of large fish, stocking of piscivorous fish and re-planting of macrophytes (Yu et al. 2016). Even though the fish population had recovered after approximately a year, the restoration was successful in re-establishing a macrophyte-dominated clear-water state (Yu et al. 2016). For this study mesocosms were placed in both restored and unrestored sections and were labelled with ^{13}C-bicarbonate and ^{15}N-ammoniumchloride. Stable isotope enrichment experiments provide a powerful tool to compare the food web community and trace carbon and nitrogen transfer through these food webs (Middelburg 2014). In the past, it has been a challenge to differentiate between particulate organic carbon and microbial groups, but nowadays the application of stable isotope analyses on biomarker lipids allows for the direct assessment of phytoplankton and bacteria through their associated biomarkers and thus allows for the inclusion of the microbial domain. Here we use phospholipid-derived fatty acids (PLFAs), membrane lipids that are produced by a wide range of organisms and which have previously been successfully applied in microbial food-web studies (Bontes et al. 2006, De Kluijver et al. 2013, Van den Meersche et al. 2004) and chapters 2 and 3 of this thesis. Subsequently, using a simple isotope model, we quantify turnover rates of microbial groups

(phytoplankton and bacteria), zooplankton, macrophytes and epiphytes and compare these between the unrestored and restored lake sections.

4.2 Material and methods

4.2.1 Study site

Lake Taihu, a large and shallow lake is China's third largest lake with a surface area of 2338 km^2. It is located near Shanghai in the Yangtze Delta and serves as an important drinking water supply for the highly industrialized and densely populated area. Intense nutrient loadings have changed the trophic state of the lake from oligotrophic until the mid-20th century to its current hypereutrophic state. Meiliang Bay, a northern basin of Lake Taihu (Fig. 4.1) is dominated by *Microcystis* blooms during summer. In 2007, a massive *Microcystis* bloom occurred near the inlet of a water plant, causing ~2 million people in Wuxi City to be without drinking water for at least a week (Qin et al. 2010). Subsequently, a restoration project was started in Wuli Lake, a basin northeast of Meiliang Bay (Fig. 4.1) in 2010. With the objective to improve water quality and restore aquatic biodiversity, a plot of 5 ha was isolated from the lake. No restoration measures were implemented in the remainder of Lake Taihu, including Meiliang Bay, making this an excellent site to compare to. Several characteristics of Meiliang Bay and restoration site Wuli Lake as measured at the start of the mesocosm experiments are summarized in table 4.1.

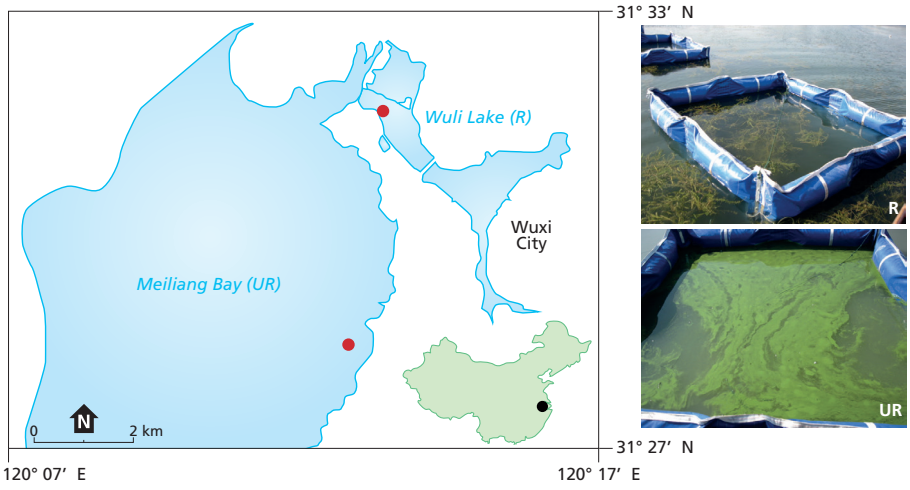

Fig. 4.1 Map showing the locations (red circles) of the experiments in unrestored Meiliang Bay and restoration site Wuli Lake. Photos on the right show mesocosm set-ups as placed in restored Wuli Lake (top) and unrestored Meiliang Bay (bottom), dominated by macrophytes and cyanobacterial blooms respectively.

Table 4.1 Characteristics of Meiliang Bay (unrestored) and Wuli Lake (restored) at the start of the experiment (T_0).

	Meiliang Bay (UR)	Wuli Lake (R)
Water depth (m)	1.6	1.9
Secchi depth (m)	0.3	1.7
Diss. Oxygen (mg L^{-1})	3.1	9.3
pH	8.2	9.1
P_{CO2} (µatm)	243	17.1
CO_2 (µmol L^{-1})	8.5	0.6
HCO_3^- (µmol L^{-1})	1366	681
CO_3^{2-} (µmol L^{-1})	114	393
Total P (mg L^{-1})	0.2	0.03
Total N (mg L^{-1})	2.2	0.6
NH_4 (mg L^{-1})	0.21	0.17
Suspended solids (mg L^{-1})	71.2	6.1
Chl. a (µg L^{-1})	45	6

4.2.2 Experimental design and sample collection

In 2011, in situ mesocosm experiments were carried out in Wuli Lake (R, restored) and Meiliang Bay (UR, unrestored) from September 28 until October 19 (22 days). For these experiments, three enclosures were placed at each location (6 in total), which were 2.5 x 2.5 m wide and anchored to the lake floor, hence their depth depended on lake depth (Table 4.1). Mesocosms were open at the bottom and top (Fig. 4.1), allowing for exchange between water column and lake sediment and atmosphere. After placement of the mesocosms, the system was allowed to accommodate for 3 days before sampling and nitrogen and carbon labelling. Mesocosms were sampled with varying intervals between sampling, from day 0 (T_0) until day 21 (T_{21}). After initial sampling (T_0), each mesocosm was labelled with ^{13}C-bicarbonate (0.2 mg L^{-1} $NaHCO_3$, >99% ^{13}C) and ^{15}N-ammonium (0.1 mg L^{-1} NH_4Cl, >98% ^{15}N), increasing the DIC concentrations relatively by 0.21% and 0.16% in Wuli Lake and Meiliang Bay respectively and the NH_4 concentrations by 19.6% and 16.1% in Wuli Lake and Meiliang Bay respectively. ^{15}N was added as ammonium since this is preferred over nitrate by most micro- and macrophytes (Gribsholt et al. 2005). Samples for dissolved inorganic carbon (DIC), dissolved organic carbon (DOC), and water samples for chlorophyll *a* (except T_5 and T_6), bulk suspended particulate matter (SPM) and PLFA biomarkers (except T_{19}) were collected after label introduction at $T_{0.5}$ and daily during the first week of the experiments, while during the last two weeks samples were collected every second day. At these days also Secchi depth and water temperature was measured. On days 0, 0.5, 1, 4, 7, 11, 15 and 21 dissolved oxygen concentrations, pH, and water temperatures were measured using a YSI Handheld Multiparameter meter (YSI6500) and samples were collected for suspended solids, nutrients, alkalinity, $\delta^{13}C$ and $\delta^{15}N$ of macrophytes, epiphytes, phytoplankton, zooplankton (extra on T_3 and daily between T_6 and T_{17}) and surface sediment.

Samples for DIC concentrations and isotopic composition were collected air-free in 20 ml headspace vials, sealed using air-tight caps and poisoned with mercury chloride. Samples were stored in the dark and upside down at room temperatures. Samples for DOC were filtered through 0.45 µm GM/F filters and stored at -20 °C until further analysis. Water samples (2

litres) for bulk SPM intended for analyses of concentrations and C and N isotopic composition of particulate organic carbon and nitrogen (POC and PON respectively) were filtered through pre-combusted and pre-weight 0.7 µm GF/F filters and dried for 24 hours at 60 °C. Water samples (3 L) for SPM intended for concentrations and carbon isotopic composition of PLFA biomarkers were also filtered through pre-combusted and pre-weighted 0.7 µm GF/F filters and stored frozen (-20 °C) until further analyses. Sediment was collected using a handheld corer. New leaves of the dominant macrophyte species (*Myriophyllum* sp.) were collected and submersed in distilled water and shaken until the epiphytes detached. The water containing epiphytes was filtered through a 0.7 µm GF/F filter and both epiphytes and macrophyte leaves were subsequently stored frozen (-20 °C) until further analyses. Zooplankton samples for bulk isotopes were hand-picked and dried overnight at 60 °C. Zooplankton numbers did not allow for separation between species, however, in Meiliang Bay mainly *Bosmina* and *Ceriodaphnia* were picked while in Wuli Lake mainly *Bosmina* and Copepods were picked.

4.2.3 Laboratory analyses

DIC concentrations of water samples were measured on a Shimadzu TOC-5050A Carbon analyzer, calibrated to an in-house seawater standard. For $\delta^{13}C$ analyses of DIC a helium headspace was created over the DIC samples, which were subsequently acidified using a H_3PO_4 solution. Carbon stable isotope values of the resulting CO_2-gas were then measured using a gas bench coupled online to an IRMS (Thermo Delta V advantage). Accuracy and precision of the carbon stable isotope analyses was better than 0.1‰, based on multiple analyses of samples and in-house (Na_2CO_3) and international (LSVEC, Li_2CO_3) standards. Samples for the analyses of DOC concentrations and the $\delta^{13}C$ of the DOC were treated and analyzed following Boschker et al. (2008) using high-performance liquid chromatography-isotope ratio mass spectrometry (HPLC-IRMS, Thermo Surveyor system coupled to a Delta V Advantage using and LC-Isolink interface).

Chlorophyll *a* (Chl *a*) samples were filtered through cellulose acetate membrane filters and extracted using acetone. Chl *a* concentrations were then measured spectrophotometrically. Samples for particulate organic carbon and nitrogen (POC, PON) concentrations and carbon and nitrogen isotopic compositions of SPM, zooplankton and sediment were decalcified by placing them overnight in a desiccator with fuming hydrochloric acid (37%) and were subsequently weighed into tin cups. Additionally, samples for TOC/TON concentrations and $\delta^{13}C$ and $\delta^{15}N$ of sediment, zooplankton, epiphytes and macrophytes were weighed in tin cups. Except for the SPM samples, all samples were freeze dried before analyses. Concentrations were measured using an elemental analyzer (EA) (Fisons Instruments NA1500), with the $\delta^{13}C$ being analyzed on an online coupled IRMS (Thermo Deltaplus). Precision and accuracy for ^{13}C and ^{15}N of SPM was better than 0.15‰ based on in-house (Graphite quartzite, Ammonium Sulfate and Nicotinamide) standards. Precision of sediment, zooplankton, epiphytes and macrophytes was better than 0.2‰ for ^{13}C and 2.2‰ for ^{15}N.

Lipids were extracted from freeze-dried SPM samples using a modified Bligh and Dyer extraction technique, followed by separation into simple lipid (SL), glycolipid (GL) and phospholipid (PL) fractions based on polarity (Dickson et al. 2009). Phospholipid-derived fatty acids in the PL fractions were converted to fatty acid methyl esters (PL-FAMEs) by mild alkaline transmethylation (White et al. 1979). C12:0 and C19:0 FAMEs were added as internal standards. Concentrations were analyzed using a gas chromatograph (HP 6890) with Helium as carrier gas set at constant pressure and fitted with a flame ionization detector (FID) and a

VF-23ms column (0.25 mm i.d.). Mass spectrometry was performed using a Thermo Trace GC Ultra, with Helium set at constant flow. Compounds were identified based on retention times and mass spectra and double-bond positions were determined after derivatization with dimethyl-disulfide (DMDS) (chapter 5). Compound-specific $\delta^{13}C$ values were determined using GC-C-IRMS with a ThermoFinnigan Delta Plus XP using the same type of column as for GC. Oven programming of GC-FID, GC-MS and GC-C-IRMS followed Middelburg et al. (2000). For all PLFAs, values are reported in ‰ vs. Vienna Peedee Belemnite (VPDB) and were corrected for the added carbon atom during methylation. Carbon isotopic values of the derivatizing agents were determined offline. Stable isotope results are reported as mean ± standard deviation of the three mesocosms at each sampling site.

4.2.4 PLFA assignments

In both Wuli Lake and Meiliang Bay, a suite of PLFAs was detected, including branched PLFAs iC14:0, iC15:0 and aC15:0. These PLFAs are abundant in gram-positive bacteria (Kaneda 1991) and also occur in some gram-negative bacteria (Haack et al. 1994). Hence, weighted isotope ratios of iC14:0, iC15:0 and aC15:0 were used to represent $\delta^{13}C$ of bacteria. In restored Wuli Lake, in addition to bacteria-derived PLFAs, also C18:3ω6, C18:3ω3, C18:4ω3, C20:4ω6 and C20:5ω3 were major PLFAs. These PLFAs are produced by different phytoplankton groups, including green algae, haptophyte algae and cyanobacteria (Dijkman and Kromkamp 2006, Gugger et al. 2002, Taipale et al. 2013). Since no cyanobacterial blooms occur in this restored lake and cyanobacteria are not considered dominant species, only PLFA C18:3ω6 can be attributed specifically to cyanobacteria (Gugger et al. 2002) and the other PLFAs are attributed in this study to phytoplankton in general.

In cyanobacteria-dominated, unrestored Meiliang Bay, phytoplankton-derived PLFAs C18:3ω6, C18:3ω3, C18:4ω3, C18:2ω6c, C18:1ω9c, C20:4ω6 and C20:5ω3 were detected. In a study on carbon flows between cyanobacteria and zooplankton in Lake Taihu, it was established that PLFAs C18:3ω6, C18:3ω3, C18:4ω3, C18:2ω6c and C18:1ω9c were major PLFAs in indigenous *Microcystis* (De Kluijver et al. 2012), which was in accordance with previous results (Ahlgren et al. 1992, Gugger et al. 2002). Hence, these PLFAs are here also attributed to cyanobacteria. Only PLFAs C20:4ω6 and C20:5ω3 are attributed to phytoplankton in general since long-chain (C20 – C22) PLFAs are not usually observed in cyanobacteria (Ahlgren et al. 1992, Gugger et al. 2002).

Phytoplankton biomass was calculated from average (T_0-T_{21}) chlorophyll *a* concentrations using a ratio of C:Chl *a* = 40 (Del Giorgio and Gasol 1995) and thus include cyanobacterial biomass. Bacterial biomass was calculated by taking the average (T_0-T_{21}) sum of bacteria-derived PLFAs iC14:0, iC15:0 and aC15:0 and applying a C:PLFA ratio of 50. Zooplankton biomass was assumed to be 0.085 mg L^{-1} (dry weight) for Wuli Lake and 0.557 mg L^{-1} (dry weight) for Meiliang Bay (Chen, unpublished data) and using a ratio of C:dry weight of 0.46 to obtain zooplankton C biomass (Andersen and Hessen 1991). Macrophyte fresh (wet) biomass (including epiphytes) in Wuli Lake was 249.8 g m^{-2} for *Myriophyllum* sp. and 628.2 g m^{-2} for total macrophytes (Guan, unpublished data). We assumed carbon to make up between 20 and 40% of fresh weight (Clarke 2002).

4.2.5 Model

A simple source-sink isotope ratio model was used to quantify incorporation of labelled carbon and nitrogen by phytoplankton, cyanobacteria, macrophytes and epiphytes, and subsequent

transfer to bacteria and zooplankton. The model was based on De Kluijver et al. (2010), Hamilton et al. (2004) and Van Oevelen et al. (2006), which, for n carbon sources, results in the following ordinary differential equation:

$$\frac{d\delta^{13}C_{sink}}{dt} = \mu_{sink} * \left[\sum_{i=1}^{n} f_i * \delta^{13}C_{source_i}\right] - \mu_{sink} * \delta^{13}C_{sink} \quad (1)$$

$$\text{with} \quad \sum_{i=1}^{n} f_i = 1$$

Here μ represents turnover of the sink compartment in d^{-1} and f_i is the fraction of source i in the uptake. In this model, $\delta^{13}C$ can be replaced with $\delta^{15}N$ for the nitrogen data. For the phytoplankton uptake, we assumed two sources, a labelled and unlabelled source (n = 2). As the dynamics of $\delta^{13}C$ and $\delta^{15}N$ of carbon/nitrogen pools and producers in the three replicate mesocosms at each site were very similar, we modelled the average for each site. Biomasses of phytoplankton and bacteria were relatively constant throughout the experiment and hence their time dynamics was not incorporated in the model for simplicity (see supplementary figure S4.1). The model was implemented in the open source software R (R Core Team 2015), using packages deSolve (Soetaert et al. 2010) and FME (Soetaert and Petzoldt 2010).

Isotopic signatures of dissolved inorganic and organic carbon pools (DIC and DOC), and of particulate organic carbon and nitrogen pools (POC and PON) were converted to forcing functions. Model equations for microbial groups, zooplankton, epiphytes and macrophytes are given in table S4.1. The model was run from T_0 to T_{21} and initial conditions were set as the average $\delta^{13}C$ at T_{-1} and T_0. As we did not measure the initial carbon isotopic composition of the labelled DIC, it was estimated based on the isotopic composition at T_0 and the amount of label added. The isotopic composition of dissolved ammonium at T_0 was assumed to be 0‰, and the isotopic composition after label addition was estimated based on the amount of label added. Varying the initial value for ammonium by ±20‰ did not affect model outcome given the high $\delta^{15}N$ values achieved by the labelling. The model was applied in two steps. The isotope source-sink model was first fitted to the carbon isotopes, after which the derived turnover parameters were subsequently imposed to the nitrogen isotopes to test the consistency among C and N dynamics.

The model was initially fitted manually to the carbon isotope data to narrow the range of parameters; after this an automatic calibration routine of the FME package was used to minimize the sum of squared residuals of model and data. Finally, the uncertainty in the parameter fits was assessed using a Markov chain Monte Carlo method (Geyer 2011), to generate a posterior probability distribution for the parameters (Soetaert and Petzoldt 2010). The number of runs in the MCMC simulation was set to 5000, resulting in 991 accepted runs for Wuli Lake and 1436 accepted runs for Meiliang Bay. For each parameter in the MCMC output, the mean and standard deviation were calculated. Production rates were calculated by multiplying turnover rates with average biomass concentrations during the experiment. For phytoplankton, we were unable to accurately differentiate between cyanobacterial biomass and biomass of other phytoplankton (section 4.2.4) hence we multiplied turnover rates for both cyanobacteria and phytoplankton with total phytoplankton biomass resulting in a minimum and a maximum production rate. Similarly, we combined macrophyte and epiphyte biomasses with epiphyte and macrophyte turnover to estimate combined macrophyte+epiphyte production.

4.3 Results

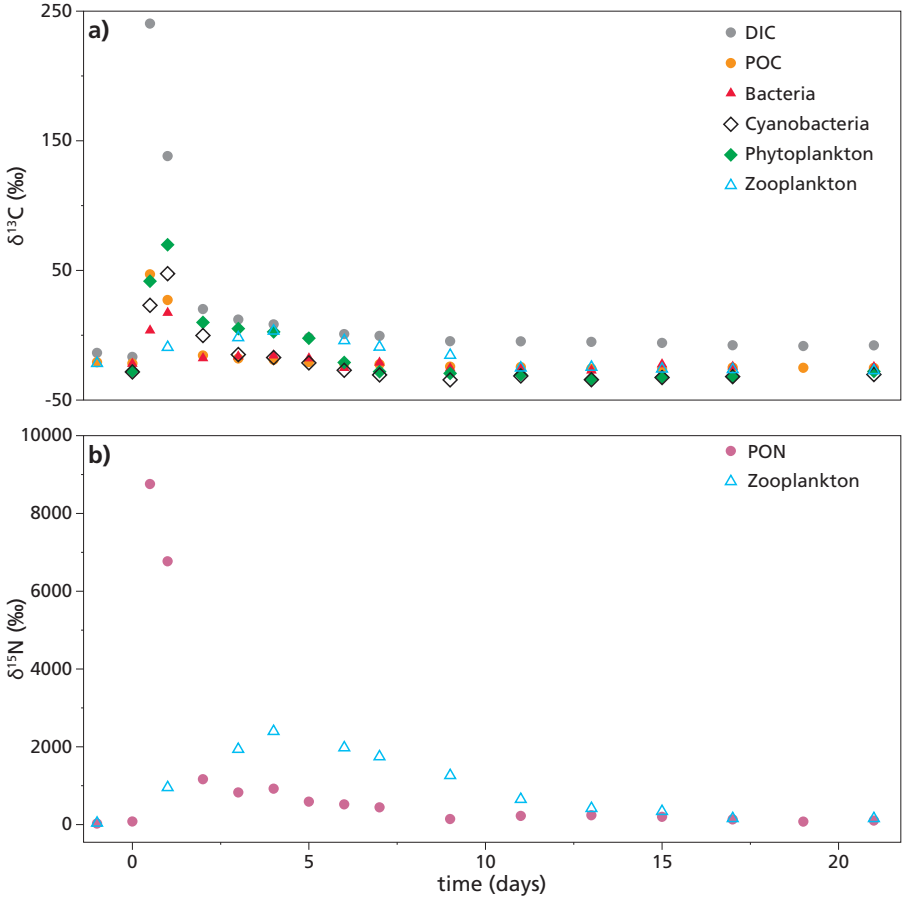

Fig. 4.2 Temporal change in isotope ratios of measured a) carbon and b) nitrogen pools in unrestored Meiliang Bay. Values in (‰ vs VPDB) are averages of three mesocosms.

4.3.1.1 Meiliang Bay isotope dynamics

Isotope dynamics in the unrestored, hypereutrophic basin Meiliang Bay from T_{-1} to T_{21}, are shown in figure 4.2a (carbon) and figure 4.2b (nitrogen), and show rapid label transfer among food-web compartments. The duration of the experiment was too short and label dilution was too high to observe label transfer to sediment and higher organisms (fish, snails). The addition of ^{13}C-bicarbonate increased the δ^{13}C of DIC from -16.7 ± 1.8‰ at T_0 to a maximum of 240.4 ± 16.0‰ at $T_{0.5}$. The isotopic composition of DIC decreased rapidly to values around 0‰ at day 5 and was back at pre-labelling values at the end of the experiment. This rapid dilution of label indicates high turnover. No label was transferred from the DIC pool to the DOC pool and values remained constant around -24.5 ± 0.7‰. Label transfer to POC reached a maximum already at $T_{0.5}$ with a δ^{13}C of 83.6 ± 33.1‰, subsequently declining rapidly to pre-labelling values at day 6 (Fig. 4.2). In corporation of labelled DIC by phytoplankton and cyanobacteria was already observed at $T_{0.5}$, but δ^{13}C reached maxima at T_1 of 69.8 ± 19.2‰ and 47.5 ±

22.3‰ respectively, declining again to pre-labelling values at day 7 (phytoplankton) and day 6 (cyanobacteria). Transfer of newly fixed ^{13}C to bacteria was similar, reaching a maximum of 17.0 ± 7.9‰ at T_1, declining rapidly to pre-labelling values at day 6. Zooplankton $\delta^{13}C$ showed a more gradual increase, reaching a maximum of 3.3 ± 6.7‰ at day 4, gradually declining to a pre-addition value at day 11.

For nitrogen, only the isotopic composition of PON and zooplankton were measured, but $\delta^{15}N$ showed a similar trend over time (Fig. 4.2b). Maximum label transfer to PON was observed at $T_{0.5}$, reaching a $\delta^{15}N$ value of 8700 ± 2000‰, which subsequently decreased to ~100 ± 14‰ at the end of the experiment. Nitrogen isotope dynamics of zooplankton also showed a similar trend as observed for carbon, with a maximum value of 2400 ± 670‰ reached at day 4. In contrast to carbon, pre-labelling values were not reached during the experiment, with $\delta^{15}N_{PON}$ remaining enriched at 160 ± 40‰ at day 21.

4.3.1.2 Meiliang Bay model output

The model fits discussed here are based on carbon isotope data, using the nitrogen data as an independent control. Reliable parameter distributions and good fits were obtained for the carbon isotope dynamics of most variables (Table 4.2 and Fig. 4.3). Most critical to obtain these good fits was the inclusion of two sources for phytoplankton, a labelled (DIC) and an unlabelled substrate (DOC), via a fraction *f* in the model. Phytoplankton carbon demand was derived mostly from labelled DIC (f = 0.79 ± 0.03), but it also comprised a significant fraction of unlabelled DOC, on average 21%. Cyanobacteria derived 56 ± 3% of their carbon from DIC and 44 ± 3% from DOC. Turnover rates were 0.79 ± 0.07 d^{-1} for phytoplankton and 0.98 ± 0.12 d^{-1} for cyanobacteria, resulting in a phytoplankton production rate between 81 and 100 µmol C L^{-1} d^{-1}. Bacterial carbon demand was derived from unlabelled DOC (14 ± 7%) and labelled POC (86 ± 7%) with a turnover rate of 0.95 ± 0.21 d^{-1} and production rate of 3.2 µmol C L^{-1} d^{-1}. Zooplankton derived similar amounts (50 ± 26%) of their carbon from POC and phytoplankton, both these pools were labelled and consequently the fraction (*f*) could not be constrained well. Zooplankton turnover was 0.24 ± 0.07 d^{-1} and the production rate was 5.1 µmol C L^{-1} d^{-1}.

Table 4.2 Model parameters ± standard deviation and turnover rates (µ, in d^{-1}) for Meiliang Bay.

	f_{DIC}	f_{DOC}	f_{POC}	f_{phyto}	µ (d^{-1})
Phytoplankton	0.79±0.03	0.21±0.03	-	-	0.79±0.07
Cyanobacteria	0.56±0.03	0.44±0.03			0.98±0.12
Bacteria	-	0.14±0.07	0.86±0.07	-	0.95±0.21
Zooplankton	-	-	0.50±0.26	0.50±0.26	0.24±0.07

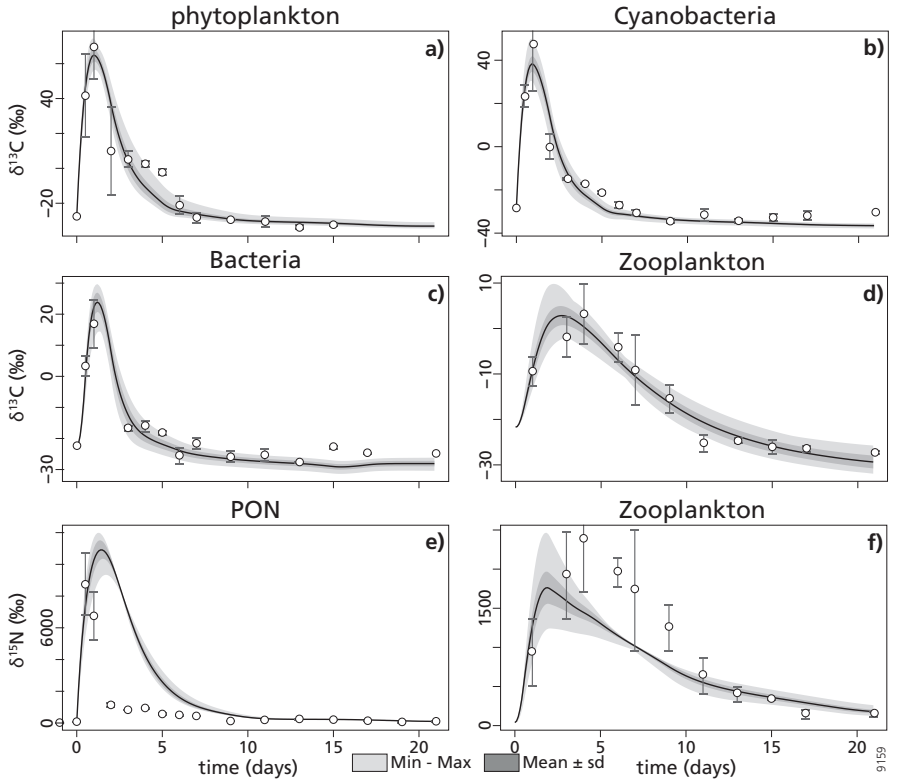

Fig. 4.3 Plots show the best fits of the model (black line) for Meiliang Bay, with light grey envelopes representing the range of minimum to maximum values and dark grey envelopes indicating the mean ± standard deviations of the MCMC analyses. The data points to which the model was fitted are shown as circles with error bars.

4.3.2.1 Wuli Lake isotope dynamics

Stable carbon and nitrogen isotope dynamics from T_{-1} to T_{21} at the restored, clear-water site Wuli Lake are shown in figure 4.4. Similar to unrestored Meiliang Bay, no label transfer was observed to higher organisms or sediment within the 22-day experiment. The addition of ^{13}C-bicarbonate increased $\delta^{13}C_{DIC}$ from -9.8 ± 2.6‰ at T_0 to 512.2 ± 15.7‰ at $T_{0.5}$ (Fig. 4.4a). Label content of DIC rapidly decreased to values around 0‰ at day 6, reaching values similar to pre-labelling conditions at day 15. Analogous to Meiliang Bay, no label was transferred from DIC to the DOC pool and values remained constant around -25.1 ± 0.5‰. Transfer of labelled carbon to POC in Wuli Lake was limited compared to Meiliang Bay, with a maximum $\delta^{13}C_{POC}$ of -2.0 ± 4.4‰ being reached at $T_{0.5}$, slowly decreasing to pre-labelling values around day 11. Phytoplankton and cyanobacteria in Wuli Lake showed highest labelling at T_1 with $\delta^{13}C$ values of 22.3 ± 6.8‰ and 16.7 ± 15‰ respectively. Phytoplankton $\delta^{13}C$ returned to pre-labelling values around day 11, but cyanobacterial $\delta^{13}C$ already recovered at day 6. Highest uptake of labelled DIC in Wuli Lake was observed in macrophytes and epiphytes, with $\delta^{13}C$ values of new leaves of macrophytes reaching 45.6 ± 14.4‰ at T_1. Macrophyte $\delta^{13}C$ remained high until day

11, but differences between mesocosms were considerable resulting in relatively high standard deviations (7.1‰ at day 21 up to 54.6‰ at day 7). Label incorporation into epiphytes, reached a similar $\delta^{13}C$ value of 43.3 ± 0.7‰ at T_1, but gradually decreased afterwards to a $\delta^{13}C$ value of -11.4 ± 2.7‰ at T_{21}. Transfer of newly labelled carbon to bacteria in Wuli Lake was limited compared to Meiliang Bay with a maximum $\delta^{13}C$ of -18.6 ± 3.2‰ at T_1, reaching pre-labelling values around day 6. Similarly, enrichment of zooplankton $\delta^{13}C$ was limited, with a maximum of -17.9 ± 0.6‰ reached at day 6. Zooplankton $\delta^{13}C$ returned to pre-labelling values at day 15.

Isotope dynamics of PON in Wuli Lake (Fig. 4.4b) showed maximum $\delta^{15}N$ values of 19000 ± 2600‰ at T_1, rapidly decreasing to a value of 1200 ± 990‰ at day 7, after which $\delta^{15}N$ of PON gradually decreases to 290 ± 110‰ at day 21, the end of the experiment. Standard deviations for PON were relatively large due to a delayed decrease in one of the mesocosms compared to the other two, but the overall trend was the same in all mesocosms. Labelling of new leaves of macrophytes and epiphytes was similar at T_1 with $\delta^{15}N$ values of 21000 ± 12300‰ and 18100 ± 7000‰ respectively. Macrophyte $\delta^{15}N$ remained high until day 15 when it decreased to 4600 ± 2500, while epiphyte $\delta^{15}N$ gradually decreased after T_1, reaching 3600 ± 680‰ at day 21, the end of the experiment. Highest zooplankton enrichment in Wuli Lake was observed at day 6, reaching a $\delta^{15}N$ value of 2400 ± 600‰, subsequently decreasing to 217 ± 34‰ at day 21.

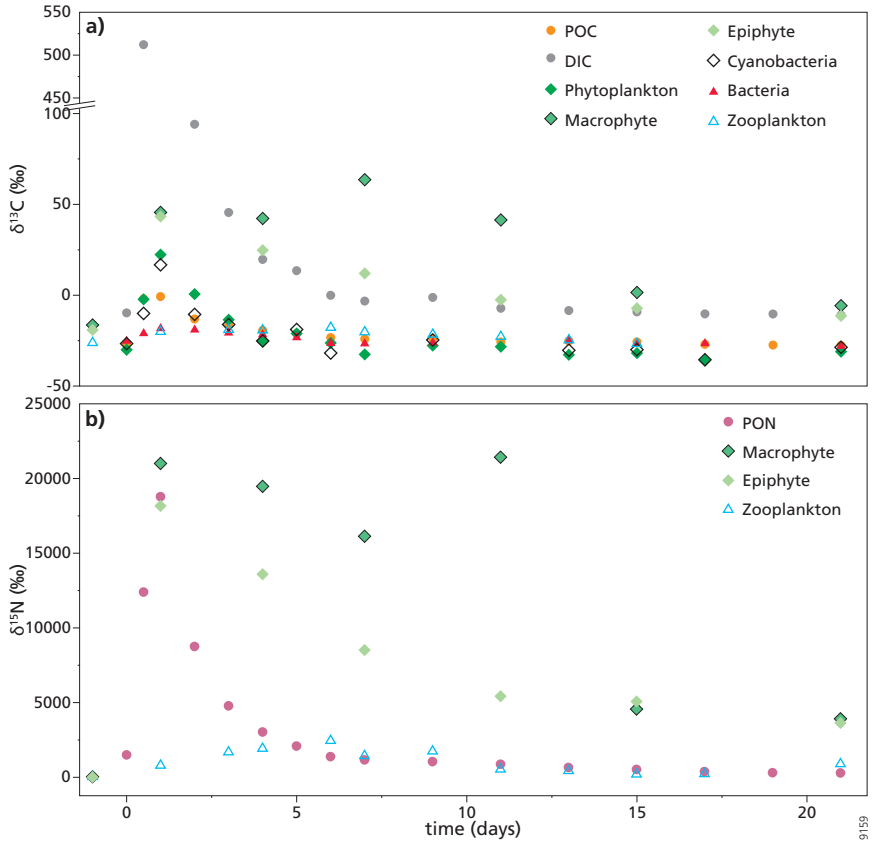

Fig. 4.4 Temporal change in isotope ratios of measured a) carbon and b) nitrogen pools in restored Wuli Lake. Values in (‰ vs. V-PDB) are averages of three mesocosms.

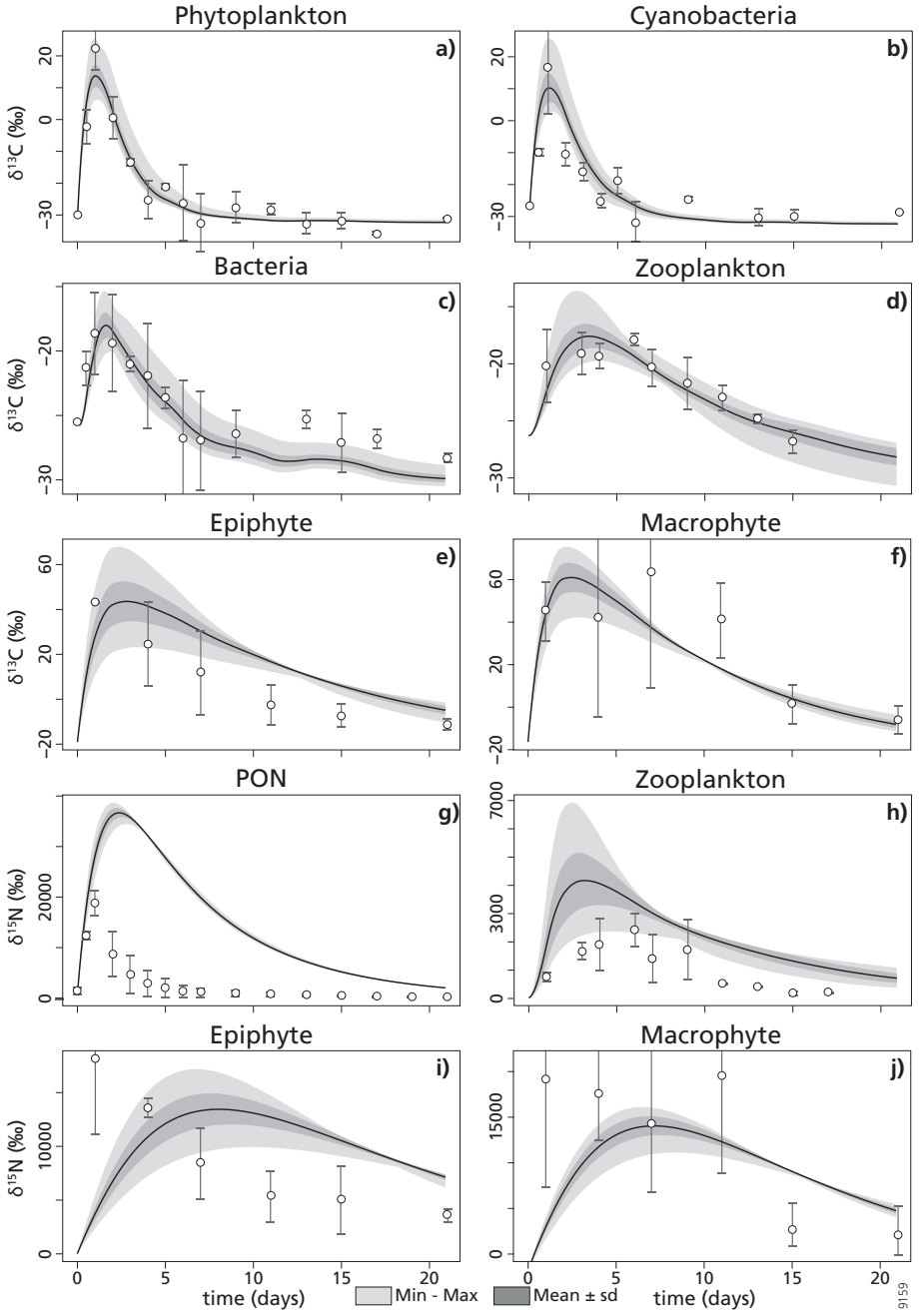

Fig. 4.5 Plots show the best fits of the model (black line) of Wuli Lake, with light grey envelopes representing the range of minimum to maximum values and dark grey envelopes indicating the mean ± standard deviations of the MCMC analyses. The data points to which the model was fitted are shown as circles with error bars.

4.3.2.2 Wuli Lake model output

Similar to Meiliang Bay, Wuli Lake carbon data could be fitted very well using the simple source-sink isotope model (Table 4.3 and Fig. 4.5). Also similar to Meiliang Bay, it was essential to include two sources, via a fraction *f*, resolving the dependence on labelled and unlabelled substrates to reproduce the data. During the experiment, phytoplankton and cyanobacteria derived only 19 ± 2% of their carbon from labelled DIC and 81 ± 2% from unlabelled DOC. Phytoplankton turnover rate was 0.79 ± 0.19 d^{-1}, but cyanobacterial turnover rate was somewhat higher at 0.89 ± 0.21 d^{-1}, resulting in combined phytoplankton production rates between 16 and 18 µmol C L^{-1} d^{-1}. Bacteria derived their carbon from unlabelled DOC (21 ± 22%) and labelled POC (79 ± 22%). The bacterial turnover rate resulting from the model run was not well constrained (0.6 ± 0.8 d^{-1}) but the resulting mean production rate of 3.1 µmol C L^{-1} d^{-1} seems plausible. Zooplankton derived its carbon in similar amounts from POC and phytoplankton, but the partitioning was poorly constrained (Table 4.3). Zooplankton turnover rate was 0.14 ± 0.44 d^{-1} with a production rate of 0.5 µmol C L^{-1} d^{-1}. Both macrophytes and epiphytes derived their carbon solely from DIC. For macrophytes and epiphytes turnover rates were 0.13 ± 0.02 d^{-1} and 0.08 ± 0.01 d^{-1} respectively, corresponding to a combined production rate between 69 and 223 µmol C L^{-1} d^{-1} for *Myriophyllum* sp. and epiphytes. Using the biomass of the total macrophyte community (628 g m^{-2}) and assuming all macrophytes have the same turnover rate as *Myriophyllum* sp. the production rate would be between 173 and 561 µmol C L^{-1} d^{-1}.

Table 4.3 Model parameters ± standard deviation and turnover rates (µ, in d^{-1}) for Wuli Lake.

	f_{DIC}	f_{DOC}	f_{POC}	f_{phyto}	µ (d^{-1})
Phytoplankton	0.19±0.02	0.81±0.02	-	-	0.79±0.19
Cyanobacteria	0.19±0.02	0.81±0.02			0.89±0.21
Bacteria	-	0.21±0.22	0.79±0.22	-	0.60±0.8
Zooplankton	-	-	0.51±0.49	0.49±0.49	0.14±0.44
Macrophyte	1.0	-	-	-	0.13±0.02
Epiphyte	1.0	-	-	-	0.08±0.01

4.4 Discussion

Before discussing in detail the carbon flows in unrestored Meiliang Bay and the restored Wuli Lake sections of Lake Taihu, it is instructive to discuss the design of our dynamic isotope model. Initially we explored the use of a commonly used simple source-sink isotope model (De Kluijver et al. 2010, Van Oevelen et al. 2006) in which producers or consumers only rely on one single carbon substrate (e.g. primary producers on DIC and bacteria on DOC). Such a model gave unacceptable fits for phytoplankton and zooplankton: it was not possible to simultaneously reproduce the initial increase and subsequent decrease of ^{13}C with only one parameter (see supplementary information figure S4.2). Similarly, it was not possible to fit the bacterial ^{13}C dynamics relying on DOC only, as the DOC pool did not become noticeably labelled during the experiment. The most simple and straightforward solution was to include one extra parameter *f,* allowing consumers to exploit two carbon substrates rather than one. Although this added some more complexity to our model (from one to two unknown parameters to be estimated) the model is still simple allowing MCMC estimation of the uncertainties in parameters.

4.4.1 Carbon and nitrogen pathways in eutrophic Meiliang Bay

4.4.1.1 Primary production

In eutrophic Meiliang Bay, the phytoplankton community is dominated by *Microcystis* sp., contributing 40-98% of the total phytoplankton biovolume from May to October (Chen et al. 2003). Calculated production rates for phytoplankton, including cyanobacteria, in Meiliang Bay were 81 – 100 μmol C L^{-1} d^{-1} (or 1.5 – 1.9 g C m^{-2} d^{-1}), which is high compared to temperate eutrophic lakes such as Lake Rotsee (16.1 μmol C L^{-1} d^{-1}, chapter 2) and Tuesday Lake (12.2 μmol C L^{-1} d^{-1}) (Carpenter et al. 1987), but not extreme compared to productivity in other tropical eutrophic lakes such as Lake Victoria (3.7 – 5.2 g C m^{-2} d^{-1}) (Darchambeau et al. 2014) or Lake George (Uganda) which has chlorophyll *a* concentrations 5-8 times higher than Meiliang Bay (Ganf 1974). The majority of phytoplankton production measured in Meiliang Bay likely derived from cyanobacteria, scum of which was visible during the experiment (Fig. 4.1). Model results indicate that cyanobacteria derived a higher fraction of their carbon demand from DOC (44 ± 3%) compared to other phytoplankton (21 ± 3%), which is expected since many species of cyanobacteria are known to be capable of assimilating organic carbon (Montesinos et al. 1997, Paerl 1991, Stebegg et al. 2012). For the order Chroococcales, to which *Microcystis* belongs, it was shown that several species are capable of photoheterotrophy (Rippka 1972).

In nitrogen stable isotope studies, PON is often used as a proxy for the phytoplankton nitrogen isotopic composition. However, when we applied the carbon-based turnover rates of phytoplankton to the isotopic composition of PON the resulting fit was poor (Fig. 4.3e), showing that PON could not be fitted as a proxy for phytoplankton. Also, we were unable to obtain a fit for POC isotopes, suggesting that both pools not only contain phytoplankton but also a substantial amount of other substrates. Since variable amounts of allochthonous material affect the POC and PON pools they should not be used directly as an approximation for the isotopic composition of phytoplankton. After the initial peak in label uptake, the stable isotopic compositions of POC and PON showed a rapid decrease in labelling in both lakes during the first few days (Fig. 4.2, 4.4), likely as a consequence of extensive remineralization (respiration) causing isotope dilution in both carbon and nitrogen sources.

4.4.1.2 Secondary production

Typically, DOC is considered the main carbon substrate for bacterial growth and its carbon isotopic composition is sometimes used to infer bacterial $\delta^{13}C$ (Taipale et al. 2008). However, our model results show that bacterial labelling derives mostly (86 ± 7%) from POC, which represents a mixture of a.o. phytoplankton, cyanobacteria, zooplankton and detritus in this experiment. Only a relatively small fraction of 14 ± 7% of bacterial carbon derived from the measured DOC pool, which itself did not become noticeably enriched during this experiment. The low bacterial dependence on DOC observed here is in line with previous results by De Kluijver et al. (2014) who observed no correlation between the $\delta^{13}C$ of bacteria and DOC in 22 lakes along a trophic gradient. Also in Lake Naarden (chapter 5) a strong correlation between phytoplankton and bacterial $\delta^{13}C$ was observed over a 17-month time series study. The minor uptake of DOC by bacteria in a highly productive system such as Meiliang Bay, might be due to the measured DOC pool consisting of mostly refractory compounds, with more easily degradable compounds being readily consumed (Tranvik 1988). This implies that although actual consumption of phytoplankton-derived carbon by bacteria may still occur via DOC, this is almost instantaneous and complete and hence does not show up in the DOC isotopic signal.

Transfer of ^{13}C-label to zooplankton biomass was slow compared to bacteria (Fig. 4.2a) as a result of lower turnover rates (Table 4.2) and hence the maximum in $\delta^{13}C_{zoo}$ was not observed until day 4. Given the similar trends in the isotopic compositions of POC and phytoplankton, it is difficult to determine their relative importance as carbon source for zooplankton. However, zooplankton uptake of both sources resulted in a better fit compared to using either POC or phytoplankton. This uncertainty is reflected in the rather large standard deviations of the best model fit with either source contributing 50 ± 26% to zooplankton carbon. In Meiliang Bay the massive abundance of *Microcystis* likely contributes substantially to the POC pool measured here (section 4.4.1.1). *Microcystis* are generally considered to be a poor food source for zooplankton, although they have been found to be an important carbon substrate for zooplankton in eutrophic lakes (Christoffersen et al. 1990, De Kluijver et al. 2012, Yu et al. 2013). In Meiliang Bay, DOM and detritus derived from *Microcystis* are important carbon sources for zooplankton, mainly via heterotrophic microbial pathways (De Kluijver et al. 2012, Luo et al. 2015). Given the lower isotopic enrichment observed in bacteria (17.0 ±7.9‰) compared to phytoplankton and detritus (69.8 ± 19‰ and 83.6 ± 33‰ respectively, Fig. 4.2a), a substantial contribution of cyanobacteria-derived ^{13}C via bacteria requires a somewhat higher turnover rate for zooplankton. A contribution of bacterial carbon up to ~50% combined with a turnover rate of 0.3 d^{-1} gives a similarly good fit to the zooplankton $\delta^{13}C$ data. A turnover rate of 0.3 d^{-1} still falls within the range given by the model for zooplankton turnover (0.24 ± 0.07 d^{-1}), showing that although the results of this experiment do not allow us to distinguish any further between carbon sources for zooplankton in Meiliang Bay, the calculated zooplankton production rates are robust.

When we applied the zooplankton turnover rate based on carbon isotopes to their $\delta^{15}N$ values, the model fits poorly (Fig. 4.3f). The resulting maximum in modelled $\delta^{15}N_{zoo}$ is too low compared to the data and is reached too early during the experiment. Uncoupling the nitrogen turnover rate from the turnover rate of zooplankton carbon allows for a higher nitrogen turnover rate (> 0.35 d^{-1}). This improves the model fit for $\delta^{15}N_{zoo}$ but still a supplementary source of nitrogen (more enriched than PON) is required. We expect that also phytoplankton and bacteria contribute to the nitrogen content of zooplankton, similar to what was discussed above for $\delta^{13}C_{zoo}$, but better constraints on the isotopic composition of nitrogen compounds (nitrate, ammonium, dissolved organic nitrogen) and the microbial food web (phytoplankton, bacteria) are required to improve model estimates for nitrogen sources and turnover rates in zooplankton.

4.4.2 Carbon and nitrogen pathways in restored Wuli Lake

4.4.2.1 Phytoplankton production in Wuli Lake

In Wuli Lake, high pH values and low DIC concentrations indicate exceptionally low dissolved CO_2 concentrations of ~17 µatm (or 0.6 µmol C L^{-1}, Table 4.1) and also low HCO_3^- concentrations of 681 µmol C L^{-1}. Similarly, ammonium made up only ~27% of the total nitrogen pool. Under these C- and N-limiting conditions, the added ^{13}C-bicarbonate and ^{15}N-ammonium was quickly removed, apparently forcing phytoplankton to take up alternative substrates such as DOC and DON/nitrate. Accordingly, DOC was implemented in the model as a second carbon source for phytoplankton and cyanobacterial production and good fits (Fig. 4.5a,b) were obtained for rather low consumption of DIC (19 ± 2% of consumed carbon) and a substantial contribution of DOC (81 ± 2%, Table 4.3). As discussed for Meiliang Bay, many cyanobacterial species are known to consume organic carbon sources and it is generally acknowledged that also many (micro)eukaryotes are able to consume dissolved organic carbon substrates (osmotrophy) as a metabolic strategy to keep up production of biomass when environmental conditions become

less favourable for photoautotrophy (e.g. low light conditions or competition for nutrients) (Lewin 1953, Stoecker 1998). Still there are many uncertainties about the degree to which DOC contributes to production of phytoplankton biomass. Algal heterotrophy has been suggested as a possible solution for the survival of algae in environments where light is limiting (e.g. below the euphotic zone or at high latitudes) (Gervais 1997, Vincent and Goldman 1980). Gervais (1997) found that uptake of glucose by cryptophytes under light limiting conditions was negligibly small compared to cellular carbon content (max 0.015% $cell^{-1}$ $hour^{-1}$), which was in line with earlier observations for cyanobacteria *Oscillatoria rubescens* (Feuillade and Feuillade 1989). However, other studies found that at least 15% of carbon in *Scenedesmus obliquus* (chlorophyte) was derived from glucose in a high-oxidation pond (Abeliovich and Weisman 1978) and in the same species also an increase in growth rates and ammonium uptake was observed when acetate was added to incubations (Combres et al. 1994). For two other species of chlorophytes (*Friedmannia* sp. and *Monoraphidium contortum*), Vincent and Goldman (1980) showed uptake of acetate near the bottom of the euphotic zone of Lake Tahoe to be substantial. However they concluded that the contribution of acetate-derived carbon could not be significant on a whole-lake scale. It should be noted that these studies mainly focused on light-limitation. In Wuli Lake we study a carbon-limited environment, and the strong dependence of phytoplankton on DOC observed here is much higher than was previously calculated. To keep up production when dissolved CO_2 is low, phytoplankton species have developed carbon concentrating mechanisms, aiding in the conversion of dissolved bicarbonate to aqueous CO_2 (Lucas and Berry 1985). Nevertheless, phytoplankton growth rates are generally assumed to decrease under CO_2-limiting conditions (Riesebell et al. 1993). In Wuli Lake, where high pH values and low DIC concentrations result in extremely low concentrations of dissolved CO_2 and also low concentrations of bicarbonate, phytoplankton have apparently adjusted their metabolic pathways and switched to mostly heterotrophic production. It hence also makes sense that no label was transferred to the DOC pool, as it is required by phytoplankton for the production of biomass.

4.4.2.2 Macrophyte production in Wuli Lake

Our study shows that, despite the CO_2-limiting conditions, both epiphytes and macrophytes use only DIC as carbon substrate, which is consistent with plant physiology, as they are not capable of mixotrophy. Macrophytes in Wuli Lake were able to keep up photosynthesis under C-limiting conditions even though phytoplankton was forced to switch to organic carbon sources. Due to their large biomass, macrophyte/epiphyte production dominates carbon dynamics in Wuli Lake, with production rates between 69 and 223 μmol C L^{-1} d^{-1} for *Myriophyllum* sp. Since we used new leaves of macrophytes to measure isotope labelling, the modelled turnover may be an overestimate compared to actual macrophyte turnover as new leaves may grow faster than old leaves and plant stems etc. Conversely, the biomass of 249.8 g m^{-2} for *Myriophyllum* sp. is only ~40% of total macrophyte biomass (628.2 g m^{-2}) in Wuli Lake, leading underestimation of production rates. Given these uncertainties, the calculated production rates are first order approximations, representing orders of magnitude only.

It is generally acknowledged that macrophytes play an important role during restoration of shallow lakes, as they stabilize sediment and reduce turbidity, they provide shelter against predation for zooplankton and they increase competition for nutrients with phytoplankton (Carpenter and Lodge 1986, De Kluijver et al. 2015, Jeppesen et al. 1997, Jeppesen et al. 1998, Van Donk and van de Bund 2002). In Wuli Lake however, a recent study on the importance of macrophyte abundance in the restoration project has shown that macrophytes promote

population growth of omnivorous fish, thereby reducing top-down control of zooplankton over phytoplankton and potentially lowering the chances of successfully restoring macrophytes and maintaining a clear-water state (Yu et al. 2016). Conversely, aquatic macrophytes including *Myriophyllum* sp. are highly proficient at extracting DIC and are thereby able to reduce DIC concentrations and increase pH levels (Madzen and Sand-Jensen 1991). It hence seems likely that the high macrophyte production in Wuli Lake resulted in more alkaline conditions and lower pCO_2 compared to Meiliang Bay. Our results thus suggest that the high macrophyte production observed in Wuli Lake may have induced a competition for DIC with the algae, forcing the algae to switch to osmotrophy.

The model fit of nitrogen isotopic composition of macrophytes and epiphytes (Fig. 4.5i,j) is not as good as the fit for carbon (Fig. 4.5e,f), especially the observed labelling at T_1 is not well captured, with error bars falling outside of the range of minimum to maximum values provided by the model. This suggests that in Wuli Lake, macrophytes and epiphytes rapidly take up ammonium when it becomes available, which is common in plants that are nitrogen-depleted (Thomas and Harrison 1987). Additionally, when comparing the model outcome of macrophytes and epiphytes, we observed that the turnover of nitrogen seems to be somewhat higher than the turnover of carbon.

4.4.2.3 Secondary production in Wuli Lake

The model results show that bacteria in Wuli Lake derived 79 ± 22% of their carbon from POC, which is similar to what was calculated by the model for Meiliang Bay (section 4.4.1.2). Bacterial turnover rates in Wuli Lake were low compared to Meiliang Bay (0.6 ± 0.8 d^{-1} and 0.95 ±0.21 d^{-1} respectively), but the resulting production rate of 3.1 µmol C L^{-1} d^{-1} in Wuli Lake was similar to the calculated bacterial production rate of 3.2 µmol C L^{-1} d^{-1} in Meiliang Bay because the biomass of heterotrophic bacteria was higher in restored Wuli Lake.

Similar to what was observed for Meiliang Bay, the results of this experiment did not allow us to differentiate clearly between carbon sources for zooplankton. Nonetheless, the model shows that zooplankton turnover rates in Wuli Lake were somewhat lower than in Meiliang Bay, with rates of 0.14 ± 0.44 d^{-1} and 0.24 ± 0.07 d^{-1} respectively. The phytoplankton community in Wuli Lake, with lower cyanobacterial biomass, would traditionally have been viewed as more nutritious to zooplankton, allowing for higher zooplankton turnover rates. As we observe here, this is not the case which further confirms the relevance of cyanobacteria as a substrate for zooplankton production as discussed in section 4.4.1.2. The model fit for zooplankton nitrogen isotopes, using the turnover rate based on modelling $\delta^{13}C_{zoo}$, resulted in higher $\delta^{15}N$ than was observed in the data and a peak in $\delta^{15}N$ occurring sooner (Fig. 4.5h), suggesting that in zooplankton, turnover of nitrogen occurred at a somewhat lower rate than turnover of carbon. However, as discussed above, better constraints on nitrogen compounds and food sources are needed to improve model estimates for zooplankton.

4.4.3 Effects of biomanipulation on ecosystem productivity and metabolism

The effects of remediation measures and biomanipulation on ecosystem metabolism have not been studied well and many uncertainties remain regarding biological feedbacks. Although it is expected that phytoplankton production decreases, this may be compensated by higher production rates by benthic algae, macrophytes and epiphytes, as a result of improved water quality and clarity (Jeppesen et al. 2012, Vadeboncoeur et al. 2003). Our study shows that the decrease in phytoplankton production due to biomanipulation measures in Wuli Lake were more

than compensated by macrophyte production (Fig. 4.6). Primary production rates of 81-100 µmol C L^{-1} d^{-1} as measured in the still eutrophic Meiliang Bay were lower than rates between 85 and 240 µmol C L^{-1} d^{-1} (sum of phytoplankton and *Myriophyllum* sp.) in restored Wuli Lake (Fig. 4.6). Hence, total carbon uptake during primary production has increased by up to 3 times due to the biomanipulation measures aimed at reducing eutrophication.

Bacterial secondary production rates are similar in both lakes and have thus not been affected much by the restoration project. However, in contrast to general belief, zooplankton production rates are higher in eutrophic Meiliang Bay compared to Wuli Lake as a result of feeding on cyanobacteria and lower zooplankton biomass in Wuli Lakes compared to Meiliang Bay. Macrophyte abundance was found to enhance development of omnivorous fish in Wuli Lake, and thereby grazing pressure on zooplankton by juvenile omnivores (Yu et al. 2016). Phytoplankton biomass is ~5 times lower in Wuli Lake and zooplankton:phytoplankton biomass ratios in Meiliang Bay and Wuli Lake are 0.2 and 0.16 respectively, showing that the manipulation measures taken in Wuli Lake (removal of planktivorous fish, stocking of omnivorous fish and planting of macrophytes) were not successful in increasing the grazing pressure on phytoplankton.

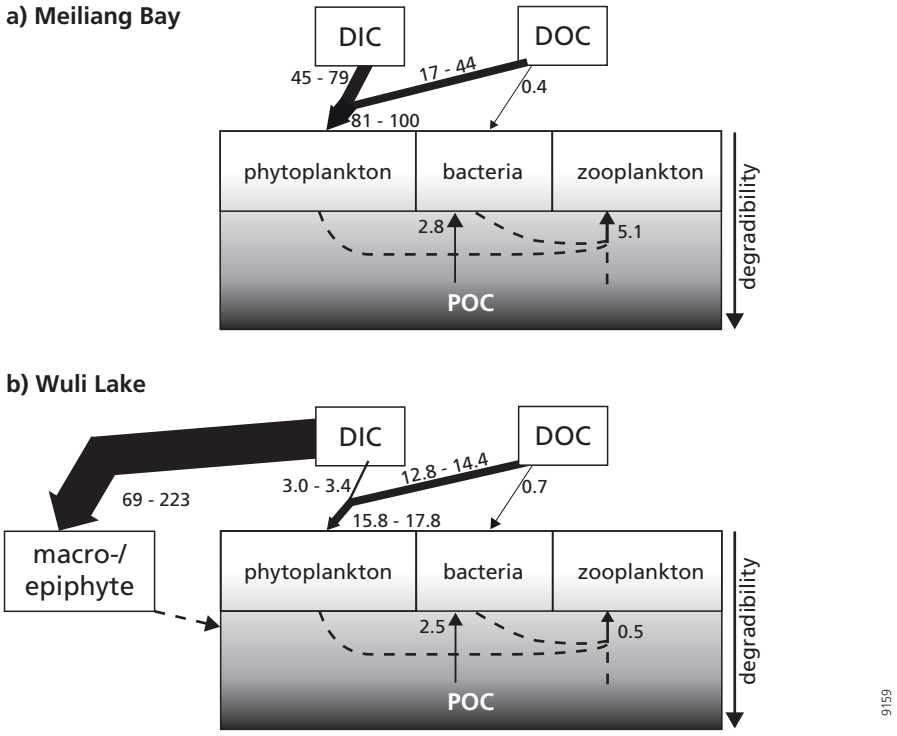

Fig. 4.6 Carbon flows through the food webs of eutrophic Meiliang Bay and restored Wuli Lake. Carbon flow rates are in µmol C L^{-1} d^{-1}. Thickness of the arrows indicates the size of the flow rate (not to scale). Dashed arrows could not be quantified.

4.5 Conclusions

The biomanipulation measures taken in Wuli Lake resulted in a shift in the pathways of nutrient cycling from being dominated by phytoplankton (cyanobacteria) to being dominated by macrophytes. The decrease in phytoplankton production in the restored section was more than compensated by higher production by macrophytes and epiphytes, with primary production rates in restored Wuli Lake being up to 3 times higher than in unrestored Meiliang Bay. In Wuli Lake, the very low concentrations of dissolved CO_2 and HCO_3^- forced phytoplankton (including cyanobacteria) to use substantial amounts of DOC (81 ± 2%) in addition to DIC (19 ± 2%) to sustain production. In contrast, macrophytes derived 100% of their carbon from DIC. Possibly, the high macrophyte production observed in Wuli Lake has caused a change in carbonate chemistry, ultimately forcing the algae to switch to osmotrophy.

Bacterial secondary production rates were similar in both lakes, around 3.2 and 3.4 µmol C L^{-1} d^{-1} in Meiliang Bay and Wuli Lake respectively. Zooplankton production rates were higher in Meiliang Bay (5.1 µmol C L^{-1} d^{-1}) than in Wuli Lake (0.5 µmol C L^{-1} d^{-1}), likely related to 1) higher phytoplankton biomass and consumption of cyanobacterial carbon in Meiliang Bay and 2) lower zooplankton biomass in Wuli Lake. Hence, grazing pressure on phytoplankton by zooplankton was lower in restored Wuli Lake as evidenced by zooplankton:phytoplankton biomass ratios of 0.2 and 0.16 in Meiliang Bay and Wuli Lake respectively.

Overall we conclude that even though nutrient cycling pathways have shifted as a result of the biomanipulation project in Wuli Lake, ecosystem productivity did not decrease but in fact seems to have increased. Furthermore, this study shows that the dominance of primary producers was changed from the pelagic to the benthic, which has implications for restoration of eutrophic shallow lakes in tropical and subtropical regions, showing that measures should focus on establishing a dominance of benthic primary production in lakes, e.g. by re-establishing submerged plants and benthic algae.

Supplementary material

Table S4.1 Model equations for the calculation of derived parameters as used for Meiliang Bay and Wuli Lake.

Phytoplankton: $\frac{d\delta^{13}C_{phyto}}{dt} = \mu_{phyto} * [f_{phyto} * \delta^{13}C_{DIC} + (1 - f_{phyto}) * \delta^{13}C_{DOC}] - \mu_{phyto} * \delta^{13}C_{phyto}$

Cyanobacteria: $\frac{d\delta^{13}C_{cyano}}{dt} = \mu_{cyano} * [f_{cyano} * \delta^{13}C_{DIC} + (1 - f_{cyano}) * \delta^{13}C_{DOC}] - \mu_{cyano} * \delta^{13}C_{cyano}$

Bacteria: $\frac{d\delta^{13}C_{bact}}{dt} = \mu_{bact} * [f_{bact} * \delta^{13}C_{DOC} + (1 - f_{bact}) * \delta^{13}C_{POC}] - \mu_{bact} * \delta^{13}C_{bact}$

Zooplankton: $\frac{d\delta^{13}C_{zoo}}{dt} = \mu_{zoo} * [f_{zoo} * \delta^{13}C_{POC} + (1 - f_{zoo}) * \delta^{13}C_{phyto}] - \mu_{zoo} * \delta^{13}C_{zoo}$

Epiphytes: $\frac{d\delta^{13}C_{epiph}}{dt} = \mu_{epiph} * \delta^{13}C_{DIC} - \mu_{epiph} * \delta^{13}C_{epiph}$

Macrophytes: $\frac{d\delta^{13}C_{macph}}{\delta t} = \mu_{macph} * \delta^{13}C_{DIC} - \mu_{macph} * \delta^{13}C_{macph}$

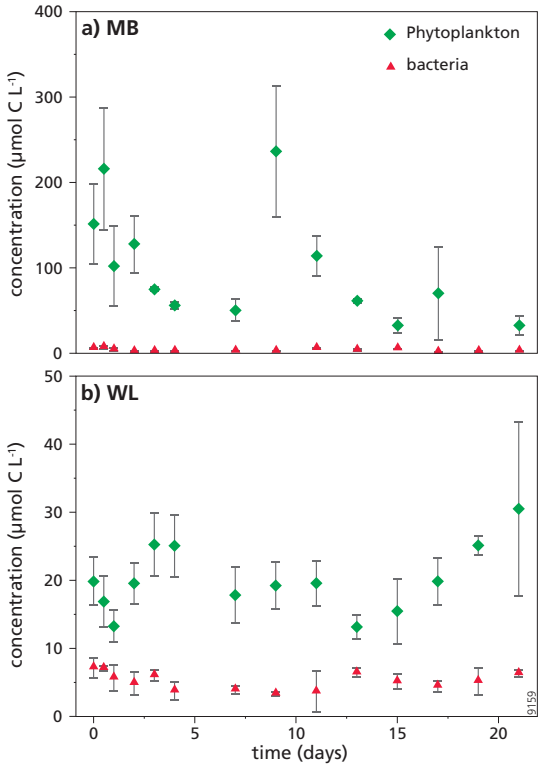

Fig. S4.1 Temporal change in phytoplankton and bacterial biomass (in µmol C L^{-1}) as averaged over three mesocosms in a) Meiliang Bay and b) Wuli Lake.

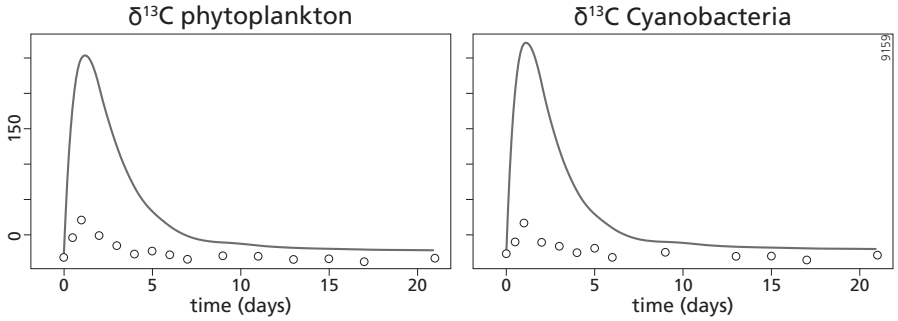

Fig. S4.2 Model outcome before fraction *f* was introduced and DIC was the only carbon source for phytoplankton and cyanobacterial production.

Chapter 5

Seasonal variability in phytoplankton isotopes and bacterial carbon sources in a shallow Dutch lake

Look straight ahead, there's nothing but blue skies
I can see clearly now the rain is gone
- Johnny Nash –

Abstract

Ecosystem metabolism of lakes strongly depends on the relative importance of local versus allochthonous carbon sources and on microbial food-web functioning and structure. Over the year ecosystem metabolism varies as a result of seasonal changes in environmental parameters such as nutrient levels, light availability, temperature and variability in the food web. Such changes are reflected in isotopic compositions of phytoplankton and bacteria. Here we present the results of a 17-month study on carbon dynamics in two basins of varying trophic states in Lake Naarden (Naardermeer), The Netherlands. Anthropogenic eutrophication affected both sites, but restoration of the lake in 1985 returned one basin to its original state, whereas the other basin remains eutrophic. We analyzed natural stable carbon isotope abundances ($\delta^{13}C$) of dissolved inorganic carbon (DIC), dissolved organic carbon (DOC) and macrophytes, and combined these data with compound-specific $\delta^{13}C$ analyses of phospholipid-derived fatty acids (PLFAs), produced by phytoplankton and bacteria. Isotopic fractionation (ε) between phytoplankton biomass and $CO_{2(aq)}$ was similar for diatoms and phytoplankton in general, and differences between sampling sites were small. Highest ε values were observed in winter with values of 23.0‰ for phytoplankton and 14.0‰ for cyanobacteria. Lowest ε values were observed in summer, with values of 9.0‰ for phytoplankton and 3.1‰ for cyanobacteria. At the different sites, the annual range in $\delta^{13}C_{bact}$ was between 6.9 and 8.2‰, while this range was between 11.6 and 13.1‰ for phytoplankton. Correlations between $\delta^{13}C_{phyto}$ and $\delta^{13}C_{bact}$ were strong at both sites. During summer and fall, bacterial biomass derives mainly from locally produced organic matter, with minor contributions from allochthonous carbon (as derived from DOC). Conversely, during winter months bacterial dependence on DOC was 39-77% at the restored site, and was 17-46% at the eutrophic site.

5.1 Introduction

Freshwater systems play an important role in the global carbon cycle despite their limited spatial extent. Inland waters process large amounts of carbon (Battin et al. 2008, Cole et al. 2007, Tranvik et al. 2009) and, compared to oceans, have a disproportionally high storage capacity resulting from high production rates and high sedimentation rates. Nevertheless, the majority of surface waters of lakes is supersaturated with respect to CO_2 (Cole et al. 1994), resulting in emission of CO_2 to the atmosphere. The imbalance between lacustrine and atmospheric partial pressures of CO_2 most often results from excess respiration compared to primary production. The carbon supporting respiration can be derived from either autochthonous (locally produced) or allochthonous (external inputs from plants and soils) sources. Ecosystem metabolism and net impact on the global carbon cycle strongly depend on the relative importance of these carbon sources and hence microbial food-web functioning and structure.

The microbial food web is not only affected by input of allochthonous organic matter but also by environmental parameters such as nutrient levels, temperature and light availability, which influence primary productivity. Even though all these factors vary strongly throughout the year, microbial food-web studies are usually snapshots representing days (Coloso et al. 2011, Staehr and Sand-Jensen 2007, Staehr et al. 2010, chapter 2) to weeks (Brett et al. 2009, Cole et al. 1988, Cole et al. 2006, De Kluijver et al. 2010, Pace et al. 2004, chapters 3, 4) because of limitations in time and resources. Studies on the effects of seasonal variability on carbon processing and the microbial food web hence are relatively scarce. The few studies of seasonal

changes in phytoplankton carbon isotopic composition generally show large variability (Bontes et al. 2006, De Kluijver et al. 2015, Finlay 2004, Van Breugel et al. 2006), resulting from changes in growth rate and carbonate chemistry (pH, pCO_2). Also seasonal variability in the dependence of zooplankton on allochthonous carbon via microbial links has been reported (Grey and Jones 2001, Van den Meersche et al. 2009).

In the past, stable carbon isotopes have been successfully applied to trace energy flow at higher food-web levels (e.g. Keough et al. (1996), Kling et al. (1992), Peterson and Fry (1987). A major challenge however, has been to separate between microbial organisms (phytoplankton, bacteria) and particulate organic carbon (POC) (Middelburg 2014). Indirect measurements such as different size classes of POC and their carbon isotopic compositions have been used to infer the $\delta^{13}C$ of phytoplankton (Marty and Planas, 2008). However, these size-based approaches are difficult to apply in turbid, eutrophic systems and estimates from dissolved inorganic carbon involve large uncertainties in terms of fractionation and correction factors (Middelburg 2014, Taipale et al. 2015). Compound-specific stable isotope analyses (CSIA) nowadays allows addressing different components of the food web, including the microbial part (Boschker et al. 1998, Middelburg et al. 2000, Van den Meersche et al. 2009). Especially phospholipid-derived fatty acids (PLFAs), components of cell membranes, are excellently suited for natural abundance isotope studies since they are generally hydrolyzed within hours to days after cell death (Harvey et al. 1986, White et al. 1979) and thus mainly represent freshly produced biomass. PLFAs are produced by a large variety of organisms and although they do not represent unique organisms, they can be used to differentiate between phytoplankton (eukaryotic algae, cyanobacteria) and heterotrophic bacteria (Boschker and Middelburg 2002, Dijkman and Kromkamp 2006, Gugger et al. 2002, Kaneda 1991, Taipale et al. 2013). Accordingly, PLFAs have been successfully applied to food-web studies (Rütters et al. 2002), including in lakes (Bontes et al. 2006, De Kluijver et al. 2014, Pace et al. 2007).

Here we investigate phytoplankton-bacteria coupling over a 17-month period in two basins of successfully restored Lake Naarden (Naardermeer), The Netherlands. Lake Naarden is a shallow (~1 m water depth) wetland lake, lying within the Naardermeer nature reserve. The lake has a surface area of 1042 ha and consists of five connected basins and canals that are surrounded by marshy woodland, open reed-marshland and meadows (Fig. 5.1). Until the 1960's, water was supplied by rainfall, groundwater discharge and water levels were maintained by pumping water to and from the river Vecht. Water supply from the river Vecht was stopped after 1960 because of eutrophication of this water. Nevertheless, eutrophication of Naardermeer continued after 1960, with increasing turbidity and decreasing aquatic vegetation (mostly charophytes and *Najas marina*). Original macrophyte vegetation gave way to species associated with eutrophication and seasonal algal blooms (Bootsma et al. 1999). A restoration project started in 1985, aiming at reducing the P-load by supplying phosphate-free water. After a decade turbidity was reduced and macrophytes had largely recovered in most of the lake (Bootsma et al. 1999). Currently, dephosphorized water is supplied from the river Vecht in dry periods (summer), but only reaches the area north of the railway (Fig. 5.1). Diatom studies have shown that water quality has recovered in particular north of the railway. The northern basin Grote Meer (GM) is considered of "very good" quality, while Bovenste Blik (BB) south of the railway is eutrophic and still moderately disturbed (Van Ee 2007). This is also reflected in Secchi depths, ranging from ~0.8 m (summer) to ~1.2 m (winter) in GM, while in BB Secchi depths vary between 0.4 and 0.8 m.

This study addresses seasonal changes in phytoplankton isotopes and carbon transfer to bacteria using stable isotope analyses of inorganic (DIC) and organic (DOC and aquatic and

terrestrial vegetation) carbon as well as compound-specific stable carbon isotope analyses of the microbial food web via PLFAs. We examine bacterial dependence on autochthonous versus allochthonous carbon sources throughout the year.

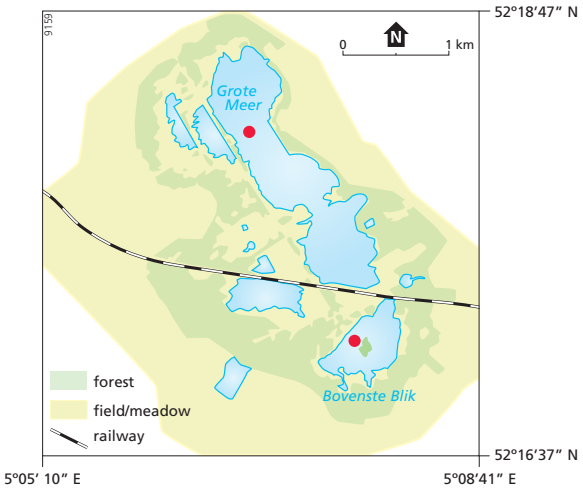

Fig. 5.1 Map of Lake Naarden and the surrounding vegetation types. Samples were taken in two basins: Grote Meer (GM) and Bovenste Blik (BB). Sampling locations are indicated by red circles.

5.2 Material and methods

5.2.1 Sample collection

Between May 2013 and September 2014 water was collected monthly from two basins of Lake Naarden: Grote Meer (GM) and Bovenste Blik (BB) (Fig. 5.1). Ten liters of water were transported to the laboratory and sampled for dissolved inorganic carbon (DIC), dissolved organic carbon (DOC), and suspended particulate matter. Samples for DIC and DOC concentrations and carbon isotopic composition were filtered through 0.45 µm GM/F filters. DIC samples were collected air-free in 20 ml headspace vials, which were sealed airtight, poisoned using mercury chloride and subsequently stored dark and upside down. After filtering, DOC samples were stored frozen (-20 °C) until analysis. Remaining water was filtered for SPM using pre-weighed and pre-combusted GF/F filters (0.7 µm) and frozen (-20 °C) until extraction. Aquatic, littoral and terrestrial vegetation was collected in September 2015 and stored (-20 °C) frozen until further analyses.

Data on temperatures, chlorophyll *a* concentrations, pH values and concentrations of carbonate species were collected and kindly provided by water company Waternet and its associated laboratory Waterproef, commissioned by Natuurmonumenten, the Society for preservation of nature monuments in The Netherlands.

5.2.2 Laboratory analyses

DIC concentrations were measured on a Shimadzu TOC-5050A carbon analyzer, using an in-house seawater standard. For $\delta^{13}C$ analyses first a helium headspace was generated and DIC samples were then acidified using H_3PO_4, creating CO_2-gas of which the $\delta^{13}C$ values were measured using a gas bench coupled online to an IRMS (Thermo Delta V advantage). Values were calibrated to the Vienna Peedee Belemnite (V-PBD) scale using Li_2CO_3 and Na_2CO_3 as standards.

DOC samples were treated and analyzed for concentrations and $\delta^{13}C$ following Boschker et al. (2008), using high-performance liquid chromatography-isotope ratio mass spectrometry (HPLC-IRMS, Thermo Surveyor system coupled to a Delta V Advantage using the LC-Isolink interface), using certified reference materials glutamic acid and sucrose for calibration.

Particulate organic carbon (POC) concentrations and $\delta^{13}C_{POC}$ were measured on small pieces (8 circles, 5 mm diameter) cut from the filters collected for SPM analyses. POC concentrations were measured using an elemental analyzer (EA) (Fisons Instruments NA1500), coupled online to an IRMS (Thermo Deltaplus) for $\delta^{13}C$ analyses. Precision for $\delta^{13}C$ was better than 0.1‰ based on an in-house (Graphite quartzite) standard and 0.2‰ based on an in-house (Nicotinamide) standard. Concentrations were relatively low and hence did not allow for replicate measurements, still, the observed trends are consistent and confirm that the internal precision is representative.

Vegetation samples were freeze dried and ground to a powder. Carbon isotopic compositions were measured on the same setup described above for analyses of POC. Standard deviations were better than 0.4‰ based on an in-house (Graphite quartzite standard) standard.

A modified Bligh and Dyer extraction method was used to extract lipids from freeze-dried SPM samples, which were then separated based on polarity into simple lipid (SL), glycolipid (GL) and phospholipid (PL) fractions (Dickson et al. 2009). Following, mild alkaline transmethylation converted phospholipid-derived fatty acids to fatty acid methyl esters (PL-FAMEs) (White et al. 1979) and C12:0 and C19:0 FAMEs were added as internal standards. Concentrations of PL-FAMEs were analyzed using a gas chromatograph (HP 6890) with Helium as carrier gas set at constant pressure and fitted with a flame ionization detector (FID) and a VF-23ms column (0.25 mm i.d.). Compounds were identified based on retention times and mass spectra following mass spectrometry, which was performed using a Thermo Trace GC Ultra, with Helium set at constant flow. Double-bond positions were determined after derivatization with dimethyl-disulfide (DMDS). DMDS was activated with iodine in diethyl ether at 40°C overnight (Buser et al. 1983). Compound-specific $\delta^{13}C$ analysis was done using gas chromatography combustion isotope ratio mass spectrometry (GC-C-IRMS) on a ThermoFinnigan Delta Plus XP using the same type of column that was used during GC-FID analyses. Oven programming of GC-FID, GC-MS and GC-C-IRMS followed Middelburg et al. (2000). Carbon isotopic values of PLFAs are reported in ‰ vs. V-PDB. These were corrected for the carbon atom that was added during methylation. Carbon isotopic values of the derivatizing agents were determined offline.

5.2.3 PLFA assignments

Main PLFAs detected in SPM samples from both sites were branched PLFAs iC14:0, iC15:0, aC15:0, and polyunsaturated fatty acids (PUFAs) C16:2ω7, C18:3ω3, C18:4ω3, C20:4ω6, C20:5ω3 and C22:6ω3. Branched PLFAs iC14:0, iC15:0 and aC15:0 are predominantly produced by gram-positive bacteria (Kaneda 1991) but have also been detected in some gram-

negative bacteria (Haack et al. 1994). PUFAs are synthesized by phytoplankton groups, including green and red algae, diatoms, dinoflagellates and haptophytes (Brett and Müller-Navarra 1997, Dijkman and Kromkamp 2006, Taipale et al. 2013). Detected PUFAs C18:3ω3, C18:4ω3, C20:4ω6 and C22:6ω3 derive from numerous phytoplankton groups while PUFAs C16:2ω7 and C20:5ω3 derive more uniquely from diatoms (Dijkman and Kromkamp 2006).

PLFA C18:3ω6, which can be used to represent cyanobacteria (Gugger et al. 2002), was found in very low concentrations and only during four months at sampling location GM and was not included in the results. At location BB however, C18:3ω6 was detected during 11 out of 17 months and concentrations allowed for $\delta^{13}C$ analyses.

5.2.4 Data analyses

$CO_{2(aq)}$ and pCO_2 were calculated from DIC concentrations, pH and water temperatures. The isotopic composition of $CO_{2(aq)}$ was calculated from $\delta^{13}C_{DIC}$ with a correction for temperature following Mook et al. (1974). Isotope discrimination, or fractionation (ε), between phytoplankton and the carbon source $CO_{2(aq)}$ was calculated as:

$$\varepsilon_{CO_2} - \text{phyto} = \frac{\delta^{13}C_{CO2} - \delta^{13}C_{\text{phyto}}}{1 + \delta^{13}C_{\text{phyto}}/1000} \quad (1)$$

where phyto can mean either phytoplankton PLFA (for $\varepsilon_{CO2-PLFA}$) or phytoplankton biomass (for $\varepsilon_{CO2-phyto}$). Carbon isotopic composition of biomass was derived from the $\delta^{13}C$ of PLFAs by correcting for the isotopic offset between PLFAs and total cells. We used a correction of +7‰ for phytoplankton, +4.5‰ for diatoms, +11‰ for cyanobacteria and +2‰ for bacteria (Taipale et al. 2015). Although depletion of lipid carbon isotopic composition with respect to biomass can vary widely (Hayes 2001, Pel et al. 2004, Schouten et al. 1998), the correction factors applied here were derived specifically for ω3-PUFAs (Taipale et al. 2015).

Concentrations of detritus (dead POC) were derived from POC by subtracting values for phytoplankton and bacteria (living POC):

$$C_{det} = C_{POC} - C_{phyto} - C_{bact} \quad (2)$$

where C_{phyto} is calculated by multiplying the concentration of chlorophyll *a* by 40 and C_{bact} is calculated using a C:FA ratio of 50 (Middelburg et al. 2000). Finally, a mass balance was constructed to calculate the carbon isotopic composition of detritus:

$$\delta^{13}C_{det} = \frac{(C_{POC} * \delta^{13}C_{POC} - C_{phyto} * \delta^{13}C_{phyto} - C_{bact} * \delta^{13}C_{bact}}{C_{det}} \quad (3)$$

5.3 Results

5.3.1 Sampling year vs. long-term averages

Temperatures – Due to their close proximity, water temperatures showed little variation between sampling locations GM and BB, hence only temperatures from location GM are shown in figure 5.2a (black diamonds), with standard deviations of average temperatures over the period 2003-2014 shown as bars. In general, monthly water temperatures during the sampling campaign corresponded well with long-term averages. The average summer temperature of 2013 was warmer than the long-term average with temperatures of 21.1 and 20.2 ˚C respectively, due to a

warm August. During the winter of '13-'14 the average temperature of 5.6 °C was also somewhat warmer than the decadal average of 4.8 °C. Conversely, the summer of 2014 was slightly colder than average with an average temperature of 19.9 °C. Both the sampling year and the long-term trend show that lowest temperatures are reached in December to February and spring warming starts in March.

Chlorophyll a – Concentrations of chlorophyll *a* at location GM during the sampling campaign fall within the range of natural variability (standard deviations of the long-term averages) (Fig. 5.2b). Chlorophyll *a* concentrations are relatively stable throughout the year, varying between 6 and 17 µg L^{-1} during most months. Highest concentrations, between 26 and 31 µg L^{-1}, were measured from January to March. At location BB, chlorophyll *a* concentrations also match well with the long-term averages but show a different seasonal trend compared to location GM (Fig. 5.2c), with two maxima observed each year: a smaller maximum in February and a more pronounced maximum in August-September. Chlorophyll *a* concentrations at site BB are much higher than at site GM, generally ranging between 14 and 31 µg L^{-1} during our sampling year, with a maximum concentration of 87 µg L^{-1} observed in September 2013. The February maximum was lower with a concentration of 61 µg L^{-1}. In 2014, there was no clear maximum observed in August/September.

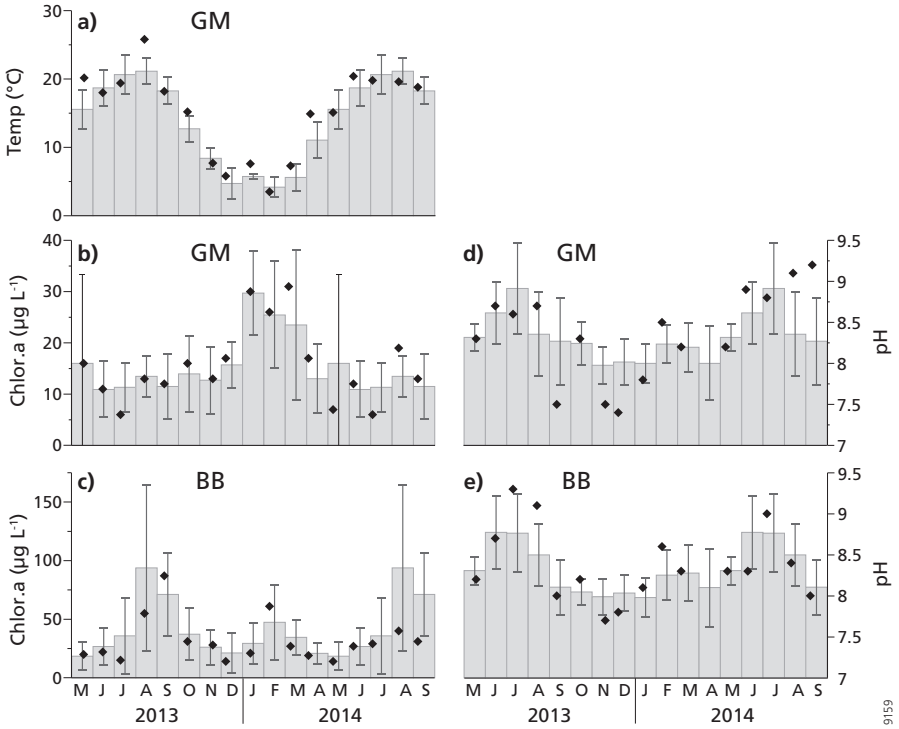

Fig. 5.2 a) water temperatures (°C), concentrations of chlorophyll *a* (µg L^{-1}) at sites b) GM and c) BB, and pH values at sites d) GM and e) BB. Values as measured during the 2013-2014 sampling campaign are shown as black diamonds. Grey-shaded bars represent long-term averages measured between 2003 and 2014.

Carbonate chemistry – At sampling location GM, pH values measured during our sampling campaign do not consistently correspond to the long-term averages (Fig. 5.2e). By definition ~1/3 of the observations is expected to fall outside the one sigma standard deviation, however, pH values appear outliers from the annual trend during three months. During the last decade average pH values generally varied between 8.0 and 8.3, with higher pH values of 8.6 and 8.9 in June and July. However, during the 2013-2014 sampling year, pH values were around 7.5 in September, November and December, which were lower than during any other year of the 2003-2014 period and clearly deviate from the trend. In 2014, pH values in August and September were higher than usual, around 9.2, but do not show a break in overall pH trend. Since it is notoriously difficult to do correct pH analyses on an absolute scale we also looked at bicarbonate concentrations (data not shown), which showed comparable values for our time series compared to the long-term averages. However, these values could not be used to calculate pH since reliability of alkalinity analyses, and hence bicarbonate concentrations, tends to be reduced in lake water due to the buffering capacity of humic substances near the endpoint of alkalinity titrations (Wilson 1979). At the moment we cannot explain the aberrant pH values compared to the long-term trend since other parameters match well. Since we cannot fully exclude analytical errors as a cause for these deviations we used long-term averages of pH values in our calculations of $CO_{2(aq)}$ and pCO_2. At site BB, the long-term averages were very similar to site GM, ranging between 8.0 and 8.3 with an average annual maximum of 8.5 to 8.8 from June-August (Fig. 5.2f). At this site, pH values during the '13-'14 sampling period correspond well with the long-term averages.

5.3.2 $\delta^{13}C$ of microbial biomass and organic carbon pools

Weighted averages of $\delta^{13}C$ values of bacterial biomass were relatively enriched in $\delta^{13}C$ during summer and relatively depleted in $\delta^{13}C$ during winter (Fig. 5.3). At site GM $\delta^{13}C_{bact}$ showed an annual range of 6.5‰, varying between -32.5 and -25.9‰. At site BB $\delta^{13}C_{bact}$ values had a higher annual span of 8.2‰, and showed more depleted $\delta^{13}C_{bact}$ ranging between -36.8 and -28.7‰.

Weighted averages of $\delta^{13}C$ values of phytoplankton biomass showed comparable seasonal changes as $\delta^{13}C_{bact}$ with enriched values during summer and depleted values during winter (Fig. 5.3, green). However, the annual range was larger than observed for bacteria. At site GM $\delta^{13}C_{phyto}$ values had an annual span of 11.6‰, ranging between -36.5 and -24.9‰. At site BB $\delta^{13}C_{phyto}$ values had a somewhat higher annual span of 13.1‰, and showed more depleted $\delta^{13}C_{phyto}$ ranging between -39.8 and -26.7‰.

Particulate organic carbon (POC) also showed clear seasonal differences at both sampling sites (Fig. 5.3, grey). Lowest, most depleted $\delta^{13}C$ values were observed during winter and early spring (November to April) with values around -31.6‰ at site GM and -34.4‰ at site BB. From April onwards, $\delta^{13}C_{POC}$ increased until maxima were reached from July to September, with values around -26.3‰ at site GM and -28.5‰ at site BB. The annual range of $\delta^{13}C_{POC}$ values was 5.3‰ at site GM and 5.7‰ at site BB. At both sampling sites, detritus was the dominant component of the POC pool. At site GM, 80-90% of POC consisted of detritus from April to October. During winter months (November to March), detritus contributed a smaller fraction of POC, between 56 and 74%, indicating highest living biomass contributions during winter, as already shown by the chlorophyll *a* data (Fig. 5.2b). Calculated stable carbon isotopic compositions of detritus at site GM varied between -26.4‰ and -30.6‰ (Fig. 5.3a). At site BB, relative contributions of detritus and living biomass to the POC pool showed more variability.

During summer months (from April to July in 2013 and until September in 2014) 72-84% of POC was detritus. From August 2013 to March 2014, the fraction of detritus was much lower, ranging between 45 and 70%, with the exception of February 2014. In this month, an exceptionally large contribution of phytoplankton biomass to POC was derived from chlorophyll *a* data and hence a low contribution resulted for detritus of ~10% of the POC pool. At site BB, calculated $\delta^{13}C_{det}$ varied between -27.3‰ and -32.2‰ (Fig. 5.3b), except for February 2014 (-9.4‰, not shown in graph) during which the calculation was strongly influenced by the unusually high chlorophyll *a* concentrations. Stable carbon isotopic compositions of dissolved organic carbon (DOC) were stable throughout the year with $\delta^{13}C$ values of -28.8±0.6‰ for GM and -29.5±0.4‰ for BB (Fig. 5.5, blue).

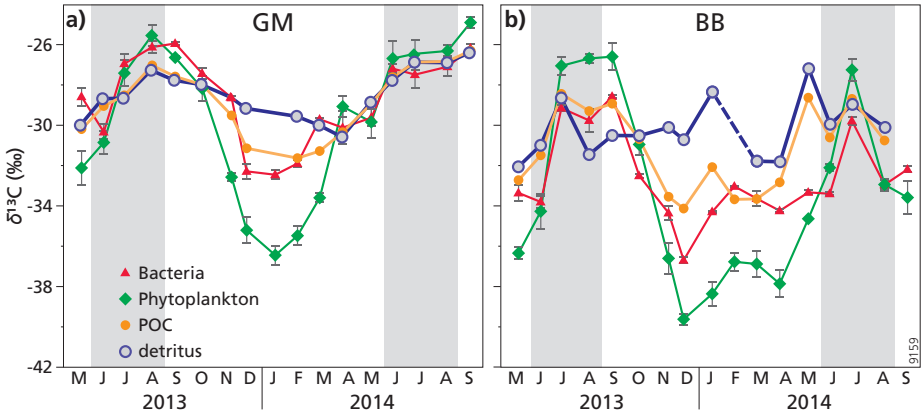

Fig. 5.3 Seasonal variations in carbon isotopic composition ($\delta^{13}C$ in ‰ vs. VPDB) of bacterial biomass (red), phytoplankton biomass (green), POC (grey) and detritus (blue) at a) site GM, and b) site BB. An outlier in $\delta^{13}C_{det}$ in February 2014 at site BB (-9.4‰) is not plotted as it is strongly influenced by exceptionally high chlorophyll *a* concentrations. Grey shaded areas correspond to summer months: June-August.

Carbon isotopic compositions of abundant species of littoral and terrestrial macrophytes (Table 5.1) were typical for vegetation using the C3 photosynthetic pathway with $\delta^{13}C$ values of -29.1±0.1‰ for *Polytrichaceae* (hair moss), -26.9±0.1‰ and -26.6±0.4‰ for *Phragmites australis* (reed) leaf and stem respectively, and -29.3±0.1‰ for *Thelypteris palustris* (marsh fern). Aquatic vegetation had $\delta^{13}C$ values of -25.5±0.1‰ for *Nymphaeaceae* (water lily), -27.8±0.4‰ for *Potamogeton lucens* (shining pontweed) and markedly different $\delta^{13}C$ value of -16.4±0.5‰ for *Characeae* (Common Stonewort) (Table 5.1). A potential contamination with $CaCO_3$ was specifically excluded using multiple decalcification steps.

Table 5.1 Average $\delta^{13}C$ values (in ‰ vs. VPDB ± SD; n=2) of terrestrial and aquatic vegetation from Lake Naarden during fall 2015.

	Vegetation	$\delta^{13}C$ (‰)
Terrestrial	Hair moss (*Polytrichaceae*)	-29.1±0.1
Terrestrial	Reed leaf (*Phragmites australis*)	-26.9±0.1
Terrestrial	Reed stem (*Phragmites australis*)	-26.6±0.4
Terrestrial	Marsh fern (*Thelypteris palustris*)	-29.3±0.1
Aquatic	Water lily (*Nymphaeaceae*)	-25.5±0.1
Aquatic	Common Stonewort (*Characeae*)	-16.4±0.5
Aquatic	Shining pontweed (*Potamogeton lucens*)	-27.8±0.4

5.3.3 $\delta^{13}C$ of inorganic carbon pools

DIC – At sampling site GM, concentrations of dissolved inorganic carbon (DIC) showed considerable variability throughout the year (Fig. 5.4a, left) with maximum concentrations around 2.0 mmol C L^{-1} in late spring/early summer (May, June) and minimum concentrations in late summer (August, September) around 1.2 and 0.85 mmol C L^{-1} in 2013 and 2014 respectively. Stable carbon isotopes of DIC at site GM were highest (more enriched) $\delta^{13}C$ values between -0.9 and -0.6‰ in June and July and lowest (most depleted) values between -4.6 and -3.8‰ during winter months November – January (Fig. 5.4b, left).

DIC concentrations at sampling site BB show a similar trend compared to site GM, but the maximum concentrations are higher, resulting in a larger annual range (Fig. 5.4a, right). Minimum concentrations of 1.5 and 1.3 mmol C L^{-1} were observed in July 2013 and 2014. During other months, DIC concentrations are relatively stable between 2.0 and 2.5 mmol C L^{-1}, with the exception of May 2013 when a peak concentration of 2.8 mmol C L^{-1} was observed. Carbon isotope values of DIC at site BB (Fig. 5.4b, right) are substantially lower than at site GM, with $\delta^{13}C$ values ranging between -9.5 and -3.8‰. Most depleted $\delta^{13}C$ values were observed in July, and November to January. The depleted $\delta^{13}C$ value in July 2013 deviates substantially from the generally more enriched values during other summer months. During this month, the observed combination of a high pH (Fig. 5.2f) and low pCO_2 (Fig. 5.4c) may have caused chemically enhanced diffusion (CED). During CED a major source of DIC in water is the reaction between atmospheric CO_2 and OH^-, instead of the more general reaction between CO_2 and H_2O. The latter reaction results in a fractionation of +8‰, compared to a fractionation of -15‰ during CED, which hence results in a more depleted $\delta^{13}C$ of DIC (Bade and Cole 2006, Bontes et al. 2006). This may explain the observed more negative values in July 2013. Overall, most enriched values were observed in August and September of both sampling years.

pCO_2 – At sampling site GM, the calculated pCO_2 values were relatively low, ranging between minima of 67 and 43 µatm in July 2013 and 2014 respectively, to maxima around 540 µatm in the winter of '13-'14 and 670 µatm in April 2014 (Fig. 5.4c, left). Variability in pCO_2 values at site BB was similar, with minimum values around 79 and 69 µatm in July 2013 and 2014 respectively and a maximum around 800 µatm in October 2013 (Fig. 5.4c, right).

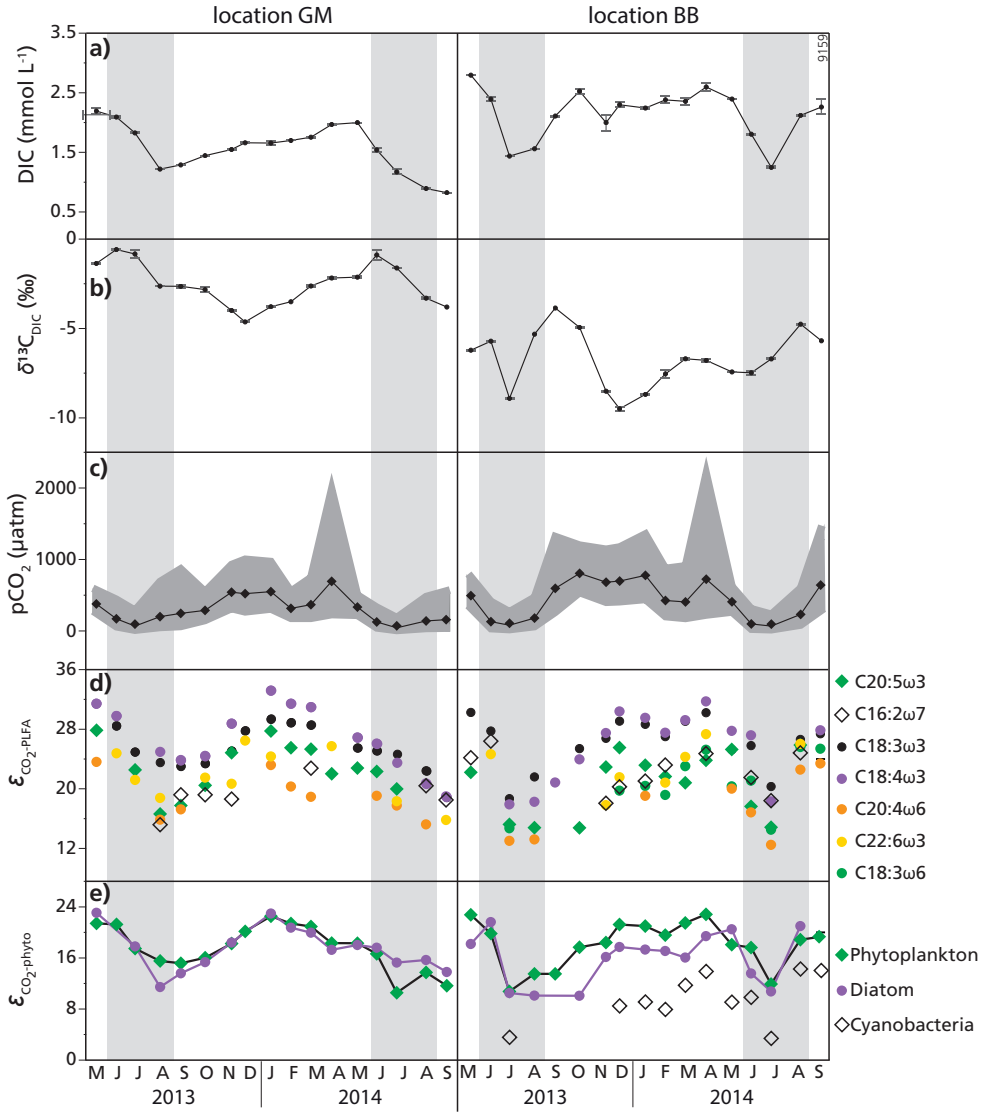

Fig. 5.4 a) DIC concentrations (mmol C L^{-1}) and b) DIC carbon isotopic compositions (‰ vs VPDB), c) average pCO_2 concentrations (µatm) with grey envelopes mean ± standard deviations as derived from pH values, d) Fractionation values (ε, in ‰ vs VPDB) of individual PLFAs relative to $CO_{2\,(aq)}$ as calculated form $\delta^{13}C_{DIC}$ at location GM (left) and BB (right). Carbon isotopic compositions of individual PLFAs were not corrected for isotopic offset between PLFA and total cells. e) Fractionation values (‰ vs VPDB) between $CO_{2\,(aq)}$ and weighted averages of phytoplankton, diatom and cyanobacterial $\delta^{13}C$ after correction for the isotopic offset between PLFA and total cells. Location GM is shown left and BB is shown right. Grey shaded areas correspond to summer months: June-August.

5.3.4 Phytoplankton fractionation

Fractionation values between phytoplankton PLFAs and the carbon source $CO_{2(aq)}$ ($\varepsilon_{CO2\text{-}PLFA}$) are shown in figure 5.4d (GM left, BB right) and show substantial differences in $\varepsilon_{CO2\text{-}PLFA}$ between individual PLFAs, with the seasonal changes being similar and in phase for the different PLFAs. At both sites lowest fractionation values were observed at the end of summer and highest fractionation values were observed during winter. Although $\delta^{13}C_{DIC}$ differs appreciably between the two basins, individual phytoplankton PLFAs displayed similar ε values at both sites, with highest fractionation values for PLFAs C18:3ω3 and C18:4ω3, ranging between 18.9 and 29.3‰ for C18:3ω3 and between 19.0 and 33.2‰ for C18:4ω3 at site GM. At site BB, ε values were similar, ranging between 18.7 and 30.3‰ for PLFA C18:3ω3 and between 17.9 and 31.7‰ for PLFA C18:4ω3. Lowest ε values at site GM were observed in PLFAs C20:4ω6 and C16:2ω7, ranging between 15.2 and 23.6‰ and between 15.2 and 22.8‰ respectively. At site BB lowest ε values were found for PLFA C20:4ω6, ranging between 12.5 and 23.4‰, and for PLFA C20:5ω3, ranging between 14.8 and 25.9‰. Additionally, cyanobacterial PLFA C18:3ω6 at location BB also showed relatively low ε values, ranging between 14.5 and 25.6‰.

Stable carbon isotopic fractionation between $CO_{2(aq)}$ and PLFA-based phytoplankton biomass ($\varepsilon_{CO2\text{-}phyto}$) are shown in figure 5.4e. Since the isotopic offset between PLFA and total cells is different for diatoms compared to other phytoplankton species (Taipale et al. 2015), the resulting $\varepsilon_{CO2\text{-}phyto}$ were plotted separately (Fig. 5.4e). At sampling site GM, there was little difference between $\varepsilon_{CO2\text{-}phyto}$ of diatoms compared to other phytoplankton (Fig. 5.4e, left), with minimum values of 11.5 and 15.2‰ respectively in 2013 and around 13.8 and 13.7‰ respectively in 2014. Maximum $\varepsilon_{CO2\text{-}\ phyto}$ values during winter were around 23‰ for both diatoms and other phytoplankton species. At site BB, the difference in $\varepsilon_{CO2\text{-}\ phyto}$ between phytoplankton and diatoms was more apparent, with generally lower ε values for diatoms (Fig. 5.4e right). Minimum $\varepsilon_{CO2\text{-}\ phyto}$ of phytoplankton was 10.8 and 11.9‰ in July 2013 and 2014 respectively, with maximum fractionation values between 19.6 and 22.8‰ from December 2013 to April 2014. Diatom fractionation decreased to around 10‰ from June to October 2013 and was stable around 17‰ during winter and early spring (November to March), reaching a maximum ε value of 20.5‰ in May 2014. A minimum fractionation of 10.7‰ was observed in July 2014. Substantially lower $\varepsilon_{CO2\text{-}phyto}$ values were observed for PLFA-based cyanobacterial biomass, with minimum values of 3.3 and 3.1‰ in July 2013 and 2014 respectively and a maximum fractionation of 13.6 and 14.0‰ observed in April and August 2014 respectively.

5.4 Discussion

5.4.1 Time series

The 17-month sampling period covered two summers and a winter, thereby capturing the full range of seasonal variability in terms of temperatures and light. Nevertheless, variability between years can still be substantial so we compared the results of several parameters to their long-term (decadal) averages and range of natural variability (Fig. 5.2). Measured water temperatures (Fig. 5.2a) were very similar to their long-term average, except for somewhat warmer temperatures in August 2013. These temperatures however, were not extreme and similarly warm months occurred in the summers of 2006 and 2010 (data not shown).

Chlorophyll *a* concentrations, representing phytoplankton biomass, varied considerably between locations GM (Fig. 5.2b) and BB (Fig. 5.2c), with much lower concentrations and only

one peak period at site GM compared to 2 annual peak periods at site BB. Higher chlorophyll *a* concentrations and multiple blooms throughout the year confirm reports based on diatom assemblages that site BB is still eutrophic and moderately disturbed, while site GM is well restored (Van Ee 2007). At site GM, chlorophyll *a* is relatively stable throughout the year, except for the months January to March, when concentrations peak. It is likely that absolute production is higher during spring (and fall) blooms but this is probably compensated by higher grazing pressures at the same time. At site BB, production which escapes grazing (i.e. net production) is highest during late summer (August, September), with a smaller peak in February. It seems that net production in BB is higher and more prone to bloom formation compared to GM. At both sites, chlorophyll *a* concentrations corresponded very well to the long-term values, indicating relative production and grazing during the sampling year can be considered normal.

Overall, variability during the period from May 2013 to September 2014 is in line with that observed over a longer timescale in terms of temperatures, phytoplankton biomass and inorganic carbon chemistry. We therefore believe that the obtained results can be interpreted as representing common conditions. Also the sampling interval used seems to nicely capture the lake's variability over the year, based on the observed gradual changes in the time series.

5.4.2 DIC concentrations and $\delta^{13}C$

In most lakes, DIC concentrations generally vary between 0.1 and 1 mmol C L^{-1} but the naturally occurring range is much larger (<0.02 to >5 mM) and concentrations within systems can be highly variable (Cole and Prairie 2009). At site GM, DIC concentrations show a large range, varying from around 2.7 mmol C L^{-1} during spring to ~1.3 mmol C L^{-1} during summer (Fig. 5.4a, left). DIC concentrations at site BB were higher during most months and were rather stable around 2.3 mmol CL^{-1} from October to March. DIC isotopic compositions at site GM (Fig. 5.4b, left) and BB (Fig. 5.4b, right) showed different values and seasonality with $\delta^{13}C_{DIC}$ values 2-7‰ lower at site BB compared to site GM. These lower values can be due to higher respiration at this more eutrophic site and/or input of small amounts of a relatively depleted source of inorganic carbon (e.g. methane with a $\delta^{13}C$ around -60‰) adding to the DIC pool in basin BB. The enhanced respiration would also explain the somewhat higher DIC concentrations. Although water from Lake Naarden typically infiltrates the ground, a contribution of groundwater-derived methane to the DIC pool at site BB seems likely, since there is at the same time also groundwater seeping into this basin (P. Schot, pers. comm).

Both DIC concentrations and $\delta^{13}C_{DIC}$ are affected by production and respiration, with primary production resulting in lower DIC concentrations and enriched $\delta^{13}C_{DIC}$ due to isotopic fractionation by phytoplankton: the preferential uptake of ^{12}C over ^{13}C during photosynthesis. Conversely, respiration releases relatively light carbon thereby increasing concentrations and lowering $\delta^{13}C_{DIC}$. At both sites, from January until summer, increasing $\delta^{13}C_{DIC}$ reveal that uptake of CO_2 (primary production) exceeds release (respiration). During and after summer, the opposite occurs, when $\delta^{13}C_{DIC}$ values decrease. Concentrations of aqueous dissolved CO_2 ($pCO_{2(aq)}$) as derived from [DIC], pH and water temperatures are lower at sampling site GM compared to site BB during most of the year (Fig. 5.4c). As expected, pCO2 concentrations decrease to very low values during periods of intense primary production (June-August), while pCO_2 maxima are observed during winter months when respiration rates are relatively high. The calculated pCO_2 trends correspond well with variability in $\delta^{13}C_{DIC}$, with minima in pCO_2 corresponding to more enriched $\delta^{13}C_{DIC}$ and maxima in pCO_2 co-occurring with more enriched

$\delta^{13}C_{DIC}$, except for July 2013 in basin BB when chemical enhanced diffusion might have been important (see above).

5.4.3 Phytoplankton $\delta^{13}C$ and fractionation

The stable carbon isotopic composition of PLFAs did not only vary clearly throughout the year, but $\delta^{13}C$ values of individual PLFAs were also different by up to 11.3‰ and 10.1‰ at locations GM and BB respectively within the same month (supplementary Table S5.1). This variation in $\delta^{13}C$ of individual PLFAs may partly result from species-specific isotopic offsets between lipids and total cells. The magnitude of this offset is not well constrained and the applied correction for this offset can be highly variable (Pel et al. 2004, Schouten et al. 1998, Taipale et al. 2015). Additionally, the $\delta^{13}C$ of phytoplankton biomass can be influenced by several species-specific factors resulting in species-specific isotopic discrimination (or fractionation, ε) between carbon source ($CO_{2(aq)}$) and consumers. For example, differences in cell size and permeability (CO_2 diffusion into or leakage out of cells) (Popp et al. 1998), the enzymatic pathway used during photosynthesis, the kinetics of carbon uptake (active vs. diffusion), and the uptake of different carbon species (see below) all result in different ε values for different species (Farquhar et al. 1989, Laws et al. 1995, O'Leary 1988, Peterson and Fry 1987). The PLFAs found in Lake Naarden have different ε values relative to $CO_{2(aq)}$ (Fig. 5.4d), which likely reflects variability in their respective source organisms.

Although the observed PLFAs may have been produced by several source organisms at the same time, the observed suite of PLFAs did allow us to distinguish between, and calculate, $\delta^{13}C$ (weighted averages) of diatoms compared to other phytoplankton and cyanobacteria (the latter at site BB only) (Fig. 5.4e). Differences in fractionation between $CO_{2(aq)}$ and phytoplankton and between $CO_{2(aq)}$ and diatoms were small. The range in ε values found here for diatoms and other phytoplankton (9.0 to 23.0‰) corresponds well with values found in other studies, e.g. 7-18‰ under different light conditions (Rost et al. 2002), 7-27 ‰ in a tidal freshwater estuary (Van den Meersche et al. 2009), 8-25‰ in lakes along a trophic gradient (De Kluijver et al. 2014) and 7-33‰ in a biomanipulation study (Bontes et al. 2006). The observed ε values of cyanobacteria at site BB were substantially lower than ε values for both diatoms and phytoplankton in general, likely related to morphological and physiological differences in e.g. cell walls, the combination of photosynthesis and respiration within the same compartment (Vermaas 2001), and the presence of carboxyzomes (microstructures involved in increasing Rubisco efficiency) in cyanobacteria. Observed fractionation values for cyanobacterial biomass are in line with an average ε value of 12.2‰ reported by Bontes et al. (2006).

The relative uptake of CO_2 and bicarbonate affects photoautotrophs fractionation values not only between species, but also throughout the year. This is a result of the ~10‰ isotopic fractionation during the conversion of $CO_{2(g)}$ to $HCO_{3\ (aq)}^{-}$ (Mook et al. 1974). Rubisco requires CO_2, which is often limiting in lacustrine environments while $HCO_{3\ (aq)}^{-}$ is abundant. To keep up photosynthesis during periods of low [$CO_{2(aq)}$], aquatic photosynthesizers have developed carbon concentrating mechanisms (Lucas and Berry 1985), e.g. using carbonic anhydrase (CA), a family of enzymes that catalyses interconversion between CO_2 and bicarbonate. A relationship between fractionation values and concentrations of $CO_{2(aq)}$ would thus be expected, with higher ε when $pCO_{2(aq)}$ is higher. This relationship has been confirmed in several studies, which have shown the response of ε to changing $pCO_{2(aq)}$ to be species-specific (Degens et al. 1968, Finlay 2004, Hoins et al. 2015, Mizutani and Wada 1982). At both sampling sites in Lake Naarden a general seasonal trend of higher $pCO_{2(aq)}$ co-occurring with higher $\varepsilon_{CO2\text{-}phyto}$ (Fig. 5.4c,e) was observed.

Calculated Pearson correlations however, showed only weak to moderate positive correlations at site GM and no to weak positive correlations at site BB (Table 5.2). This probably reflects phytoplankton isotopic discrimination depending on many other factors as well, such as growth rates (μ), with higher growth rates resulting in lower ε values. Correspondingly, other studies observed stronger correlations between ε values and $\mu/[CO_{2(aq)}]$ (Bontes et al. 2006, Keller and Morel 1999, Laws et al. 1995, Popp et al. 1998, Van Breugel et al. 2006). Additionally, irradiance and light cycles have also been shown to have a major influence on $\varepsilon_{CO2\text{-}phyto}$, stronger even than $pCO_{2(aq)}$ and growth rates (Burkhardt et al. 1999, Rost et al. 2002). As copious factors influence $\varepsilon_{CO2\text{-}phyto}$ and a large variety in correlations has been observed (positive and negative, linear and nonlinear), it is practically impossible to determine which factors exactly contributed to the annual variability we observed in the natural system studied here. Still, it is clear that highest ε is observed when pCO_2 is highest during periods of typically low production rates. Additionally, ε values decrease during spring and summer when pCO_2 decreases and production rates are typically enhanced. This trend is suggestive of uptake of bicarbonate as an alternative carbon source during periods when the concentration of $CO_{2(aq)}$ is low (Hoins et al. 2016).

Table 5.2 Pearson correlations between $\varepsilon_{CO2\text{-}phyto/diatom/cyano}$ and pCO_2 at both sampling sites, where n.d. means not detected. R values for diatoms and cyanobacteria were not statistically significant due to low R value (diatoms) or low n (cyanobacteria).

	Location GM	Location BB
$\varepsilon_{CO2\text{-}phyto}$	R = 0.518 ($p < 0.05$)	R = 0.415 ($p < 0.10$)
$\varepsilon_{CO2\text{-}diatom}$	R = 0.491 ($p < 0.10$)	R = 0.265
$\varepsilon_{CO2\text{-}cyano}$	n.d.	R = 0.423

5.4.4 Particulate organic carbon

Particulate organic carbon contains living biomass of phytoplankton and bacteria, as well as dead organic matter (detritus) from these and other organisms, but it can also contain allochthonous organic carbon, such as small pieces of terrestrial vegetation. At site GM, seasonal changes in the carbon isotopic position of POC were similar to the seasonality observed in the $\delta^{13}C$ of bacterial and phytoplankton biomass, except during winter, when $\delta^{13}C_{phyto}$ decreases to more depleted values compared to $\delta^{13}C_{bact}$ and $\delta^{13}C_{POC}$ (Fig. 5.3, left). This suggests that the phytoplankton dynamics control the stable isotopic composition of the total POC pool, even though living phytoplankton forms a relatively small contribution (5-36%). At site BB, $\delta^{13}C_{bact}$ and $\delta^{13}C_{POC}$ are similar during most months, but the amplitude of variation in $\delta^{13}C_{phyto}$ is higher, showing more enriched values during summer and more depleted values during winter (Fig. 5.3, right), which is in line with bacterial biomass making up a relatively larger part of the POC pool in BB (1.7-9.9%) compared to site GM (0.9-7.9%). Overall the isotopic composition of the POC pools at BB and GM differ considerably, but both consist mostly of detritus throughout the year.

Carbon isotopic compositions of terrestrial and aquatic vegetation from Lake Naarden between -25.5 and -29.3‰ are typical for vegetation using the C3 photosynthetic pathway, with aquatic vegetation showing somewhat more enriched $\delta^{13}C$ compared to terrestrial vegetation (Table 5.1). Only Characeae, or Common Stonewort, had a substantially more enriched $\delta^{13}C$ of -16.4‰ despite careful decalcification steps during sample preparation. In general, $\delta^{13}C$ values of

POC are more depleted than $\delta^{13}C$ values of the aquatic and terrestrial vegetation (Fig. 5.3). Both terrestrial and aquatic vegetation sources likely contribute to the POC pool, stabilizing values, with the more negative values resulting from enhanced phytoplankton production.

5.4.5 Carbon subsidies to bacteria

Bacterial production can be sustained by locally produced fresh algal biomass, its detritus, macrophytes and locally produced or allochthonous DOC. The seasonal trend observed in the isotopic composition of bacterial carbon ($\delta^{13}C_{bact}$) is similar to the trend observed in POC (Fig. 5.3) and phytoplankton biomass ($\delta^{13}C_{phyto}$, Fig. 5.3, 5.5), albeit with a smaller amplitude than phytoplankton. Strong positive correlations were observed between $\delta^{13}C_{phyto}$ and $\delta^{13}C_{bact}$ at site GM ($R = 0.909$, $p < 10^{-5}$) and site BB ($R = 0.935$, $p < 10^{-5}$), indicating that the seasonal variation in $\delta^{13}C_{bact}$ derives mostly from variations in $\delta^{13}C$ of autochthonous, fresh organic matter. However, $\delta^{13}C_{bact}$ had an annual range of 6.9 and 8.2‰ at sites GM and BB respectively, while this range was 11.6 and 13.1‰ for phytoplankton, indicative of contributions from another carbon source. Because the correlation between phytoplankton and bacterial $\delta^{13}C$ is strong but the effects of seasonal variability in $\delta^{13}C_{phyto}$ are dampened in bacteria, the carbon isotopic signature of the supplementary carbon source must have a relatively stable value throughout the year.

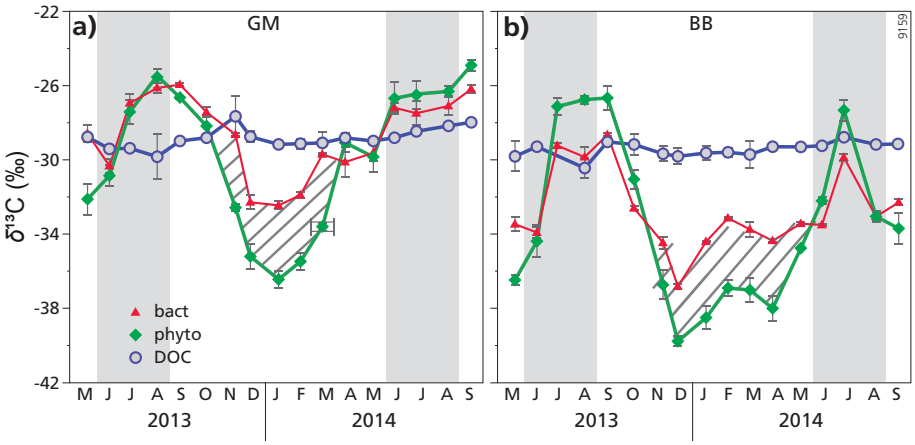

Fig. 5.5 Seasonal variations in carbon isotopic composition ($\delta^{13}C$ in ‰ vs. VPDB) of bacterial biomass (red), phytoplankton biomass (green), and DOC (blue) at a) site GM, and b) site BB. The grey hatched areas represent offset of $\delta^{13}C_{bact}$ from $\delta^{13}C_{phyto}$, likely as a result of enhanced contribution of DOC (allochthonous carbon) to bacterial biomass. Grey shaded areas correspond to summer months: June-August.

Terrestrial vegetation using atmospheric carbon dioxide shows limited isotopic variability and bacterial utilization of terrestrial plants or DOC derived from terrestrial plants might explain the attenuated seasonality (Fig. 5.3, 5.5). The DOC pool has a constant carbon isotopic composition throughout the year, with rather low values around -28.8±0.6‰ at site GM and -29.5±0.4‰ at site BB (Fig. 5.5a,b). The stability of $\delta^{13}C_{DOC}$ may indicate that concentrations of locally produced phytoplankton-derived DOC are much lower than allochthonous DOC and hence too

low to affect the isotopic signal of the large total DOC pool. In a productive system such as Lake Naarden, low contributions of phytoplankton organic matter to the DOC pool are a result of rapid turnover, as fresh phytoplankton biomass is generally easily degradable. We therefore assume the DOC pool in Lake Naarden to consist mainly of allochthonous carbon and we use $\delta^{13}C_{phyto}$ to represent the autochthonous organic carbon source to bacteria. Bacterial dependence on autochthonous (phytoplankton biomass) versus allochthonous (DOC) carbon was calculated from a standard one-isotope-two-sources isotope mixing model. We realize that the DOC pool has a highly variable composition (Fry et al. 1998) and that there is likely variability in the $\delta^{13}C$ of the individual compounds making up the DOC. Since certain compounds will be preferentially consumed, the carbon isotopic composition of the DOC pool as a whole may be somewhat different from the actual food used from that pool by bacteria. Still, even terrestrially derived DOC, although traditionally assumed to be aged and refractory, has been shown to fuel at least parts of the food web (Battin et al. 2008, Cole et al. 2006) and here $\delta^{13}C_{DOC}$ represents the best approximation for allochthonous carbon.

During some months, carbon isotopic compositions of potential sources (phytoplankton, macrophytes and DOC) and bacteria were very similar and thus could not be used to accurately calculate bacterial dependence (Fig. 5.5a). Still, it is clear that during most of the year, $\delta^{13}C_{bact}$ closely follows $\delta^{13}C_{phyto}$, especially at site GM (Fig. 5.5), suggesting that most bacterial carbon derives from phytoplankton (autochthonous) production. At site BB it seems that, in addition to phytoplankton, a more ^{13}C-depleted carbon sources is used by bacteria, since bacterial biomass is depleted compared to phytoplankton by 1-2‰ even during summer months that are characterized by high phytoplankton productivity. As discussed before, a contribution of soil-water derived methane seems likely at site BB, also in view of the very depleted values observed. Whether this is the legacy of sustained eutrophication at this site or results from methane from deeper peat layers and upwelling groundwater cannot be resolved here.

During winter and spring substantial differences were observed between bacterial biomass and phytoplankton biomass and DOC (Fig. 5.5). During these months, bacterial dependence on DOC varied between 39 and 77% at site GM and between 17 and 46% at site BB. These numbers are in line with previous studies (De Kluijver et al. 2015), in which also lower allochthonous contributions were observed in a more eutrophic lake (Cole et al. 2006). However, if methanotrophic bacteria contribute to the bacterial biomass in basin BB, the dependence on allochthonous carbon calculated here are minimum values and still could be similar to the dependence observed in GM. The period when DOC contributes substantially to bacterial biomass seems to last longer at the more eutrophic site BB (November to May) compared to the restored site GM (November to March). Hence, given the longer period of DOC consumption and potential contribution by methanotrophs, net consumption of allochthonous carbon on an annual basis may be higher in BB. This suggests that in the more eutrophic lake more allochthonous carbon is being processed, potentially as a result of larger bacterial standing stocks.

5.5 Conclusions

In the two sub-basins of Lake Naarden fractionation between individual phytoplankton PLFAs and $CO_{2(aq)}$ differed by up to 11.3‰ within the same month, but showed similar seasonal variation during the sampling period. Differences in $\delta^{13}C$ values between individual PLFAs were likely related to differences in source organisms and different species-specific fractionation values.

Fractionation values between phytoplankton biomass and $CO_{2(aq)}$ were similar for phytoplankton and diatoms and differences between sampling sites were small. Highest ε values were observed in winter, with values of 23.0‰ for phytoplankton and 14.0‰ for cyanobacteria. Lowest ε values were observed in summer, with values of 11.6‰ for phytoplankton and 3.1‰ for cyanobacteria. Many factors (light, growth rates etc.) affect phytoplankton fractionation values, but weak positive Pearson correlations between $\varepsilon_{CO2\text{-}biomass}$ and pCO_2 and general correspondence in trends show highest ε values co-occurring with highest pCO_2 (during periods of typically low production rates).

During most months bacterial biomass derives mainly from phytoplankton (autochthonous) production and dependence on allochthonous carbon is very low. During winter and spring however, bacterial dependence on DOC was considerable, varying between 39 and 77% at site GM, and between 17 and 46% at site BB. Possibly, methanotrophic bacteria contributed to $\delta^{13}C_{bact}$ in basin BB, in which case the calculated dependence on DOC are minimum values and could be closer to DOC-dependence observed in GM. Additionally, the period in which DOC contributed to bacterial biomass continued somewhat longer in BB and hence net consumption of allochthonous carbon is likely higher than in GM on an annual basis.

GM month	Bacteria				Phytoplankton				
	iC14:0	iC15:0	aC15:0	C18:3ω3	C18:4ω3	C20:4ω6	C16:2ω7	C20:5ω3	C22:6ω3
May-13	-32.9±1.0	-30.8±0.2	-29.1±0.6		-40.9±1.1	-33.6±0.1		-37.6±1.0	
June-13	-35.4±0.7	-31.5±0.2	-30.9±0.4	-37.6±0.5	-38.9±0.8				-34.2±0.3
July-13	-32.7±0.2	-28.7±0.7	-28.4±0.4	-34.4±0.6				-32.2±0.9	-30.9
August-13		-27.8±0.2	-27.2±0.4	-34.2	-35.6	-26.9±0.3	-26.2±0.1	-27.6±0.9	-29.7±0.7
Sept-13	-31.0±0.1	-27.3±0.2	-27.6	-34.5	-35.3	-29.0±0.1	-30.9	-29.5±0.5	
Oct-13	-32.4±0.3	-29.4±0.2	-28.8±0.4	-35.4±0.8	-36.3±0.2		-31.4±1.4	-32.6±0.4	-33.6±0.4
Nov-13	-32.2±0.9	-30.5	-30.5±0.1	-39.0	-42.4±0.8		-32.9±0.7	-38.8±0.2	-34.8±0.9
Dec-13	-33.7±0.9	-34.0±0.4	-34.6±0.4	-42.3±0.7					-41.1±0.4
Jan-14	-34.5±0.1	-34.4±0.3	-34.5±0.2	-42.8±0.3	-46.3±0.8	-37.0±0.4		-41.3±0.9	-38.1
Feb-14	-34.8±0.2	-33.6±0.2	-33.9±0.2	-42.5±0.7	-44.9±0.2	-34.5±0.2		-39.4±0.2	
March-14	-32.5±0.4	-31.2	-31.9±0.1	-40.9±0.2	-43.2	-31.9±0.5	-35.5±0.7	-37.9±0.4	
April-14	-32.1±0.8							-33.5±0.6	-37.0
May-14	-34.0±0.2	-31.5±0.2	-30.9±0.8	-36.7±0.9	-38.0±0.9			-34.1±0.6	
June-14	-31.1±0.1	-28.9±0.2	-29.0±0.4	-34.5±1.0	-35.4±1.1	-28.8±0.3		-31.9±1.0	
July-14	-30.3±0.5	-29.4±0.7	-29.0±0.7	-34.9	-33.8	-28.3±0.6		-30.5±0.9	-28.7±0.7
August-14	-29.9±0.3	-29.4±0.6	-28.0±0.6	-34.4±0.1	-32.8±0.8	-27.6±0.6	-32.5±0.1		
Sept-14	-30.5±0.7	-27.7	-27.0±0.2	-31.7±0.3	-31.8±0.6		-31.3		-28.8±1.1

$\delta^{13}C$ values of individual PLFAs (in ‰ vs. VPDB ± SD; n=2) at sampling site GM

BB		Bacteria				Phytoplankton				Cyanobacteria
month	iC14:0	iC15:0	aC15:0	C18:3ω3	C18:4ω3	C20:4ω6	C16:2ω7	C20:5ω3	C22:6ω3	C22:6ω3
May-13	-36.4±0.3	-35.6±0.3	-34.9±0.6	-44.6±0.1			-38.9±0.2	-37.1±1.5		
June-13	-37.7±1.2	-36.2	-34.9±0.5	-41.7±0.9			-40.5±1.8		-38.8±0.4	-32.6±0.1
July-13	-34.0±0.6	-31.0±0.3	-31.0	-36.4±0.4	-35.7±1.0	-31.0±0.1		-33.1±1.0		
August-13	-34.3±1.0	-32.0±0.5	-30.5±0.5	-34.8±0.1	-31.7±0.8	-26.9±0.8		-28.4±1.0		
Sept-13		-30.5	-30.9±0.2		-33.7±0.7					
Oct-13	-35.7±0.4	-34.3±0.1	-34.5±0.1	-39.3±0.5	-37.9±0.6			-29.2±0.3		
Nov-13		-36.3±0.4	-36.7±0.4	-45.0±0.7	-45.7±0.2		-36.8±0.6	-41.4	-36.6±3.8	
Dec-13		-38.8±0.2	-38.8±0.2	-48.3±0.1	-49.5±0.3		-40.0±0.8	-45.0±0.4	-41.3±0.8	-39.6±0.1
Jan-14	-36.6±0.2	-36.4±0.1	-36.4±0.1	-47.0±0.5	-47.8±1.2	-38.0±0.4	-39.9±1.1	-41.9±0.5		-39.2±0.6
Feb-14	-37.3	-35.5±0.1	-35.4	-44.8±0.7	-45.3±0.1		-41.2±0.9	-39.8±0.2	-39.0±0.2	-37.5±1.0
March-14		-35.3±0.3	-36.1±0.5	-45.5±0.6	-45.7±1.6			-37.8±0.7	-41.1±0.7	-39.9±1.7
April-14	-37.8±0.1	-36.0	-36.4±0.2	-45.7±0.7	-47.1±1.7		-40.6±0.4	-39.7±0.4	-43.0±0.2	-41.0±0.5
May-14	-36.1±0.3	-35.1±0.1	-35.7±0.1	-41.7	-44.1	-36.8±0.4		-41.7		-37.1±0.5
June-14	-36.3±0.1	-35.6±0.2	-35.2	-41.7±0.3	-42.9±0.1	-33.2±0.1	-37.6±1.0	-34.0		-37.2±0.5
July-14	-33.9±0.2	-31.1±0.2	-31.7±0.3	-35.8±0.8	-33.9±0.1	-28.4±0.5	-34.0±0.1	-30.6±0.2		-30.3±0.4
August-14		-34.7±0.4	-35.2±0.2	-40.0		-36.2±0.8	38.3±0.5	-39.3±0.1	-39.4±0.8	-39.0±0.9
Sept-14		-34.4	-34.2±0.4	-41.5±0.7	-42.0±1.0	-37.8±1.1				-39.7±1.1

$\delta^{13}C$ values of individual PLFAs (in ‰ vs. VPDB ± SD; n=2) at sampling site BB

References

Abeliovich A, Weisman D (1978) Role of Heterotrophic Nutrition in Growth of the Alga *Scenedesmus obliquus* in High-Rate Oxidation Ponds. Applied and Environmental Microbiology 35:32-37

Ahlgren G, Gustafsson IB, Moberg M (1992) Fatty acid content and chemical composition of freshwater microalgae. Journal of Phycology 28:37-50

Andersen T, Hessen DO (1991) Carbon, nitrogen, and phosphorus content of freshwater zooplankton. Limnology and Oceanography 36:807-814

Bade DL, Cole JJ (2006) Impact of chemically enhanced diffusion on dissolved inorganic carbon stable isotopes in a fertilized lake. Journal of Geophysical Research 111

Baines SB, Pace ML (1991) The production of dissolved organic matter by phytoplankton and its importance to bacteria: Patterns across marine and freshwater systems. Limnology and Oceanography 36:1078-1090

Battin TJ, Luyssaert S, Kaplan LA, Aufdenkampe AK, Richter A, Tranvik LJ (2009) The boundless carbon cycle. Nature Geoscience 2:598-600

Battin TJ, Kaplan LA, Findlay S, Hopkinson CS, Marti E, Packman AI, Newbold JD, Sabater F (2008) Biophysical controls on organic carbon fluxes in fluvial networks. Nature Geoscience 1:95-100

Bauersachs T, Compaoré J, Hopmans EC, Stal LJ, Schouten S, Sinninghe Damsté JS (2009) Distribution of heterocyst glycolipids in cyanobacteria. Phytochemistry 70:2034-2039

Blaga CI, Reichart GJ, Vissers EA, Lotter AF, Anselmetti FS, Sinninghe Damsté JS (2011) Seasonal changes in glycerol dialkyl glycerol tetraether concentrations and fluxes in a perialpine lake: Implications for the use of the TEX_{86} and BIT proxies. Geochimica et Cosmochimica Acta 75:6416-6428

Bloesch J, Stadelmann P, Buhrer H (1977) Primary Production, Mineralization, and Sedimentation in the Euphotic Zone of Two Swiss Lakes. Limnology and Oceanography 22:511-526

Bodelier PLE, Bär Gillisen MJ, Hordijk K, Sinninghe Damsté JS, Rijpstra WIC, Geenevasen JAJ, Dunfield P (2009) A reanalysis of phospholipid fatty acids as ecological biomarkers for methanotrophic bacteria. The ISME Journal 3:606-617

Bontes BM, Pel R, Ibelings BW, Boschker HTS, Middelburg JJ, Van Donk E (2006) The effects of biomanipulation on the biogeochemistry, carbon isotopic composition and pelagic food web relations of a shallow lake. Biogeosciences 3:69-83

Bootsma MC, Barendregt A, Van Alphen JCA (1999) Effectiveness of reducing external nutrient load entering a eutrophicated shallow lake ecosystem in the Naardermeer nature reserve, The Netherlands. Biological Conservation 90:193-201

Boschker HTS, Moerdijk-Poortvliet TCW, van Breugel P, Houtekamer M, Middelburg JJ (2008) A versatile method for stable carbon isotope analysis of carbohydrates by high-performance liquid chromatography/isotope ratio mass spectrometry. Rapid Communications in Mass Spectometry 22:3902-3908

Boschker HTS, Middelburg JJ (2002) Stable isotopes and biomarkers in microbial ecology. FEMS Microbiology Ecology 40:85-95

Boschker HTS, Nold SC, Wellsbury P, Bos D, de Graaf W, Pel R, Parkes RJ, Cappenberg TE (1998) Direct linking of microbial populations to specific biogeochemical processes by ^{13}C-labelling of biomarkers. Nature 392:801-805

Bossard P, Gammeter S, Lehmann C, Schanz F, Bachofen R, Bürgi HR, Steiner D, Zimmerman U (2001) Limnological description of the Lakes Zürich, Lucerne, and Cadagno. Aquatic Sciences 63:225-249

Bossard PP, Stettler R, Bachofen R (2000) Seasonal and spatial community dynamics in the meromictic Lake Cadagno. Archives of Microbiology 174:168-174

Bowman JP, Sly LI, Nichols PD, Hayward AC (1993) Revised taxonomy of the methanotrophs – description of *Methylobacter* gen.nov., emendation of *Methylococcus*, validation of *Methylosinus* and *Methylocystis* species, and a proposal that the family *Methylococcaceae* includes only the group-I methanotrophs. International Journal of Systematic Bacteriology 43:735-753

Bowman JP, Skerratt JH, Nichols PD, Sly LI (1991) Phospholipid fatty acid and lipopolysaccharide fatty acid signature lipids in methane-utilizing bacteria. FEMS Microbiology Ecology 85:15-22

Brand A, Bruderer H, Oswald K, Guggenheim C, Schubert CJ, Wehrli B (2016) Oxygenic primary production below the oxycline and its importance for redox dynamics. Aquatic Sciences 78:727-741

Bratbak G, Thingstad TF (1985) Phytoplankton-bacteria interactions: an apparent paradox? Analysis of a model system with both competition and commensalism. Marine Ecology Progress Series 25:23-30

Brett MT, Arhonditsis GB, Chandra S, Kainz MJ (2012) Mass flux calculations show strong allochthonous support of freshwater zooplankton production is unlikely. PLoS ONE 7

Brett MT, Kainz MJ, Taipale SJ, Seshan H (2009) Phytoplankton, not allochthonous carbon, sustains herbivorous zooplankton production. PNAS 106:21197-21201

Brett MT, Müller-Navarra DC (1997) The role of highly unsaturated fatty acids in aquatic foodweb processes. Freshwater Biology 38:483-499

Bürgi HR, Stadelmann P (2002) Alteration of phytoplankton structure in Lake Lucerne due to trophic conditions. Aquatic Ecosystem Health and Management 5:45-59

Bürgi HR, Heller C, Gaebel S, Mookerji N, Ward JV (1999) Strength of coupling between phyto- and zooplankton in Lake Lucerne (Switzerland) during phosphorus abatement subsequent to a weak eutrophication. Journal of Plankton Research 21:485-507

Burkhardt S, Riesebell U, Zondervan I (1999) Stable carbon isotope fractionation by marine phytoplankton in response to daylength, growth rate, and CO_2 availability. Marine Ecology Progress Series 184:31-41

Buser HR, Arn H, Guerin P, Rauscher S (1983) Determination of double bond position in mono-unsaturated acetates by mass spectrometry of dimethyl disulfide adducts. Analytical Chemistry 55:818-822

Canadell JG, Le Quéré C, Raupach MR, Field CB, Buitenhuis ET, Ciais P, Conway TJ, Gillet NP, Houghton RA, Marland G (2007) Contributions to accelerating atmospheric CO_2 growth from economic activity, carbon intensity, and efficiency of natural sinks. PNAS 104:18866

Canuel EA, Martens CS (1993) Seasonal variations in the sources and alteration of organic matter associated with recently-deposited sediments. Organic Geochemistry 20:563-577

Carpenter SR, Caraco NF, Correll DL, Howarth RW, Sharpley AN, Smith VH (1998) Nonpoint pollution of surface waters with phosphorous and nitrogen. Ecological Applications 8:559-568

Carpenter SR, Kitchell JF, Hodgson JR, Cochran PA, Elser JJ, Elser MM, Lodge DM, Kretchmer D, He X, von Ende CN (1987) Regulation of lake primary productivity by food web structure. Ecology 68:1863-1876

Carpenter SR, Lodge DM (1986) Effects of submersed macrophytes on ecosystem processes. Aquatic Botany 26:341-370

Chen Y, Qin B, Teubner K, Dokulil MT (2003) Long-term dynamics of phytoplankton assemblages: *Microcystis*-domination in Lake Taihu, a large shallow lake in China. Journal of Plankton Research 25:445-453

Christoffersen K, Riemann B, Hansen LR, Klysner A, Sørensen HB (1990) Qualitative importance of the microbial loop and plankton community structure in a eutrophic lake during a bloom of cyanobacteria. Microbial Ecology 20:253-272

Clarke SJ (2002) Vegetation growth in rivers: influences upon sediment and nutrient dynamics. Progress in Physical Geography 26:159-172

Cole JJ, Carpenter SR, Kitchell JF, Pace ML, Solomon CT, Weidel BC (2011) Strong evidence for terrestrial support of zooplankton in small lakes based on stable isotopes of carbon, nitrogen, and hydrogen. PNAS 108:1975-1980

Cole JJ, Prairie YT (2009) Dissolved CO_2. In: Likens GE (ed) Encyclopedia of Inland Waters, 2nd edn. Elsevier, Oxford, pp 30-34

Cole JJ, Prairie YT, Caraco NF, McDowell WH, Tranvik LJ, Striegl RG, Duarte CM, Kortelainen P, Downing JA, Middelburg JJ, Melack JM (2007) Plumbing the global carbon cycle: integrating inland waters into the terrestrial carbon budget. Ecosystems 10:171-184

Cole JJ, Carpenter SR, Pace ML, van de Bogert C, Kitchell JF, Hodgson JR (2006) Differential support of lake food webs by three types of terrestrial organic carbon. Ecology Letters 9:558-568

Cole JJ, Pace ML, Carpenter SR, Kitchell JF (2000) Persistence of net heterotrophy in lakes during nutrient addition and food web manipulations. Limnology and Oceanography 45:1718-1730

Cole JJ, Caraco NF, Kling GW, Kratz TK (1994) Carbon dioxide supersaturation in the surface waters of lakes. Science 265:1568-1570

Cole JJ, Findlay S, Pace ML (1988) Bacterial production in fresh and saltwater ecosystems: a cross-system overview. Marine Ecology Progress Series 43:1-10

Coloso JJ, Cole JJ, Pace ML (2011) Difficulty in discerning drivers of lake ecosystem metabolism with high-frequency data. Ecosystems 14:935-948

Combres C, Laliberté G, Reyssac J, Noüe JDL (1994) Effect of acetate on growth and ammonium uptake in the microalga *Scenedesmus obliquus*. Physiologia Plantarum 91:729-734

Coplen TB (2011) Guidelines and recommended terms for expression of stable-isotope-ratio and gas-ratio measurement results. Rapid Communications in Mass Spectometry 25:2538-2560

Cotner JB, Biddanda BA (2002) Small players, large role: microbial influence on biogeochemical processes in pelagic aquatic ecosystems. Ecosystems 5:105-121

Darchambeau F, Sarmento H, Descy JP (2014) Primary production in a tropical large lake: The role of phytoplankton composition. Science of the Total Environment 473-474:178-188

Davison IR (1991) Environmental effects on algal photosynthesis: temperature. Journal of Phycology 27:2-8

De Bie MJM, Starink M, Boschker HTS, Peene JJ, Laanbroek HJ (2002) Nitrification in the Schelde estuary: Methodological aspects and factors influencing its activity. FEMS Microbiology Ecology 42:99-107

De Kluijver A, Ning J, Liu Z, Jeppesen E, Gulati RD, Middelburg JJ (2015) Macrophytes and periphyton carbon subsidies to bacterioplankton and zooplankton in a shallow eutrophic lake in tropical China. Limnology and Oceanography 60:375-385

De Kluijver A, Schoon PL, Downing JA, Schouten S, Middelburg JJ (2014) Stable carbon isotope biogeochemistry of lakes along a trophic gradient. Biogeosciences 11:6265-6276

De Kluijver A, Soetaert K, Czerny J, Schulz KG, Boxhammer T, Riesebell U, Middelburg JJ (2013) A ^{13}C labelling study on carbon fluxes in Arctic plankton communities under elevated CO_2 levels. Biogeosciences 10:1425-1440

De Kluijver A, Yu J, Houtekamer M, Middelburg JJ, Liu Z (2012) Cyanobacteria as a carbon source for zooplankton in eutrophic Lake Taihu, China, measured by ^{13}C labeling and fatty acid biomarkers. Limnology and Oceanography 57:1245-1254

De Kluijver A, Soetaert K, Schulz KG, Riesebell U, Bellerby RGJ, Middelburg JJ (2010) Phytoplankton-bacteria coupling under elevated CO_2 levels: a stable isotope labelling study. Biogeosciences 7:3783-3797

Degens ET, Guillard RRL, Sackett WM, Helleburst JA (1968) Metabolic fractionation of carbon isotopes in marine plankton: Temperature and respiration experiments. Deep-Sea Research 15:1-9

Del Giorgio PA, Cole JJ (1998) Bacterial growth efficiency in natural aquatic systems. Annual Review of Ecology and Systematics 29:503-541

Del Giorgio PA, Cole JJ, Cimberlis A (1997) Respiration rates in bacteria exceed phytoplankton production in unproductive systems. Nature 385:148-151

Del Giorgio PA, Gasol PM (1995) Biomass distribution in freshwater plankton communities. The American Naturalist 146:135-152

Del Giorgio PA, Peters RH (1994) Patterns in planktonic P:R ratios in lakes: influence of lake trophy and dissolved organic carbon. Limnology and Oceanography 39:772-787

Dickson L, Bull ID, Gates PJ, Evershed RP (2009) A simple modification of a silicic acid lipid fractionation protocol to eliminate free fatty acids from glycolipid and phospholipid fractions. Journal of Microbiological Methods 78:249-254

Dijkman NA, Boschker HTS, Middelburg JJ, Kromkamp JC (2009) Group-specific primary production based on stable-isotope labeling of phospholipid-derived fatty acids. Limnology and Oceanography: Methods 7:612-625

Dijkman NA, Kromkamp JC (2006) Phospholipid-derived fatty acids as chemotaxonomic markers for phytoplankton: application for inferring phytoplankton composition. Marine Ecology Progress Series 324:113-125

Ducklow H, Carlson C, Church M, Kirchman D, Smith D, Steward G (2001) The seasonal development of the bacterioplankton bloom in the Ross Sea, Antarctica, 1994 – 1997. Deep-Sea Research II 48:4199-4221

Ducklow H, Carlson C, Smith W (1999) Bacterial growth in experimental plankton assemblages and seawater cultures from the *Phaeocystis antarctica* bloom in the Ross Sea, Antarctica. Aquatic Microbial Ecology 19:215-227

Farquhar GD, Ehlinger JR, Hubick KT (1989) Carbon isotope discrimination and photosynthesis. Annual review of plant physiology and plant molecular biology 40:503-537

Fernando CH (1994) Zooplankton, fish and fisheries in tropical freshwaters. Hydrobiologia 272:105-123

Feuillade M, Feuillade J (1989) Heterotrophic capabilities of the blue-green alga *Oscillatoria rubescens*. Archiv für Hydrobiologie 117:61-76

Finlay FC (2004) Patterns and controls of lotic algal stable carbon isotope ratios. Limnology and Oceanography 49:850-861

Fogg GE (1983) The ecological significance of extracellular products of phytoplankton photosynthesis. Botanica Marina 26:3-14

Fry B, Hopkinson CSJ, Nolin A, Wainwright SC (1998) $^{13}C/^{12}C$ composition of marine dissolved organic carbon. Chemical Geology 152:113-118

Fulton RS, Paerl HW (1988) Effects of the blue-green alga *Microcystis aeruginosa* on zooplankton competitive relations. Oecologia 76:383-389

Galand PE, Saarnio S, Fritze H, Yrjälä K (2002) Depth related diversity of methanogen Archaea in Finnish oligotrophic fen. FEMS Microbiology Ecology 42:441-449

Ganf GG (1974) Phytoplankton biomass and distribution in a shallow eutrophic lake (Lake George, Uganda). Oecologia 16:9-29

Gervais F (1997) Light-dependent growth, dark survival, and glucose uptake by Cryptophytes isolated from a freshwater chemocline. Journal of Phycology 33:18-25

Geyer C (2011) Introduction to Markov Chain Monte Carlo. In: Brooks S, Gelman A, Jones GL, Meng XL (eds) Handbook of Markov Chain Monte Carlo. CRC Press, New York

Granum E, Kirkvold S, Myklestad SM (2002) Cellular and extracellular production of carbohydrates and amino acids by the marine diatom *Skeletonema costatum*: diel variations and effects of N depletion. Marine Ecology Progress Series 242:83-94

Grey J, Jones RI (2001) Seasonal changes in the importance of the source of organic matter to the diet of zooplankton in Loch Ness, as indicated by stable isotope analysis. Limnology and Oceanography 46:505-513

Gribsholt B, Boschker HTS, Struyf E, Andersson M, Tramper A, De Brabandere L, Van Damme S, Brion N, Meire P, Dehairs F, Middelburg JJ, Heip CHR (2005) Nitrogen processing in a tidal freshwater marsh: A whole-ecosystem ^{15}N labeling study. Limnology and Oceanography 50:1945-1959

Grosse J, van Breugel P, Boschker HTS (2015) Tracing carbon fixation in phytoplankton – compound specific and total ^{13}C incorporation rates. Limnology and Oceanography: Methods 13:288-302

Guckert JB, Ringelberg DB, White DC, Hanson RS, Bratina BJ (1991) Membrane fatty acids as phenotypic markers in the polyphasic taxonomy of methylotrophs within the Proteobacteria. Journal of General Microbiology 137:2631-2641

Guezennec J, Fialamedioni A (1996) Bacterial abundance and diversity in the Barbados trench determined by phospholipid analysis. FEMS Microbiology Ecology 19:83-93

Gugger M, Lyra C, Suominen I, Tsitko I, Humbert JF, Salkinoja-Salonen MS, Sivonen K (2002) Cellular fatty acids as chemotaxonomic markers of the genera *Anabaena*, *Aphanizomenon*, *Microcystis*, *Nostoc* and *Planktothrix* (cyanobacteria). International Journal of Systematic and Evolutionary Microbiology 52:1007-1015

Gyllström M, Hansson LA, Jeppesen E, García-Criado F, Gross E, Irvine K, Kairesalo T, Kornijow W, Miracle MR, Nykänen M, Nõges T, Romo S, Stephen D, Van Donk E, Moss B (2005) The role of climate in shaping zooplankton communities of shallow lakes. Limnology and Oceanography 50:2008-2021

Haack SK, Garchow H, Odelson DA, Forney LJ, Klug MJ (1994) Accuracy, reproducibility, and interpretation of fatty acid methyl ester profiles of model bacterial communities. Applied Environmental Microbiology 60:2483-2493

Hama T, Miyazaki T, Ogawa Y, Iwakuma T, Takahashi M, Otsuki A, Ichimura S (1983) Measurement of photosynthetic production of a marine phytoplankton population using a stable ^{13}C isotope. Marine Biology 73:31-36

Hamilton SK, Tank JL, Raikow DF, Siler ER, Dorn NJ, Leonard NE (2004) The role of instream vs allochthonous N in stream food webs: modeling the results of an isotope addition experiment. Journal of the North American Benthological Society 23:429-448

Hammes F, Vital M, Egli T (2010) Critical evaluation of the volumetric "bottle effect" on microbial batch growth. Applied and Environmental Microbiology 76:1278-1281

Hancke K, Glud RN (2004) Temperature effects on respiration and photosynthesis in three diatom-dominated benthic communities. Aquatic Microbial Ecology 37:265-281

Hanson PC, Pace ML, Carpenter SR, Cole JJ, Stanley EH (2015) Integrating landscape carbon cycling: research needs for resolving organic carbon budgets of lakes. Ecosystems 18:363-375

Harvey HR, Fallom RD, Patton JS (1986) The effect of organic matter and oxygen on the degradation of bacterial membrane lipids in marine sediments. Geochimica et Cosmochimica Acta 50:795-805

Havens KE, Work KA, East TL (2000) Relative efficiencies of carbon transfer from bacteria and algae to zooplankton in a subtropical lake. Journal of Plankton Research 22:1801-1809

Hayes JM (2001) Fractionation of carbon and hydrogen isotopes in biosynthetic processes. In: Valley JW, Cole D (eds) Stable isotope geochemistry, Reviews in Mineralogy & Geochemistry, vol. 43 edn. Mineralogical Society of America, pp 225-277

Heimann M (2009) Searching out the sinks. Nature Geoscience 2:3-4

Hessen DO (1992) Dissolved organic carbon in a humic lake: effects on bacterial production and respiration. Hydrobiologia 229:115-123

Hoins M, Eberlein T, Van de Waal DB, Sluijs A, Reichart GJ, Rost B (2016) CO_2-dependent carbon isotope fractionation in dinoflagellates relates to their inorganic carbon fluxes. Journal of Experimental Marine Biology and Ecology 481:9-14

Hoins M, Van de Waal DB, Eberlein T, Reichart GJ, Rost B, Sluijs A (2015) Stable carbon isotope fractionation of organic cyst-forming dinoflagellates: Evaluating the potential for a CO_2 proxy. Geochimica et Cosmochimica Acta 160:267-276

Hoppe HG, Breithaupt P, Walther K, Koppe R, Bleck S, Sommer U, Jürgens K (2008) Climate warming in winter affects the coupling between phytoplankton and bacteria during the spring bloom: a mesocosm study. Aquatic Microbial Ecology 51:105-115

Humayoun SB, Bano N, Hollibaugh JT (2003) Depth distribution of microbial diversity in Mono Lake, a meromictic soda lake in California. Applied and Environmental Microbiology 69:1030-1042

Iglesias C, Goyenola G, Mazzeo N, Meerhoff M, Rodó E, Jeppesen E (2007) Horizontal dynamics of zooplankton in subtropical Lake Blanca (Uruguay) hosting multiple zooplankton predators and aquatic plant refuges. Hydrobiologia 584:179-189

IPCC (2013) Climate Change 2013: The Physical Science Basis. Contribution of Working Group I to the Fifth Assessment Report of the Intergovernmental Panel on Climate Change. Cambridge University Press, Cambridge

IPCC (2007) Climate Change 2007: The Physical Science Basis. Contribution of Working Group I to the Fourth Assessment Report of the Intergovernmental Panel on Climate Change. Cambridge University Press, Cambridge

Jeppesen E, Jensen JP, Søndergaard M, Lauridsen T (1999) Trophic dynamics in turbid and clearwater lakes with special emphasis on the role of zooplankton for water clarity. Hydrobiologia 408/409:217-231

Jeppesen E, Søndergaard M, Søndergaard M, Christoffersen K (1998) The structuring role of submerged macrophytes in lakes. Springer, New York

Jeppesen E, Jensen JP, Søndergaard M, Lauridsen T, Pedersen LJ, Jensen L (1997) Top-down control in freshwater lakes: the role of nutrient state, submerged macrophytes and water depth. Hydrobiologia 432-343:151-164

Jeppesen E, Søndergaard M, Lauridsen TL, Davidson TA, Liu Z, Mazzeo N, Trochine C, Özkan K, Jensen HS, Trolle D, Starling F, Lazzaro X, Johansson LS, Bjerring R, Liboriussen L, Larsen SE, Landkildehus F, Egemose S, Meerhoff M (2012) Biomanipulation as a restoration tool to combat eutrophication: recent advances and future challenges. Adv Ecol Res. doi: 10.1016/B978-0-12-398315-2.00006-5

Jones HLJ, Leadbeater BSC, Green JC (1994) The haptophyte algae. Systematics Association and Clarendon Press, Oxford

Kaneda T (1991) Iso-fatty and anteiso-fatty acids in bacteria – biosynthesis, function and taxonomic significance. Microbiological reviews 55:288-302

Keller K, Morel FMM (1999) A model of carbon isotopic fractionation and active carbon uptake in phytoplankton. Marine Ecology Progress Series 182:295-298

Keough JE, Sierzen M, Hagley C (1996) Analysis of a Lake Superior coastal food web with stable isotopes. Limnology and Oceanography 41:136-146

Kling GW, Fry B, O'brien WJ (1992) Stable isotopes and planktonic trophic structures in Arctic lakes. Ecology 73:561-566

Koizumi Y, Kojima H, Oguri K, Kitazato H, Fukui M (2004) Vertical and temporal shifts in microbial communities in the water column and sediment of saline meromictic Lake Kaiike (Japan), as determined by a 16S rDNA-based analysis, and related to physicochemical gradients. Environmental Microbiology 6:622-637

Kok B (1956) On the inhibition of photosynthesis by intense light. Biochimica et Biophysica Acta 21:234-244

Kolzau S, Wiedner C, Rücker J, Köhler J, Köhler A, Dolman AM (2014) Seasonal patterns of nitrogen and phosphorus limitation in four German lakes and the predictability of limitation status from ambient nutrient concentrations. PLoS ONE 9

Koshikawa H, Harada S, Watanabe M, Sato K, Akehata K (1996) Relative contribution of bacterial and photosynthetic production to metazooplankton as carbon sources. Journal of Plankton Research 18:2269-2281

Lapierre JF, Seekell DA, Del Giorgio PA (2015) Climate and landscape influence on indicators of lake carbon cycling through spatial patterns in dissolved organic carbon. Global Change Biology 21:4425-4435

Lapierre JF, Del Giorgio PA (2014) Partial coupling and differential regulation of biologically and photochemically labile dissolved organic carbon across boreal aquatic network. Biogeosciences 11:5969-5985

Laws EA, Popp BN, Bidigare RR, Kennicutt MC, Macko SA (1995) Dependence of phytoplankton carbon isotopic composition on growth rate and $[CO_2]_{aq}$: Theoretical considerations and experimental results. Geochimica et Cosmochimica Acta 59:1131-1138

Le Quéré C, Raupach MR, Canadell JG, Marland G, Bopp L, Ciais P, Conway TJ, Doney SC (2009) Trends in the sources and sinks of carbon dioxide. Nature Geoscience 2:831-836

Lewin JC (1953) Heterotrophy in diatoms. Journal of General Microbiology 9:305-313

Lipski A, Spieck E, Makolla A, Altendorf K (2001) Fatty acid profiles of nitrite-oxidizing bacteria reflect their phylogenetic heterogeneity. Systematic and Applied Microbiology 24:377-384

Lucas WJ, Berry JA (1985) Inorganic carbon transport in aquatic photosynthetic organisms. Physiologia Plantarum 65:539-543

Luo X, Liu Z, Gulati RD (2015) Cyanobacterial carbon supports the growth and reproduction of *Daphnia*: an experimental study. Hydrobiologia 743:211-220

Lyche A, Andersen T, Christoffersen K, Hessen DO, Hansen PHB, Klysner A (1996) Mesocosm tracer studies. 2. The fate of primary production and the role of consumers in the pelagic carbon cycle of a mesotrophic lake. Limnology and Oceanography 41:475-487

Madzen TV, Sand-Jensen K (1991) Photosynthetic carbon assimilation in aquatic macrophytes. Aquatic Botany 41:5-40

Meerhoff M, Fosalba C, Bruzzone C, Mazzeo N, Noordhoven W, Jeppesen E (2006) An experimental study of habitat choice by *Daphnia*: plants signal danger more than refuge in subtropical lakes. Freshwater Biology 51:1320-1330

Meili M (1992) Sources, concentrations and characteristics of organic matter in softwater lakes and streams of the Swedish forest region. Hydrobiologia 229:23-41

Middelburg JJ (2014) Stable isotopes dissect aquatic food webs from the top to the bottom. Biogeosciences 11:2357-2371

Middelburg JJ, Barranguet C, Boschker HTS, Herman PMJ, Moens T, and Heip CHR (2000) The fate of intertidal microphytobenthos carbon: An in situ ^{13}C-labeling study. Limnology and Oceanography 45:1224-1234

Mizutani H, Wada E (1982) Effects of high atmospheric CO_2 on $\delta^{13}C$ of algae. Origins of Life 12:377-390

Montesinos ML, Herrero A, Flores E (1997) Amino acid transport in taxonomically diverse cyanobacteria and identification of two genes encoding elements of a neutral amino acid permease putatively involved in recapture of leaked hydrophobic amino acids. Journal of Bacteriology 179:853-862

Mook WG, Bommerson JC, Staverman WH (1974) Carbon isotope fractionation between dissolved bicarbonate and gaseous carbon dioxide. Earth and Planetary Science Letters 22:169-176

Moore KA, Shields EC, Jarvis JC (2010) The role of habitat and herbivory on the restoration of tidal freshwater submerged aquatic vegetation populations. Restoration Ecology 18:596-604

Morana C, Roland FAE, Crowe SA, Llirós M, Borgers AV, Darchambeau F, Bouillon S (2016) Chemoautotrophy and anoxygenic photosynthesis within the water column of a large meromictic tropical lake (Lake Kivu, East Africa). Limnology and Oceanography 61:1424-1437

Morita RY (1982) Starvation-survival of heterotrophs in the marine environment. Advances in Microbial Ecology 6:171-198

Morris DP, Lewis WM (1988) Phytoplankton nutrient limitation in Colorado mountain lakes. Freshwater Biology 20:315-327

Moss B (2010) Climate change, nutrient pollution and the bargain of Dr Faustus. Freshwater Biology 55:175-187

Naeher S, Peterse F, Smittenberg RH, Niemann H, Zigah PK, Schubert CJ (2014) Sources of glycerol dialkyl glycerol tetraethers (GDGTs) in catchment soils, water column and sediments of Lake Rotsee (Switzerland) – Implications for the application of GDGT-based proxies for lakes. Organic Geochemistry 66:164-173

Necchi Jr O, Zucchi MR (2001) Photosynthetic performance of freshwater Rhodophyta in response to temperature, irradiance, pH and diurnal rhythm. Phycological Research 49:305-318

Nichols PD, Smith GA, Antworth CP, Hanson RS, White DC (1985) Phospholipid and lipoploysaccharide normal and hydroxy fatty-acids as potential signatures for methane-oxidizing bacteria. FEMS Microbiology Ecology 31:327-335

O'Leary MH (1988) Carbon isotopes in photosynthesis. BioScience 38:325-336

Oswald K, Milucka J, Brand A, Littmann S, Wehrli B, Kuypers MMM, Schubert CJ (2015) Light-dependent aerobic methane oxidation reduces methane emissions from seasonally stratified lakes. PLoS ONE 10

Øvreås L, Forney L, Daae FL, Torsvik V (1997) Distribution of bacterioplankton in meromictic Lake Saelenvannet, as determined by denaturing gradient gel electrophoresis of PCR-amplified gene fragments coding for 16S rRNA. Applied and Environmental Microbiology 63:3367-3373

Pace ML, Carpenter SR, Cole JJ, Coloso JJ, Kitchell JF, Hodgson JR, Middelburg JJ, Preston ND, Solomon CT, Weidel BC (2007) Does terrestrial organic carbon subsidize the planktonic food web in a clear-water lake?. Limnology and Oceanography 52:2177-2189

Pace ML, Prairie YT (2005) Respiration in lakes. In: del Giorgio PA, Williams PJl (eds) Respiration in Aquatic Ecosystems. Oxford University Press Inc., New York, pp 103-121

Pace ML, Cole JJ, Carpenter SR, Kitchell JF, Hodgson JR, van de Bogert C, Bade DL, Kritzberg ES, Bastviken D (2004) Whole-lake carbon-13 additions reveal terrestrial support of aquatic food webs. Nature 427:240-243

Pacheco FS, Roland F, Downing JA (2013) Eutrophication reverses whole-lake carbon budgets. Inland Waters 4:41-48

Paerl HW, Huisman J (2008) Blooms like It hot. Science 320:57-58

Paerl HW, Fulton RS, Moisander PH, Dyble J (2001) Harmful freshwater algal blooms, with an emphasis on cyanobacteria. TheScientificWorld 1:76-113

Paerl HW (1991) Ecophysiological and trophic implications of light-stimulated amino acid utilization in marine picoplankton. Applied and Environmental Microbiology 57:473-479

Pel R, Floris V, van Hoogveld H (2004) Analysis of planktonic community structure and trophic interactions using refined isotopic signatures determined by combining fluorescence-activated cell sorting and isotope-ratio mass spectrometry. Freshwater Biology 49:546-562

Peterson BJ, Fry B (1987) Stable isotopes in ecosystem studies. Annual Review of Ecology and Systematics 18:293-320

Petit JR, Jouzel J, Raynaud D, Barkov NI, Barnola J-, Basile I, Benders M, Chappellaz J, Davis M, Delaygue G, Delmotte M, Kotlyakov VM, Legrand M, Lipenkov VY, Lorius C, Pépin L, Ritz C, Saltzman E, Stievenard M (1999) Climate and atmospheric history of the past 420,000 years from the Vostok ice core, Antarctica. Nature 399:429-436

Popp BN, Laws EA, Bidigare RR, Dore JE, Hanson KL, Wakeham SG (1998) Effect of phytoplankton cell geometry on carbon isotopic fractionation. Geochimica et Cosmochimica Acta 62:69-77

Prairie YT, Bird DF, Cole JJ (2002) The summer metabolic balance in the epilimnion of southeastern Quebec lakes. Limnology and Oceanography 47:316-321

Qin B, Zhu G, Gao G, Zhang Y, Li W, Paerl HW, Carmichael WW (2010) A drinking water crisis in Lake Taihu, China: linkage to climatic variability and lake management. Environmental Management 45:105-112

R Core Team (2015) R: A language and environment for statistical computing.

Raymond PA, Hartmann J, Lauerwald R, Sobek S, McDonald C, Hoover M, Butman D, Striegl RG, Mayorga E, Humborg C, Kortelainen P, Dürr H, Meybeck M, Ciais P, Guth P (2013) Global carbon dioxide emissions from inland waters. Nature 503:355-387

Richey JE, Melack JM, Aufdenkampe AK, Ballester VM, Hess LL (2002) Outgassing from Amazonian rivers and wetlands as a large tropical source of atmospheric CO_2. Nature 416:617-621

Riesebell U, Wolf-Gladrow DA, Smetacek V (1993) Carbon dioxide limitation of marine phytoplankton growth rates. Nature 361:249-251

Rippka R (1972) Photoheterotrophy and chemoheterotrophy among unicellular blue-green algae. Archives of Microbiology 87:93-98

Roberts EC, Laybourn-Parry J (1999) Mixotrophic cryptophytes and their predators in the Dry Valley lakes of Antarctica. Freshwater Biology 41:737-746

Rost B, Zondervan I, Riesebell U (2002) Light-dependent carbon isotope fractionation in the coccolithophorid *Emiliania huxleyi*. Limnology and Oceanography 47:120-128

Rütters H, Sass H, Cypionka H, Rullkötter J (2002) Phospholipid analysis as a tool to study complex microbial communities in marine sediments. Journal of Microbiological Methods 48:149-160

Sanders RW, Porter KG (1988) Phagotrophic phytoflagellates. Advances in Microbial Ecology 10:167-192

Sarmiento JL, Gruber N (2006) Ocean Biogeochemical Dynamics. In:. Princeton University Press, Princeton, NJ

Scheffer M, Hosper SH, Meijer ML, Moss B, Jeppesen E (1993) Alternative Equilibria in Shallow Lakes. Trends in Ecology and Evolution 8:275-279

Schindler DE, Carpenter SR, Cole JJ, Kitchell JF, Pace ML (1997) Influence of food web structure on carbon exchange between lakes and the atmosphere. Science 277:248-251

Schindler DW (2006) Recent advances in the understanding and management of eutrophication. Limnology and Oceanography 51:356-363

Schouten S, Breteler W, Blokker P, Schogt N, Rijpstra WIC, Grice K, Baas M, Sinninghe Damsté JS (1998) Biosynthetic effects on the stable carbon isotopic compositions of algal lipids: Implications for deciphering the carbon isotopic biomarker record. Geochimica et Cosmochimica Acta 62:1397-1406

Schubert CJ, Lucas FS, Durisch-Kaiser E, Stierli R, Diem T, Scheidegger O, Vazquez F, Müller B (2010) Oxidation and emission of methane in a monomictic lake (Rotsee, Switzerland). Aquatic Sciences 72:455-466

Scott JH, O'Brien DM, Emerson D, Sun H, McDonald GD, Salgado A, Fogel ML (2006) An examination of the carbon isotope effects associated with amino acid biosynthesis. Astrobiology 6:867-880

Seekell DA, Lapierre JF, Ask J, Bergström AK, Deininger A, Rodríguez P, Karlsson J (2015) The influence of dissolved organic carbon on primary production in northern lakes. Limnology and Oceanography 60:1276-1285

Shishlyannikov SM, Klimenkov IV, Bedoshvili YD, Mikhailov IS, Gorshkov AG (2014) Effect of mixotrophic growth on the ultrastructure and fatty acid composition of the diatom Synedra acus from Lake Baikal. Journal of Biological Research-Thessaloniki 21:15-23

Smith EL (1938) Limiting factors in photosynthesis: light and carbon dioxide. Journal of General Physiology 22:21-35

Smith WOJ, Barber RT, Huntsman SA (1977) Primary production off the coast of northwest Africa: excretion of dissolved organic matter and its heterotrophic uptake. Deep-Sea Research 24:35-47

Soetaert K, Petzoldt T (2010) Inverse modelling, sensitivity and Monte Carlo analysis in R using package FME. Journal of Statistical Software 33:1-28

Soetaert K, Petzoldt T, Setzer RW (2010) Solving differential equations in R: package deSolve. Journal of Statistical Software 33:1-25

Soetaert K, Hofmann AF, Middelburg JJ, Meysman FJR, Greenwood J (2007) The effect of biogeochemical processes on pH. Marine Chemistry 105:30-51

Søndergaard M, Jensen JP, Jeppesen E (2003) Role of sediment and internal loading of phosphorus in shallow lakes. Hydrobiologia 506-509:123-145

Staehr PA, Bade D, van de Bogert MC, Koch GR, Williamson C, Hanson P, Cole JJ, Kratz TK (2010) Lake metabolism and the diel oxygen technique: State of the science. Limnology and Oceanography 8:628-644

Staehr PA, Sand-Jensen K (2007) Temporal dynamics and regulation of lake metabolism. Limnology and Oceanography 52:108-120

Stebegg R, Wurzinger B, Mikulic M, Schmetterer G (2012) Chemoheterotrophic growth of the cyanobacterium *Anabaena* sp. strain PCC 7120 dependent on a functional cytochrome c oxidase. Journal of Bacteriology 194:4601-4607

Stoecker D (1998) Conceptual models of mixotrophy in planktonic protists and some ecological and evolutionary implications. European Journal of Protistology 34:281-290

Sundh I, Bell RT (1992) Extracellular dissolved organic carbon released from phytoplankton as a source of carbon for heterotrophic bacteria in lakes of different humic content. Hydrobiologia 229:93-106

Taipale SJ, Peltomaa E, Hiltunen M, Jones RI, Hahn MW, Biasi C, Brett MT (2015) Inferring phytoplankton, terrestrial plant and bacteria bulk $\delta^{13}C$ values from compound specific analyses of lipids and fatty acids. PLoS ONE 10

Taipale SJ, Strandberg U, Peltomaa E, Galloway AWE, Ojala A, Brett MT (2013) Fatty acid composition as biomarkers of freshwater microalgae: analysis of 37 strains of microalgae in 22 genera and in seven classes. Aquatic Microbial Ecology 71:165-178

Taipale SJ, Kankaala P, Tiirola M, Jones RI (2008) Whole-lake dissolved inorganic ^{13}C additions reveal seasonal shifts in zooplankton diets. Ecology 89:463-474

Tan CK, Johns MR (1996) Screening of diatoms for heterotrophic eicosapentaenoic acid production. Journal of Applied Phycology 8:59-64

Teixeira-de Mello F, Meerhoff M, Pekcan-Hekim Z, Jeppesen E (2009) Substantial differences in littoral fish community structure and dynamics in subtropical and temperate shallow lakes. Freshwater Biology 54:1202-1215

Thomas TE, Harrison PJ (1987) Rapid ammonium uptake and nitrogen interactions in five intertidal seaweeds grown under field conditions. Journal of Experimental Marine Biology and Ecology 107:1-8

Tranvik LJ, Downing JA, Cotner JB, Loiselle SA, Striegl RG, Ballatore TJ, Dillon P, Finlay K, Fortino K, Knoll LB, Kortelainen PL, Kutser T, Larsen S, Laurion I, Leech DM, Leigh McCallister SL, McKnight DM, Melack JM, Overholt E, Porter JA, Prairie Y, Renwick WH, Roland F, Sherman BS, Schindler DW, Sobek S, Tremblay A, Vanni MJ, Verschoor AM, von Wachenfeldt E, Weyhenmeyer GA (2009) Lakes and reservoirs as regulators of carbon cycling and climate. Limnology and Oceanography 65:2298-2314

Tranvik LJ (1988) Availability of dissolved organic carbon for planktonic bacteria in oligotrophic lakes of different humic content. Microbial Ecology 16:311-322

Travers M, Shin YJ, Jennings S, Cury P (2007) Towards end-to-end models for investigating the effects of climate and fishing in marine ecosystems. Progress in Oceanography 75:751-770

Vadeboncoeur Y, Jeppesen E, Vander Zanden MJ, Schierup HH, Christoffersen K, Lodge DM (2003) From Greenland to green lakes: Cultural eutrophication and the loss of benthic pathways in lakes. Limnology and Oceanography 48:1408-1418

Van Breugel Y, Schouten S, Paetzel M, Sinninghe Damsté JS (2006) Seasonal variation in the stable carbon isotopic composition of algal lipids in a shallow anoxic fjord: evaluation of the effect of recycling of respired CO_2 on the $\delta^{13}C$ of organic matter. American Journal of Science 306:367-387

Van den Meersche K, van Rijswijk P, Soetaert K, Middelburg JJ (2009) Autochthonous and allochthonous contributions to mesozooplankton diet in a tidal river and estuary: Integrating carbon isotope and fatty acid constraints. Limnology and Oceanography 54:62-74

Van den Meersche K, Middelburg JJ, Soetaert K, van Rijswijk P, Boschker HTS, Heip CHR (2004) Carbon-nitrogen coupling and algal-bacterial interactions during an experimental bloom: Modeling a ^{13}C tracer experiment. Limnology and Oceanography 49:862-878

Van Donk E, van de Bund WJ (2002) Impact of submerged macrophytes including charophytes on phyto- and zooplankton communities: allelopathy versus other mechanisms. Aquatic Botany 72:261-274

Van Ee G (2007) Naardermeer op weg naar volledig herstel. In: Diatomededelingen 31

Van Gaever S, Moodley L, Pascotti F, Houtekamer M, Middelburg JJ, Danovaro R, Vanreusel A (2009) Trophic specialisation of metazoan meiofauna at the Håkon Mosby Mud Volcano: Fatty acid biomarker isotope evidence. Marine Biology 156:1289-1296

Van Oevelen D, Moodley L, Soetaert K, Middelburg JJ (2006) The trophic significance of bacterial carbon in a marine intertidal sediment: Results of an in situ stable isotope labeling study. Limnology and Oceanography 51:2349-2359

Vermaas WFJ (2001) Photosynthesis and respiration in cyanobacteria. In: Encyclopedia of Life Sciences. Nature Publishing Group, London, pp 245-251

Vincent WF, Goldman CR (1980) Evidence for algal heterotrophy in Lake Tahoe, Calofornia-Nevada. Limnology and Oceanography 25:89-99

Waiser MJ, Robarts RD (2000) Changes in composition and reactivity of allochthonous DOM in a prairie saline lake. Limnology and Oceanography 45:763-774

Weyhenmeyer GA, Kosten S, Wallin MB, Tranvik LJ, Jeppesen E, Roland F (2015) Significant fraction of CO_2 emissions from boreal lakes derived from hydrologic inorganic carbon inputs. Nature Geoscience 8:933-936

White DC, Stair JO, Ringelberg DB (1996) Quantitative comparisons of in situ microbial biodiversity by signature biomarker analysis. Journal of Industrial Microbiology 17:185-196

White DC, David WM, Nickels JS, King JD, Bobbie RJ (1979) Determination of the sedimentary microbial biomass by extractible lipid phosphate. Oecologia 40:51-62

Wilson DE (1979) The influence of humic compounds on titrimetric determinations of organic carbon in freshwater. Archiv für Hydrobiologie 87:379-384

Wolf-Gladrow DA, Zeebe RE, Klaas C, Körtzinger A, Dickson AG (2007) Total alkalinity: The explicit conservative expression and its application to biogeochemical processes. Marine Chemistry 106:287-300

Wright RT, Shah NM (1975) The trophic role of glycolic acid in coastal seawater. I. Heterotrophic metabolism in seawater and bacterial cultures. Marine Biology 33:175-183

Yu J, Liu Z, He H, Zhen W, Guan B, Chen F, Pi K, Zhong P, Teixeira-de Mello F, Jeppesen E (2016) Submerged macrophytes facilitate dominance of omnivorous fish in a subtropical shallow lake: implications for lake restoration. Hydrobiologia 775:97-107

Yu J, Li Y, Liu X, Li K, Chen F, Gulati R, Liu Z (2013) The fate of cyanobacterial detritus in the food web of Lake Taihu: a mesocosm study using ^{13}C and ^{15}N labeling. Hydrobiologia 710:39-46

Zeebe RE, Wolf-Gladrow DA (2001) CO_2 in seawater: equilibrium, kinetics, isotopes

Zelles L (1999) Fatty acid patterns of phospholipids and lipopolysaccharides in the characterisation of microbial communities in soil: a review. Biology and Fertility of Soils 29:111-129

Zepp Falz K, Holliger C, Grosskopf R, Liesack W, Nozhevnikova AN, Müller B, Wehrli B, Hahn D (1999) Vertical distribution of methanogens in the anoxic sediment of Rotsee (Switzerland). Applied Environmental Microbiology 65:2402-2408

Zhang CL, Huang Z, Cantu J, Pancost RD, Brigmon RL, Lyons TW, Sassen R (2005) Lipid biomarkers and carbon isotope signatures of a microbial (Beggiatoa) mat associated with gas hydrates in the Gulf of Mexico. Applied and Environmental Microbiology 71:2106-2112

Summary

Present-day increases in atmospheric carbon dioxide concentrations represent only about 50% of total anthropogenic carbon emissions; the remainder has been absorbed by terrestrial and aquatic reservoirs. Freshwater ecosystems, although relatively small in volume, have a disproportionately large carbon storage capacity compared to oceans, as a result of relatively high production rates and fast accumulation rates. Although of clear importance to the global carbon cycle, the role of lakes in terms of processing and storage of organic carbon is not very well characterized. Also, complete lacustrine carbon budgets are scarce and need to be better constrained in order to provide a more consistent view on the functioning of freshwater systems in the global carbon cycle. Whether lakes function as a net source or sink for carbon depends on the balance between rates of primary production and respiration. Respiration may be enhanced by input of allochthonous organic carbon and hence it is thought that most lakes are sources of CO_2 to the atmosphere.

At the base of the food web, the microbial segment plays a crucial role in lacustrine food-web functioning and carbon transfer, thereby influencing carbon storage and CO_2 emission and uptake in freshwater environments. The microbial food web is particularly sensitive to variability in nutrient supply, oxygenation, temperature, light and atmospheric CO_2 levels. In freshwater ecosystems most of these parameters vary with depth, allowing different microbial communities to occur simultaneously at different depths of the water column. Additionally, these parameters also change seasonally, affecting microbial communities and relative rates of (phytoplankton) production and consumption throughout the year. Between freshwater systems, differences in nutrient availability cause variation in lacustrine food webs in terms of the relative sizes of compartments and carbon fluxes. Generally, when nutrient availability increases, phytoplankton production increases and the role of the microbial food web becomes more important. Nutrient availability often increases as result of anthropogenic activities, resulting in eutrophication of freshwater systems. Anthropogenic eutrophication is one of the most serious and extensive environmental problems worldwide, degrading ecosystems by causing cyanobacterial blooms, reducing oxygen concentrations and lowering biodiversity.

The aim of this thesis is to increase understanding of the processes within food webs that affect lacustrine carbon budgets, focusing specifically on the effects of variability with depth, varying trophic states, and seasonality on microbial carbon processing.

Switzerland

Variability in microbial carbon processing with depth was investigated in two peri-alpine Swiss lakes. Lake Rotsee is a small and relatively shallow eutrophic lake, which is vertically stratified during most of the year with an anoxic hypolimnion. Nearby Lake Lucerne is a large, oligotrophic lake, with limited terrestrial input and a fully oxygenated water column. In both lakes, in situ ^{13}C-bicarbonate-labelled incubations were carried out in early summer 2011 at six different depth intervals under ambient light conditions to trace total and group-specific primary production, and the transfer of this newly fixed carbon to secondary producers. In parallel, incubations under dark conditions and using ^{13}C-glucose as a tracer were carried out at the same depth intervals, to quantify bacterial production in terms of assimilation and respiration. The studies showed depth-dependence of primary production and the microbial community, with 1) different PLFAs produced at different depths corresponding to different metabolic processes, 2) variability with water depth in the release of extracellular carbon by phytoplankton and 3) depth-dependence of consumption of recently fixed carbon by bacteria. A comparison between the lakes showed that production rates were substantially lower in oligotrophic Lake

Lucerne compared to eutrophic Lake Rotsee and the greater depth of the photic zone could not compensate for differences in volumetric production rates. Phytoplankton-bacteria coupling was stronger in Lake Lucerne, where bacteria fully consumed the newly produced organic matter, showing that they were well adapted to rapidly respond to periods of increased productivity. Also, results suggest that both Rotsee and Lake Lucerne were net autotrophic during the experiments.

Additionally, in Lake Lucerne, a mesocosm labelling experiment using ^{13}C-bicarbonate as a tracer was carried out during spring, showing a much weaker coupling between phytoplankton and bacterial production, indicating that potentially more organic matter can escape recycling at this time and can be transported to the lake floor.

China

The effects of biomanipulation and restoration measures on food-web dynamics and carbon flows were studied in two basins of Chinese Lake Taihu, one of which is hypereutrophic and dominated by cyanobacterial blooms (Meiliang Bay) and the other was the subject of biomanipulation and restoration measures and has returned to a clear-water state (Wuli Lake). Mesocosm labelling experiments were carried out in both lakes. Isotope analyses on microbial lipids, zooplankton, epiphytes and macrophytes were combined with a simple isotope model. This study showed that as a result of restoration measures, carbon flows shifted from phytoplankton(cyanobacteria)-dominated in Meiliang Bay to macrophyte-dominated in Wuli Lake and primary production in the restored lake was 2-7 times higher compared to the unrestored lake. The study also showed that the dominance of primary producers was changed from pelagic to benthic, which has implications for restoration of eutrophic, shallow lakes in tropical and subtropical regions, indicating that measures should focus on establishing a dominance of benthic primary production in lakes, e.g. by re-establishing submerged plants and benthic algae.

The Netherlands

Seasonal variability in phytoplankton and bacterial stable carbon isotopes, and changes in bacterial carbon sources were studied in two basins of Lake Naarden, a shallow Dutch peat lake with one basin in a restored state and the other somewhat eutrophic. Samples were collected during 17 months, capturing the full range of seasonal variability in terms of temperatures and light. Natural abundance stable carbon isotopes were analyzed on carbon pools, macrophytes and microbial membrane lipids (PLFAs). Isotope fractionation (ε) between phytoplankton biomass and $CO_{2(aq)}$ was lowest during summer (11.6‰), when productivity is high, and highest ε values were observed during winter (23.0‰). At both sites, correlations between phytoplankton and bacterial carbon isotopes were strong during most of the year, suggesting that most bacterial carbon derives from phytoplankton (autochthonous) production. Bacterial dependence on locally produced organic carbon was lowest during winter and we found that during this period, bacterial dependence on DOC (allochthonous carbon) was higher at the restored site (39-77%) compared to the eutrophic site (17-46%). It hence seems that bacterial dependence on allochthonous carbon was mostly related to the availability of locally-produced organic matter.

Main conclusions

In summary, the results presented in this thesis show that there is strong variability in microbial carbon processing in the freshwater systems studied and we found, 1) substantial variability in terms of absolute and relative amounts of production and consumption of organic matter,

concluding that nutrient levels are of clear importance to microbial metabolic activities and thereby in-lake carbon processing. 2) Nonetheless, despite lower nutrient levels in the macrophyte-dominated part of Lake Taihu we found total ecosystem productivity to be much higher compared to the still eutrophic basin. 3) We observed that carbon cycling pathways had shifted from phytoplankton-dominated to macrophyte-dominated, confirming the increased importance of the microbial food web as a consequence of eutrophication. 4) We found that severe DIC-limitation forced phytoplankton to derive significant amounts of their carbon from DOC, in addition to DIC. 5) In addition to variation among lakes, also large variability with depth was found in the relative importance of production and consumption and the microbial communities and metabolic processes dominating at each depth, showing that multiple sampling depths are of crucial importance, especially in vertically stratified lakes such as Rotsee. 6) We found that coupling between phytoplankton and bacterial production seems related to trophic state with stronger coupling in oligotrophic Lake Lucerne compared to eutrophic Lake Rotsee. 7) Additionally, we found that phytoplankton-bacteria coupling varied with water depth and during the year. We conclude that the potential for burial of organic matter in lake sediments is not only highly variable among different systems but also throughout the year and hence mass flux calculations and carbon budget calculations should be based on multiple sampling depths and campaigns.

Nederlandse samenvatting

1 Klimaatverandering en de mondiale koolstofkringloop in het Antropoceen

Het chemische element koolstof (C) is niet alleen een belangrijk bestanddeel van het leven op aarde, het speelt ook een essentiële rol in de energiebalans en daarmee het klimaat van onze planeet. De gasvormen van koolstof, koolstofdioxide (CO_2) en methaan (CH_4) houden warmte vast door warmtestraling (infrarood) te absorberen, dit maakt ze tot de voornaamste broeikasgassen in de atmosfeer. Door het gebruik van fossiele brandstoffen, het kappen van bossen en het produceren van cement heeft de mens de natuurlijke koolstofkringloop veranderd, met als resultaat een recordtoename van CO_2 in de atmosfeer tussen het begin van de industrialisatie (~280 parts per million) en nu (~400 ppm). Dit is reden tot zorg, aangezien er sterke aanwijzingen zijn voor een correlatie tussen de concentratie CO_2 in de atmosfeer en stijgende temperaturen.

Hoewel de waargenomen toename in atmosferisch CO_2 substantieel is, is het slechts ongeveer 50% van de totale antropogene CO_2 uitstoot. De rest wordt opgeslagen door verschillende reservoirs in de mondiale koolstofkringloop. Van de oceanen op aarde is al bekend dat ze CO_2 opnemen, aangezien het oplost in en reageert met (zee)water, resulterend in diwaterstofcarbonaat (H_2CO_3), bicarbonaat (HCO_3^-) en carbonaat (CO_3^{2-}), samen bekend als Dissolved Inorganic Carbon (DIC). Koolstofbudgetstudies buiten de oceanen richten zich doorgaans op de biosfeer als voornaamste opnamebron, welke ongeveer 30% van de uitgestoten koolstof opslaat. Er blijft echter veel onzeker met betrekking tot de houdbaarheid van deze opnamebronnen, alsook gaten en tegenstrijdigheden in koolstofbudgetten.

2 De rol van meren in de mondiale koolstofkringloop

Pas sinds een paar jaar worden zoetwatersystemen herkend als plekken waar koolstofverwerking plaats vindt en als mogelijke opslagplaats van substantiële hoeveelheden koolstof. Hoewel meren slechts ~1% van het totale aardoppervlak beslaan hebben ze een grote opslagcapaciteit dankzij hoge productie- en sedimentatiesnelheid. Zoetwaterstelsels ontvangen 1.9 – 2.9 Pg C y^{-1} van hun omgeving via rivieren, grondwater en afwatering, en het meeste hiervan blijft opgeslagen in de meren zelf. Vanwege hun relatieve belang zouden meren meegenomen moeten worden in de schattingen van de mondiale koolstofkringloop maar complete lacustriene koolstofbudgetten zijn schaars en moeten beter worden afgebakend om een consistenter beeld te krijgen van de rol van meren in de mondiale koolstofkringloop. Zo zijn meren voornamelijk bronnen van CO_2 in de atmosfeer ondanks hun grote opslagcapaciteit en hoewel organisch koolstof komend vanaf land over het algemeen als ontoegankelijke en inefficiënte voedselbron wordt beschouwd, kan het toch worden opgenomen in bepaalde delen van het voedselweb. Veel vragen blijven dus nog onbeantwoord, niet alleen met betrekking tot de in- en uitstromen van de meren als geheel, maar ook over de stromen in de meren zelf, en de organismen en processen betrokken bij de koolstofkringloop in meren. Dit proefschrift probeert verduidelijking te brengen in de interne processen (binnen voedselwebben) die invloed hebben op lacustriene koolstofbudgetten in meren met contrasterende productiviteit.

3 Koolstofkringloop in lacustriene voedselwebben

Waar traditionele studies naar voedselwebben beperkt waren tot het analyseren van grotere organismen en het gebruiken van indirecte proxies voor het microbiële domein, beschikken we tegenwoordig over lipidenchemie voor een directe analyse van microbiële producenten en consumenten. Dit proefschrift richt zich specifiek op microbiële koolstofverwerking in vier verschillende zoetwaterstelsels met variërende nutriëntenconcentraties: 1) Rotsee, een relatief ondiep, eutroof meer in Zwitserland, 2) het meer van Lucerne, een groot, oliotroof meer in Zwitserland, 3) twee delen van het Taihu meer in China, één sterk eutroof en gekenmerkt door giftige algenbloei en één waarin biomanipulatie en restauratiepogingen werden toegepast en welke nu gekenmerkt wordt door macrofyten (waterplanten), en 4) het Naardermeer, een ondiep veenmeer in Nederland.

3.1 Primaire productie en koolstofpoelen

Onderin het voedselweb nemen fytoplankton (microfyten) en macrofyten gedurende fotosynthese DIC op, en produceren organische materie. De hoeveelheden DIC in zoet water schommelen gewoonlijk tussen de 100 en 1000 µmol C L^{-1} en zijn zelden in evenwicht met de atmosfeer omdat de uitwisselingssnelheid met de atmosfeer (een kwestie van maanden) veel langzamer is dan de snelheid van de biologische processen die de hoeveelheid DIC in de waterkolom beïnvloeden. Concentraties van de verschillende soorten DIC ($CO_{2(aq)}$, H_2CO_3, HCO_3^- en CO_3^{2-}) in meren zijn een functie van pH, met HCO_3^- als dominante soort in de meeste natuurlijke wateren, en $CO_{2(aq)}$ komt slechts in hele kleine hoeveelheden voor. Om productie te waarborgen hebben de meeste soorten fytoplankton en macrofyten mechanismen ontwikkeld om koolstof te concentreren. Deze mechanismen helpen bij het omzetten van HCO_3^- naar $CO_{2(aq)}$. Echter, er wordt gewoonlijk aangenomen dat fytoplanktonproductie afneemt als de concentraties $CO_{2(aq)}$ beperkt zijn.

De verse organische materie die de micro- en macrofyten door fotosynthese aanmaken kan ofwel direct opgenomen worden door zoöplankton, danwel omgezet worden in opgelost organisch koolstof (Dissolved Organic Carbon, DOC) door middel van microbiële afbraak. Daarnaast kan fytoplankton ook direct organische materie uitstoten (EOC) als de fotosynthetische koolstoffixatie groter is dan de productie van biomassa. De uitstoot van organisch koolstof in zoetwatersystemen neemt toe met de snelheid van primaire productie, hetzij langzamer. Daarnaast kan DOC in meren worden geproduceerd door celveroudering, slordig foerageren van zoöplankton, virale lyse en degradatie van deeltjes organisch koolstof (Particulate Organic Carbon, POC). Op deze manieren dragen alle producenten en consumenten binnen een meer bij aan de DOC poel, aanvullend op allochtone bronnen uit sediment en omliggende stroompjes en bodems. Als resultaat hiervan kan de samenstelling (en daarmee de afbreekbaarheid) en concentratie DOC sterk variëren tussen het ene zoetwaterstelsel en het andere. Vervolgens blijkt dat verschillen in DOC concentraties de koolstoffluxen in het microbiële voedselweb kunnen beïnvloeden door bijvoorbeeld het beperken van fotosynthese (als gevolg van het verminderen van de hoeveelheid licht) en het stimuleren van bacterieel metabolisme.

Alle organismen in het voedselweb dragen bij aan de POC poel, die bestaat uit zowel levende (biomassa) en dode (detritus) fracties. POC wordt doorgaans geproduceerd in de bovenste waterlagen, terwijl afbraak meestal dieper in de waterkolom plaatsvindt, daarom zijn de concentraties het grootst bij het wateroppervlak, afnemend met de diepte.

3.2 Secundaire productie en respiratie door bacteriën

Bacteriën spelen een belangrijke rol in het voedselweb omdat ze organische verbindingen remineraliseren en significant bijdragen aan het totaal aan secundaire productie. Productie door heterotrofe bacteriën is sterk gekoppeld aan de productie van fytoplankton, waarbij de bacteriële productie varieert tussen de 20 en 30% van de productie van fytoplankton. Het grootste deel van de totale bacteriële koolstofbehoefte komt voort uit fytoplankton met berekende afhankelijkheden variërend van 70% tot ~100%. Daarnaast wordt geschat dat bacteriën tussen de 13 en 32% van hun koolstofbehoefte uit EOC halen, afhankelijk van de bacteriële groei-efficiëntie. Bacterieel metabolisme draagt niet alleen significant bij aan het totaal aan secundaire productie, maar ook aan respiratie in meren. In zoetwaterstelsels wordt respiratie doorgaans gestimuleerd door allochtone koolstofbronnen, resulterend in respiratiesnelheden die hoger zijn dan de primaire productie. Als gevolg zijn veel aquatische stelsels netto heterotroof en bronnen van CO_2 in de atmosfeer. Relatieve productie en respiratiesnelheden variëren met de diepte van het water, waardoor ze de diepteprofielen van bijvoorbeeld zuurstof en DIC concentraties beïnvloeden. Primaire productie (zuurstofproductie en DIC consumptie) vindt doorgaans boven in de waterkolom plaats, terwijl remineralisatie (zuurstofconsumptie en DIC productie) ook in dieper, donkerder waterlagen gebeurt. Diepte-afhankelijkheid van de samenstelling en verwerking van koolstof door microbiële gemeenschappen wordt nader besproken in hoofdstuk twee en drie van dit proefschrift.

3.3 Zoöplankton en vis

Zoöplankton kan zowel direct fytoplankton biomassa consumeren, of via de DOC-bacteriën route. Deze twee bronnen zijn van gelijk belang voor de productie van zoöplankton, hoewel beide manieren relatief inefficiënt blijken te zijn. De omvang van de zoöplanktonpopulatie wordt gereguleerd door plankton-etende vissen hogerop in het voedselweb. Omgekeerd zorgen macrofyten voor een schuilplaats tegen roofdieren en verminderen daarmee de top-down beperking van zoöplankton.

4 Effecten van de hoeveelheid voedingsstoffen en eutrofiëring op microbiële voedselwebben

Met name op microbieel niveau in het voedselweb hangen productie en consumptie niet alleen af van de beschikbaarheid van koolstofsubstraten, maar spelen de concentraties van voedingsstoffen, stikstof (N) en fosfor (P) ook een belangrijke rol. Veel onderzoeken hebben aangetoond dat de relatieve grootte van de compartimenten en fluxen – zoals hierboven beschreven – veranderen onder verschillende nutriëntenconcentraties. Kort gezegd, bij lage nutriëntenconcentraties is de primaire productie beperkt maar respiratie niet omdat het gestimuleerd kan worden door de input van allochtoon organisch koolstof. Hieruit volgt dat in oligotrofe meren de productie doorgaans lager is dan respiratie waardoor deze meren bronnen zijn van CO_2 in de atmosfeer (zie boven). Aangezien de meeste beschikbare voedingsstoffen en organisch koolstof in oligotrofe meren in DOC-vorm zijn, hebben bacteriën het voordeel en spelen ze dus een belangrijk rol. Neemt de hoeveelheid voedingsstoffen toe dan stijgt ook de productie van fytoplankton (maar het percentage van extracellulaire uitstoot neemt juist af). Omdat de concentraties van POC toenemen worden organismen die zich voeden met deeltjes, zoals zoöplankton, protozoa en vissen, belangrijker en bacteriën dus relatief minder belangrijk. Echter, in absolute getallen, wordt

de rol van het microbiële voedselweb groter als de hoeveelheid voedingsstoffen toeneemt omdat cyanobacteriën belangrijker worden en zoöplankton verschuift naar kleinere schaaldieren en raderdieren. Tot slot kan in voedselrijke (eutrofe) meren met hoge primaire productie de export van organisch materiaal een onbalans tussen $CO_{2(aq)}$ en de atmosfeer teweeg brengen, wat de meren juist plekken van opslag van CO_2 in plaats van bronnen maakt.

Naast natuurlijke oorzaken kan eutrofiëring van meren ook veroorzaakt worden door buitensporige nutriëntentoevoer door menselijk toedoen, bijvoorbeeld de toevoer van rioolwater, agrarische afwatering en neerslag uit de atmosfeer. Antropogene eutrofiëring is mondiaal gezien een van de meest ernstige milieuproblemen omdat het ecosystemen ontwricht wanneer fytoplanktonproductie gedomineerd wordt door bloeivorming. Dit resulteert in verhoogde troebelheid en minder licht, wat het einde betekent voor macrofyten en de organismen die afhankelijk zijn van macrofyten als habitat (zoöplankton en vis). Tot slot vermindert de degradatie van grote hoeveelheden biomassa geproduceerd tijdens bloeiperioden de hoeveelheid zuurstof, waardoor vissen doodgaan. Met name cyanobacteriën staan er om bekend te bloeien, soms met lagen schuim op het water en de productie van stoffen die giftig zijn voor mens en dier.

Om eutrofiëring tegen te gaan, de vorming van fytoplankton (cyanobacteriëel) biomassa te reduceren en helder water te herstellen zijn maatregelen om input van nutriënten terug te brengen cruciaal maar vaak niet toereikend. Daarom worden ze vaak gecombineerd met biomanipulatie gericht op het verhogen van de graasdruk op fytoplankton. Voorbeelden zijn het herplanten van macrofyten, het verwijderen van zoöplankton-etende vissen en toevoegen van vis-etende vissen. Op deze manier wordt fytoplankton productie in de voedselketen niet alleen beperkt van beneden naar boven (elimineren van voedingsbronnen), maar ook van boven naar beneden. De aanwezigheid van macrofyten beperkt de grootte van de fytoplanktonpopulatie door met fytoplankton te concurreren voor DIC en voedingsstoffen. Daarnaast kan een overvloed aan macrofyten de verhouding zoöplankton:fytoplankton verbeteren omdat ze een schuilplaats bieden aan zoöplankton en daarmee de graasdruk op fytoplankton verhogen. Tot noch toe hebben restauratiepogingen wisselend succes geboekt en blijven er nog veel vragen over de effecten op de lange termijn. Over het algemeen lijken vispopulaties zich te herstellen maar ook macrofyten kunnen zich volledig herstellen als het grazen niet te heftig is en er een bron van zaden is. Er is ook beperkt informatie over de effecten van biomanipulatie in warme (sub) tropische zoetwaterstelsels waar de biologische feedback en voedselweb interactie verschilt van die in meren met een meer gematigde temperatuur. Zo zijn bijvoorbeeld schuilplaatsen voor zoöplankton in macrofyten in tropische meren minder effectief omdat vissen er geneigd zijn te verzamelen.

In dit proefschrift worden meren van verschillende trofische gradiënten bestudeerd, variërend van oligotroof (hoofdstuk 3) tot eutroof (hoofdstuk 2) en hypereutroof, gedomineerd door cyanobacteriële bloei (hoofdstuk 4). Aanvullend vergelijken we in hoofdstuk 4 koolstofverwerking in een hypereutroof subtropisch meer (Taihu, China) met een hersteld deel van hetzelfde meer.

5 Effecten van seizoenen op koolstofverwerking in zoetwater voedselwebben

In aanvulling op de hoeveelheid voedingsstoffen en de input van allochtoon organisch materiaal wordt fytoplanktonproductie en daarmee het hele (microbiële) voedselweb beïnvloed door abiotische parameters zoals de beschikbaarheid van licht en de temperatuur. Al deze parameters

variëren gedurende het jaar en beïnvloeden zo de fytoplanktongroepen en productie. De mate van limitatie van voedingsstoffen en ook welke voedingsstof de productie beperkt bijvoorbeeld, kunnen variëren tussen de herfst en de lente. Daarnaast is het bekend dat verschillen in temperatuur van invloed zijn op primaire productie en respiratie doordat ze het metabolisme beïnvloeden, maar het is ook een beperkende factor voor koolstofchemie (pH, pCO_2) en dus de beschikbaarheid van anorganisch koolstof. De hoeveelheid licht, een voorwaarde voor fotosynthese, heeft ook invloed op de primaire productie. Als de hoeveelheid fotosynthetisch actieve straling te hoog (photo-inhibition) of te laag (low-light limitation) is hindert dit de fotosynthese. Productie en respiratie kunnen anders en met een verschillende snelheid reageren op seizoensgebonden veranderingen zoals hierboven beschreven, zo kan bijvoorbeeld respiratie onder toenemende temperaturen sneller stijgen dan productie. Het blijkt dat de capaciteit van zoetwaterstelsels om organisch materiaal op te nemen sterk afhangt van seizoensgebonden veranderingen in parameters in het milieu.

Vanwege hun snelle cyclus reageren fytoplankton en bacteriën snel op veranderingen in milieugebonden parameters, met seizoensgebonden stratificatie en mogelijke zuurstofuitputting als gevolg. Seizoensvariatie bij microbiële groepen is ook zichtbaar in biomarkers en isotopensamenstellingen van fytoplankton. In dit proefschrift bestuderen we seizoensgebonden verschillen bij fytoplankton en bacteriële koolstofbronnen in het Naardermeer (hoofdstuk 5).

6 Reconstructie van microbiële koolstofverwerking met fosfolipide vetzuren als biomarkers

Biomarkers zijn organische moleculen, voornamelijk lipiden, die kunnen worden gekoppeld aan specifieke organismen en/of processen. In voedselwebstudies worden biomarkers, zoals fosfolipide vetzuren (Phospholipid-derived fatty acids PLFA's), gebruikt om de aanwezigheid van bepaalde groepen organismen vast te stellen en hun aantallen te berekenen. Fosfolipiden maken deel uit van celmembranen en bestaan uit een hydrofiele fosfaatkop verbonden (via een glycerolmolecuul) aan twee hydrofobe staarten van vetzuur. Verzeping bevrijdt de staarten van vetzuur, welke variabele lengtes hebben alsook diverse structuren met bijvoorbeeld rechte ketens en (iso- of anteiso) methylgroepen of ringstructuren. De vetzuren in de staarten kunnen verzadigd of onverzadigd zijn met verschillende aantallen van dubbele bindingen op verschillende posities in de koolstofketen. Deze structurele variatie in PLFA moleculen wordt weergegeven in hun informele biochemische naam als C*a*:*b*ω*c*, waarbij *a* staat voor de lengte van de keten, *b* voor het aantal dubbele bindingen en *c* voor de positie van de (eerste) dubbele binding geteld vanaf het einde (ω) van de vetzuurketen. PLFA's zijn bijzonder bruikbaar bij voedselweb onderzoek omdat ze snel hydroliseren nadat de cel sterft en dus voornamelijk vers geproduceerde biomassa vertegenwoordigen. De combinatie van PLFA's met stabiele isotopenlabelling experimenten blijken een krachtige manier om het voedselweb te vergelijken en koolstof- en stikstofstromen door het microbiële voedselweb te volgen.

PLFA's komen voor in een breed scala aan organismen en vertegenwoordigen dus niet specifieke organismen. Ze kunnen echter wel gebruikt worden om verschillende groepen producenten van elkaar te onderscheiden. Vertakte PLFA's (bijv. i/aC15:0) worden voornamelijk geproduceerd door grampositieve bacteriën, maar ze zijn ook aangetroffen in gramnegatieve bacteriën. Meervoudig onverzadigde vetzuren zoals C18:3ω3, C18:4ω3 en C20:5ω3 worden geproduceerd door eukaryotisch fytoplankton (groene/rode algen, diatomeeën, haptofyten

enz.). Dit maakt het mogelijk om, door de aanwezigheid van PLFA's te combineren met isotopenlabelling, het onderscheid te maken tussen primaire producenten (autotrofen), secundaire producenten (heterotrofe bacteriën) en detritus (dode materie), en om groep-specifieke productie te kwantificeren.

7 Probleemstelling en samenvatting

Dit proefschrift is gericht op koolstofverwerking in het microbiële voedselweb in verschillende zoetwatersystemen en de invloed daarop van nutriëntenconcentraties, biomanipulatie en seizoensveranderingen. Om dit doel te bereiken werden veldexperimenten uitgevoerd om het verwerken van koolstof en het functioneren van voedselwebben te onderzoeken. We hebben stabiele koolstof- en stikstofisotopen in hun natuurlijke abundantie of na het toevoegen van label gemeten van zowel totale koolstof- en stikstofreservoirs als van specifieke membraanlipiden (PLFA's).

Hoofdstuk 2 van dit proefschrift beschrijft de resultaten van een ^{13}C-labelling experiment dat uitgevoerd werd op zes verschillende dieptes van het eutrofe meer Rotsee, in Zwitserland. Twaalf flessen werden gevuld met water van zes verschillende dieptes. Aan zes lichtdoorlatende flessen werd ^{13}C-bicarbonaat toegevoegd als label, met als doel het kwantificeren van totale en groep-specifieke primaire productie en het doorgeven van deze gefixeerde koolstof naar secundaire producenten. Zes donkere flessen werden gelabeld met ^{13}C-glucose om bacteriële productie (assimilatie en respiratie) te kwantificeren. Dit onderzoek toont dat zowel primaire productie als microbiële gemeenschappen afhankelijk zijn van de waterdiepte, waarbij 1) verschillende PLFA's, behorend bij verschillende metabolische processen, werden geproduceerd op verschillende dieptes, 2) uitstoot van extracellulaire koolstof door fytoplankton varieerde met de diepte en 3) opname van recent gefixeerde koolstof door bacteriën was afhankelijk van de waterdiepte. De resultaten doen vermoeden dat Rotsee netto autotroof was tijdens de experimenten.

Hoofdstuk 3 beschrijft de resultaten van twee ^{13}C-labelling experimenten in het oligotrofe meer van Lucerne (Zwitserland). Een vergelijkbaar experiment zoals beschreven werd in hoofdstuk 2, met transparante en donkere flessen, toonde aan dat productiesnelheden substantieel lager waren dan in het dichtbij gelegen meer Rotsee. De diepere lichtdoorlatende waterlaag kon niet compenseren voor de verschillen in productiesnelheden per volume. Bacteriën in het meer van Lucerne waren in staat om snel te reageren op verhoogde productie, zoals tijdens de periode die hier werd bestudeerd (juni), en consumeerden het vers geproduceerde organisch materiaal volledig. Daarnaast beschrijft hoofdstuk 3 de resultaten van een mesocosm experiment in het voorjaar waarin ^{13}C-bicarbonaat werd toegevoegd. In dit tweede experiment werd een veel zwakkere koppeling gevonden tussen fytoplankton en bacteriële productie, wat er op wijst dat tijdens deze periode mogelijk meer organisch materiaal kan ontsnappen en naar de bodem van het meer kan zakken.

In **hoofdstuk 4** werd het effect bestudeerd van herstelmaatregelen op koolstofstromen in een marofiet-gedomineerd (het meer Wuli) en fytoplankton-gedomineerd (Meiliang Baai) deel van een ondiep Chinees meer. Mesocosm experimenten met ^{13}C en ^{15}N als label werden in beide meren uitgevoerd. In dit onderzoek combineren we isotoopanalyse op microbiële lipiden, zoöplankton, epifyten en macrofyten met een eenvoudig isotoopmodel. Als gevolg van de herstelmaatregelen verschoven de koolstofstromen van gedomineerd door fytoplankton (cyanobacteriën) in Meiliang Baai naar gedomineerd door macrofyten in het meer Wuli.

Primaire productie in het herstelde meer was 2-7 keer hoger dan in het eutrofe meer. Door zeer lage concentraties CO_2 in het Wuli meer werd het fytoplankton gedwongen om flinke hoeveelheden koolstof uit DOC te halen. Macrofyten daarentegen namen alleen koolstof uit DIC op. Stikstofisotoopdata waren slechts beperkt betrouwbaar, maar bevestigden de resultaten van de koolstofisotopen.

In **hoofdstuk 5** werden verschillen in stabiele koolstofisotopen van fytoplankton en bacteriën door het jaar heen in een ondiep Nederlands veenmeer bestudeerd. Gedurende 17 maanden werden watermonsters verzameld uit twee delen van het Naardermeer, het ene deel was hersteld en het andere nog enigszins eutroof. We analyseerden stabiele koolstofisotopen (natuurlijke abundantie) van koolstofbronnen, macrofyten en microbiële membraanlipiden (PLFA's). Isotoopfractionatie tussen de biomassa van fytoplankton en opgelost CO_2 was het laagst (11.6‰) in de zomer, wanneer productiesnelheden het hoogst zijn. De correlatie tussen koolstofisotopen van fytoplankton en bacteriën was sterk op beide locaties, waarbij de afhankelijkheid van bacteriën van lokaal geproduceerd koolstof het grootst was tijdens de zomer en het laagst in de winter. Tijdens de winter was de bacteriële afhankelijkheid van DOC hoger op de herstelde locatie (39-77%) dan op de eutrofe locatie (17-46%).

Dit proefschrift toont aan dat er grote verschillen zijn in het verwerken van koolstof door microben in verschillende zoetwatersystemen. Het is duidelijk dat nutriëntenconcentraties van groot belang zijn voor het metabolisme van microben en daardoor voor koolstofverwerking in meren en er waren grote verschillen in zowel de absolute als relatieve hoeveelheden organisch materiaal die werden geproduceerd en opgenomen. Desondanks vonden we dat de totale productiviteit in het door macrofyten gedomineerde deel van het meer Taihu, veel hoger was dan in het eutrofe deel waarin de nutriëntenconcentraties veel hoger zijn. De verwerking van koolstof verschoof in dit meer van gedomineerd door fytoplankton naar gedomineerd door macrofyten, wat bevestigt dat het microbiële deel van het voedselweb belangrijker is in eutrofe systemen. Niet alleen werd er variatie tussen verschillende meren geobserveerd, maar ook binnen hetzelfde meer was er grote variatie met de waterdiepte in de relatieve hoeveelheden van productie en consumptie, de opbouw van microbiële gemeenschappen en het belang van verschillende metabolische processen. Het bemonsteren van meerdere waterdieptes is dus van groot belang, in het bijzonder in gestratificeerde meren zoals Rotsee. De koppeling tussen productie door fytoplankton en bacteriën lijkt afhankelijk te zijn van de nutriëntenstatus, met een sterkere koppeling in het oligotrofe meer van Lucerne dan in het eutrofe Rotsee. Daarbovenop bleek de koppeling tussen fytoplankton en bacteriën ook te variëren met waterdiepte (hoofdstuk 2 en 3) en door het jaar heen (hoofdstuk 3 en 5). Het potentieel voor opslag van organisch materiaal in het sediment op de bodem van meren varieert dus sterk en berekeningen van massastromen moeten gebaseerd worden op monsters die genomen zijn op meerdere momenten in het jaar en meerdere dieptes van de waterkolom.

Dankwoord

elke morgen
elke middag
elke avond
ik kan er niet omheen
ik kan het niet alleen
- De Dijk –

… en daarom wil ik graag de mensen bedanken die voor mij onmisbaar zijn geweest tijdens het werken aan dit proefschrift.

Beste Gert-Jan, al meer dan een decennium heb je me begeleid tijdens scripties, veldwerk en alligators in Florida en dan uiteindelijk het onderzoek in dit proefschrift. Ik heb ontzettend veel van je geleerd. Bedankt voor de hulp, het optimisme, de inzichten en de gezelligheid!
Beste Jack, bedankt voor je goede plan voor de combinatie tussen organische en environmental geochemie tijdens het schrijven van het onderzoeksvoorstel. Bedankt dat je altijd tijd maakte, voor de ideeën, je enthousiasme en je snelle reacties als ik om hulp vroeg!
Gert-Jan en Jack, ik wil jullie allebei bedanken voor het vertrouwen dat jullie vanaf het begin in mij hadden en dat de data toch echt wel interessant was. Maar vooral bedankt dat jullie er altijd in hebben geloofd dat het uiteindelijk goed zou komen en dat jullie me de tijd hebben gegeven om eerst aan mijn gezondheid en pas daarna aan het proefschrift te werken.

Dear Carsten, thank you for your welcoming me on my fieldwork trips to Switzerland! Thanks for your help and suggestions during the design and carrying-out of the experiments and also many thanks for facilitating the lab work. I promise I won't pollute your lake anymore!
Also many thanks to the other people at EAWAG in Kastanienbaum who helped me out and made me feel welcome during my trips. Special thanks to Alois Zwyssig, Magdalene Klockowksi, Captain Gregor, Michael Schurter en natuurlijk Gijs Nobbe, die eerst al in Utrecht en daarna in Zwitserland voor me klaar stond.

Karline, dankjewel voor je de introductie in de wondere wereld van het modelleren en programmeren! Ik vond het zo leuk dat ik er maar mee verder ben gegaan!
Ook een woord van dank voor de technici en andere mensen van het NIOZ in Yerseke voor hun hulp in tijden van IRMS-crisis en voor het meten van mijn DOC monsters, Marco, Pieter, Peter, Dick en Eric. Ik vond het altijd gezellig om op in Yerseke op bezoek te zijn! Een speciaal bedankje voor Francesc, voor het varen van de boot op het meer van Lucerne!

Natuurlijk wil ik ook de technici aan de UU bedanken voor hun hulp want monsters worden niet vanzelf data! Bedankt Michiel, Anita, Dominika, Arnold, Coen, Natasja, Jan en Dineke voor jullie hulp en de gezelligheid in het lab.
Voor de administratieve en secretariële ondersteuning wil ik graag Pien, Annuska, Marjolein en Tjitske bedanken. En Ton en Margot bedankt voor de hulp met het opmaken van dit boekje.

Zhengwen Liu, even though we haven't met in person, I would like to thank you for your help with the manuscript, and Guan Baohua and Chen Feizhou for sending me more data and answering my questions. Many thanks also to the technical staff at NIGLAS in Wuxi (China) for their help preparing and carrying-out the fieldwork.

Ook wil ik Annemieke Ouwehand van Natuurmonumenten bedanken en Anneke en Rob en hun collega's van Waterproef voor het verzamelen van de watermonsters op het Naardermeer elke maand. Sonja Viester en Renske Diek van Waternet wil ik bedanken voor de lange-termijn-data van het Naardermeer en voor hun hulp bij mijn vragen.

Verder mijn collega's en oud-collega's uit Utrecht. Els, mijn eerste begeleider en steun van het eerste uur, bedankt voor de gezelligheid tijdens en buiten werk, de kopjes thee en al je hulp! Angie, thanks for your help on my fieldwork trips, your excitement, honesty and advice! It was fun to do fieldwork with you! Also thanks for all the work you've done in China, it was worth it:-) Su, thanks for the good times we've had in Utrecht and Switzerland! Anna, bedankt voor je adviezen en de gezelligheid.
Ook de rest van de mensen die kortere of langere tijd mijn collega's zijn geweest: Linda, Klaas, Francien, Frédérique, Emily, Paul, Jiefei, Tjerk, Margot, Lotti, Jorien, Joost, David, Chris, Caroline, Chloé, Laura, Johan, Julia, Eveline, Cornelia, Elisabeth, Jos, Marie-Louise, nog een Laura, Mohammed, Lennart, Karoliina, Tom, Emmy, Peter Bijl, Appy, Francesca, Timme, Rike, Niels, Daarnaast de collega's van Geochemie in PP9: Fatimah, Matthias, Nikki, Itzel, Peter Kraal, Alwina, Alejandra, Anne, Marie, José, Regina and Caroline en de mensen die ik ongetwijfeld vergeet hier te nomen. Also of course my roommates during the last year or so, Amalia and Jiawang. Iedereen bedankt voor de gezelligheid!

Een speciaal bedankje voor Loes en Mathilde, ik vind het een eer dat jullie mijn paranimfen willen zijn. We kennen elkaar nu al jaren en ik ben blij dat jullie er al die tijd waren voor hulp, steun, vragen en vooral ook voor onzinnig geklets bij een kopje koffie of thee!

Een promotieonderzoek overleef je niet zonder mensen van buiten de universiteit, dus wil ik ook die vrienden bedanken: Robine, Freek, Nanda, Redmer, Evelien, Thomas, Merel en Esther. Eefje, dank je voor het begrijpen,het luisteren en het vragen. Ook mijn oudste vriendinnen nog van voor de basisschool: Doortje en Rosanne, dank jullie wel voor het samen delen, het vertrouwen in mij, de afleiding, het lachen en de gezelligheid!

Mijn broers, en mijn schoonfamilie, dank jullie wel voor de steun, de interesse en de gezelligheid! Mijn liefste paps en mams, niet alleen tijdens de afgelopen jaren maar al mijn hele leven zijn jullie er altijd voor mij geweest. Dank jullie voor de vrijheid, het stimuleren en de liefde die jullie me gaven. Het oneindige vertrouwen in mij en de steun en zorgzaamheid die ik altijd heb gevoeld hebben mij gemaakt tot wie ik ben en hebben dit boekje mogelijk gemaakt. Ik hou van jullie!

Ruben en Ella, vanaf nu heb ik weer tijd! Lieve Ella, van zo klein tot mijn prachtige, vrolijke meid, voor jou alles, altijd! You run the world! Ruben, mijn rots, mijn beste vriend en mijn lief. Tijdens de ups en de downs, en gelukkig toen weer ups, stond jij altijd naast me. Het is moeilijk te beschrijven hoe belangrijk je steun en je aanwezigheid geweest zijn tijdens de afgelopen jaren. We hebben het samen overleefd. Je bent mijn verleden, mijn heden en mijn toekomst. Laat het maar komen!

Dive down deeper
Still, all I need is you
You're all I need to breathe
- Børns -

Curriculum Vitae

Marieke Lammers was born on April 17th in Gouda, The Netherlands. She graduated from secondary school at the Goudse Waarden in Gouda (gymnasium) in 2003. After completing physics and chemistry courses at the James Boswell Institute in Utrecht, she enrolled in the Bachelor's program in Earth Sciences at Utrecht University in 2004, which she finished with distinction in 2007. Afterwards, she started with a prestige Master's program (System Earth Modelling), focusing on geochemistry. For her final Master's research project she was involved in a field study in Florida and spent a three-month internship at Woods Hole Oceanographic Institution (Woods Hole, USA) under supervision of Tim Eglinton. In 2009 she obtained her Master's degree (with distinction). She continued to work in the organic geochemistry group as a laboratory assistant whilst working on a PhD research proposal in collaboration with Gert-Jan Reichart and Jack Middelburg. She also worked on for the Darwin Center for Biogeosciences, in collaboration with the Junior College in Utrecht, developing a teaching module on system evolution for secondary schools (VWO). Once the research proposal was funded she started working on a PhD project on microbial carbon cycling in freshwater systems. During her PhD, Marieke organized field studies in Switzerland and The Netherlands, with help from the people of EAWAG (Switzerland) and Natuurmonumenten (The Netherlands). Finally, her work culminated into this PhD thesis.